

## Answer to Reviewer #1

Thank you very much for your comments and support for the publication of our manuscript. Below we address one by one the comments made during this review. All answers are in blue font.

### 5 Specific comments

10 In my opinion, the comparison between observed and simulated methane emissions would however benefit from using an upscaling approach to avoid issues arising from the mismatch of scales. This was done for the chamber measurements, but it remains unclear how representative the flux tower footprint is of the entire grid cell. Comparing flux measurements from a single location to the entire grid cell is only meaningful if the grid cell is characterized by spatially homogeneous methane emissions. This is only rarely the case for such high-latitude landscapes (e.g., Sachs et al., 2010; Parmentier et al., 2011; Helbig et al., 2017).

15 We agree that the comparison between model methane fluxes and those from observations, specifically from eddy covariance, is a challenge. In our manuscript, we use a scaling factor for the chamber data by considering chamber measurements that were done under exclusively wet and under exclusively dry summer conditions. We then make use of the total fraction of inundated areas in the model grid cell (IF) modeled with the TOPMODEL approach to scale the total chamber fluxes. This scaling approach takes into consideration that the model methane fluxes represent the emissions from only the portion of the grid cell that is inundated, i.e. with water at or above the soils surface.

20 In the case of the eddy covariance fluxes, following the concerns of the reviewer, we re-evaluated our approach for this comparison. In the revised version of this manuscript we include now a thorough analysis of the footprint area of the eddy covariance fluxes as part of a new Appendix A on “Details on in-situ flux observations”. This appendix also includes details on the eddy covariance flux data uncertainty assessment and more detailed results on the chamber measurements, as requested below also by the reviewer. This appendix is included at the end of the revised ms.

25 In this new appendix, we analyze the type of vegetation and its coverage in the footprint area of the EC tower, from remote sensing images as a metric to identify wet and dry areas. It has been recently shown in the literature that the type of vegetation in tundra landscapes is a good indicator of the spatial distribution and variation of CH<sub>4</sub> fluxes (Davidson et al., 2017) and it is also expected that the majority of the CH<sub>4</sub> fluxes are emitted from wetlands in tundra ecosystems (Helbig et al., 2017).

30 In the Chersky floodplain, areas with dominant cotton grasses, specifically *Eriophorum angustifolium*, are indicators of predominant wet soils, while tussocks, specifically *Carex appendiculata* in our study area, and shrubs are indicators of predominant dry soil conditions. It is important noting that *C. appendiculata*, can be also found in wet areas, but is predominant in dry areas.

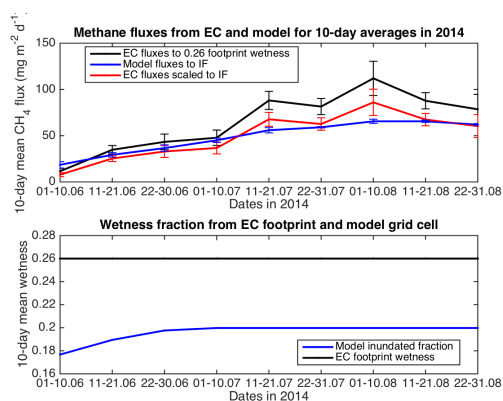
35 For the model, the vegetation distribution per grid cell is too coarse to consider this metric similar as that for the remote sensing data in the EC footprint area, however the total abundance of C3 grasses in the grid cell A is 33.3 % as given for the model (with the rest of the grid cell dominated by deciduous shrubs and extra tropical evergreen trees), but there is no discrimination between cotton grasses and tussocks.

40 The footprint of the eddy covariance tower in the Chersky floodplain covers an approximate area of 400 m x 400 m, similar to that one depicted in Fig. 1 of Kittler et al. 2016 (cited in discussion ms) (see new Appendix B at the end of this response for footprint area for the EC tower used in this manuscript). The remote sensing analysis revealed that cotton grasses are present in about 26 % of the footprint area, which would translate into the same portion of the footprint area as fully wet zones during the “wet months”: after spring melt in June and until August when most annual precipitation in the region takes place, covering most of the growing season. As will be shown below in this response, CH<sub>4</sub> fluxes measured by chambers (footprint of 60 cm x 60 cm) revealed that during the growing season in dry soil areas of the Chersky floodplain that are characterized by a water table below the surface, the emission of methane during the growing season is negligible with even some atm. CH<sub>4</sub> uptake by soil (i.e. negative CH<sub>4</sub> flux rates) (data shown in new Appendix A). Under this consideration, and as confirmed recently by Helbig et al., 2017, the majority of the CH<sub>4</sub> fluxes measured by the EC tower would represent fluxes from fraction of wetland in the footprint area, i.e. 26 %.

50 In case of the model grid cell where the location of the EC tower falls (grid cell A in Fig. 1 of the dis-

55 cussion ms), the IF for June-July-August during 2014 shows growing inundation values from 17.7 %  
to 19.9 % (for 10-day mean values for those three months) representing the percentage of total wet  
areas in the grid cell area. These values are slightly smaller than the 26 % wetness area in the EC  
footprint, and denote the area of the grid cell where the model methane emissions take place (i.e., no  
emissions in dry areas, in agreement to the chamber measurements).

60 With this basis and to make a closer comparison between EC flux measurements and model data for  
the growing season months, we scaled linearly the 10-day mean EC methane fluxes to the IF from the  
model, and calculated the standard deviation of the 10-day mean. In the next figure, we show: TOP  
panel, the original 10-day mean EC methane flux measurements that would represent the emissions of  
a 26 % wet area between June and August 2014 (black line), the 10-day mean EC methane fluxes  
65 scaled to the 10-day mean IF from the model for the same period of time (red line) and 10-day mean  
model methane emissions for grid cell A, which imply emissions from the IF from the model (blue  
line). Error bars in all lines are one standard deviation of the 10-day mean flux values. The BOTTOM  
panel shows the 10-day mean IF from the model used to scale the EC fluxes (blue line), and the constant  
70 wetness percentage of the footprint area calculated from the vegetation coverage remote sensing  
images (i.e., 26 %).



We observe that the scaled EC methane fluxes decreased as a lower IF is considered within the footprint, and those new calculated fluxes become closer to those from the model, and in most cases the latter fall within the 10-day standard deviation of the EC fluxes.

90 Unfortunately, it is not possible to obtain a temporal varying wetness area for the EC footprint all year, based on our approach of only considering the vegetation cover, thus wouldn't be appropriate to scale all of the EC fluxes for 2014 and 2015 to the IF from the model without any reference for spring and winter wet footprint areas. However, from this analysis we learn that: 1) considering the vegetation cover as indicator of soil wetness, the EC footprint area holds a very similar area to that of the model grid cell through which the majority of the methane is emitted to the atmosphere and 2) the net offsets between methane flux model and EC data can largely be attributed to differences in wetness levels.

95 Summarizing, we assume that for both the model grid cell and the eddy covariance footprint, methane emissions are not spatially homogeneous, but bound to the distribution of wet (inundated) areas. Accordingly, a meaningful agreement between model and observations can only be obtained if two factors are fulfilled: (i) the fraction of wet surfaces agrees between both data sets, and (ii) the flux rates from wet surfaces agree between both datasets. Through correcting the offsets in inundated fraction, we could demonstrate that the flux rates between model and eddy covariance observations agree very well, emphasizing the sound setup of the model algorithms and parameter settings. The analysis presented here is included into the new Appendix A to complement the discussion on scaling fluxes for comparison between EC and model data.

100

105

110 The authors should also address how representative the location of tower and chamber flux measurements is of the entire grid-cell. The authors estimate the fraction of inundated land for the grid-cell and demonstrate how this fraction is an important predictor for methane emissions. The same should apply for flux tower measurements where the fraction of wetlands is tightly coupled to the magnitude of methane emissions (see for example Helbig et al., 2017). How would the wetland fraction at the grid cell-scale compare to the same fraction at a smaller scale at the study sites?

115 We approached this comment with the answer above. By evaluating the vegetation cover types within the footprint area of the EC tower, we identified the wet areas and assume that the methane fluxes measured with this tower represent the emissions from the wetlands within the footprint. Equivalent to the grid cell area, the inundated fractions determined with the TOPMODEL approach, represent the areas where methane is emitted at grid cell scale. Those are comparable and to show this, a scaling exercise for growing season methane emissions in 2014 was presented above.

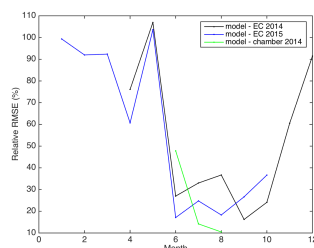
120 The authors report “comparable” (line 30) methane emissions when comparing model and measurements. The analysis could be much stronger if the authors give a quantitative measure for the performance (e.g. Root Mean Square Error or any other suitable metric).

125 As suggested by the reviewer, we include now in the revised ms the relative RMSE calculation in percentage (e.g.  $RMSE / \text{mean}(CH_4\_obs) * 100$ ) between model and flux measurements from Eddy Covariance (for 2014 and 2015) and chambers (only for the available three months in 2014). We calculated this error on a monthly basis, using the daily resolution fluxes. Results are shown in the table and figure below.

130

Month	Rel. RMSE (%) (model – EC) 2014	Rel. RMSE (%) (model – chambers) 2014	Rel. RMSE (%) (model – EC) 2015
Jan	-	-	99.3
Feb	-	-	91.9
Mar	-	-	92.4
Apr	76.1	-	60.7
May	106.9	-	103.6
Jun	26.9	47.8	17.1
Jul	33.0	14.2	24.7
Aug	36.7	10.5	18.3
Sep	16.2	-	26.6
Oct	24.1	-	36.6
Nov	60.5	-	-
Dec	91.4	-	-

135



140

145 The relative RMSE results show the relative variation between the model and the observations. A larger variation is observed in the first five and last month of the year (winter and spring) between model and measured EC fluxes, while the lowest variations are observed during the growing season and autumn (June to October). The summer variation is larger in 2014 between model and EC data and lowest in July and August between the model and chamber measurements in 2014. This information will be included in the revised ms to quantitatively support the evaluation of the model results.

150

The authors state that the aim of the work is to “improve our understanding”. However, in my opinion, the manuscript mainly focuses on improvements in methane modeling and an evaluation of the performance of a revised methane model. The authors may consider reframing their research objectives and focus results and discussion on the specific research questions.

155

The reviewer is correct that the stated aim is not reflecting the bottom line of our manuscript. Following this suggestion, we reframed the aim to be clearer and now it reads: “The aim of this work is to analyze the performance of an improved process-based methane model, designed for Arctic tundra and wetlands underlain by permafrost, when applied to a regional domain in Northeast Siberia. Our intention is to evaluate the potential of a refined process-based methane model as a proof of concept, for its application to a larger than site level scales. For this, year-round CH<sub>4</sub> emissions are modeled and differentiated among distinct pathways: plant-mediated, ebullition, and diffusion.” We also focus the discussion towards this aim in the revised ms.

160

165

Large areas in northern Siberia are covered by polygonal tundra. The distinct microtopography of these landscapes has important implications for surface hydrology and thus also surface inundation (see Cresto-Aleina et al., 2013; Helbig et al., 2013; Liljedahl et al., 2016). I was wondering if such polygonal tundra covers a significant proportion of the study area?

170

And if yes, what would be the consequences of distinct microtopography on the performance of the TOPMODEL and on the simulated methane emissions. Using a mean water table for methane modeling in such heterogeneous landscapes can lead to significant underestimation of methane emissions (Cresto-Aleina et al., 2016).

175

The reviewer is right that a good portion of the Siberian tundra is characterized as polygonal tundra. However, our area of study does not contain these particular micro-topographic structures since it is mostly located in a floodplain that naturally becomes inundated at the end of the melt season (spring). Towards summer, most of the water recedes to streams and to the Kolyma River and nearby tributaries only to lead to a typical wetland landscape. Still, some polygonal structures are present, but they are not a dominant feature of the landscape within our model domain, as opposed to e.g. the Lena River delta. Therefore, the application of TOPMODEL in the Chersky floodplain is suitable and there is no need to consider polygonal structures.

180

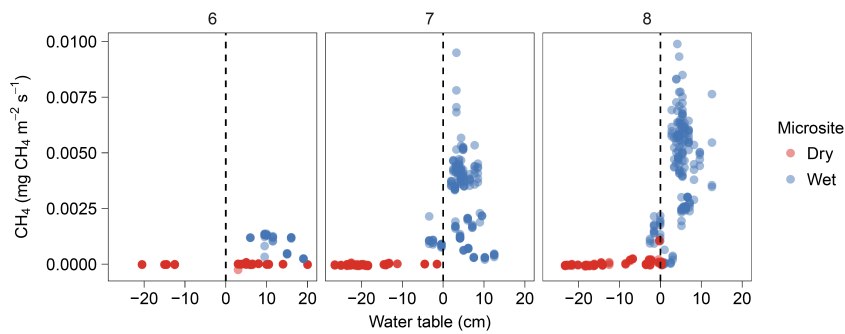
With the TOPMODEL approach, the authors can distinguish between inundated and non-inundated land. However, many peatlands are characterized by a water table just below the peat surface and are thus not inundated. Nevertheless, they can emit large amounts of methane, which would be neglected in the current modeling approach.

185

We are aware of the limitations on the use of TOPMODEL in those particular cases where the water table is located below the surface and those were discussed briefly in the discussion manuscript. The study of Kwon et al. (2016) (cited in the discussion ms) reported the flux chamber measurements in the same Chersky floodplain site subject to our study. The authors reported CH<sub>4</sub> fluxes measured in plots where the water table was 10 cm below the surface and found negligible contribution of CH<sub>4</sub> from these soils. Specifically, areas with water table 5 cm below the surface showed net CH<sub>4</sub> emissions but flux rates were not as high as in areas with standing water (see figure below). Also, as shown in the new Appendix A at the end of the revised ms, chamber flux measurements of CH<sub>4</sub> in dry soils with water tables ca. 10 cm below the surface show none or negligible methane emissions to the atmosphere in this area of study. Taking into account these findings, in our model configuration the fact that no methane emissions take place in dry soils, would not pose a constraint to the total modeled methane fluxes per grid cell in this area of study, however, the role of methane oxidation could be better evaluated.

190

195



200

The figure above shows results of CH<sub>4</sub> chamber fluxes (mg CH<sub>4</sub> m<sup>-2</sup> s<sup>-1</sup>) measured from June to August (numbers at the top of the figure indicate the month of the year: 6 is June, 7 is July and 8 is August) in 2014 for the dry and wet plots and their corresponding water table (in x-axis). “Dry” plots have mostly water tables at or below the surface during July and August with mostly uptake of CH<sub>4</sub> from the atmosphere (on average 3 mg CH<sub>4</sub> m<sup>-2</sup> d<sup>-1</sup>), whereas the wet plots characterized by water tables located above the surface, showed average emissions of 332 mg CH<sub>4</sub> m<sup>-2</sup> d<sup>-1</sup> over the same period of time.

205

Despite this agreement, we are aware that the low CH<sub>4</sub> uptake in dry areas might not apply to other tundra areas, e.g. in Zona et al., (2016) in the Alaskan tundra the highest fall and winter CH<sub>4</sub> fluxes were observed in upland tundra sites characterized by having a water table below the surface during summer. In future studies, our model scheme should also be tested in other areas such the Alaskan tundra to assess and improve further the model configuration especially in the TOPMODEL scheme.

210

215 At the same time, lakes (i.e., inundated land) may be characterized by lower methane emissions than these peatlands due to a lack of fresh organic carbon input. What are the implications of this for the modeling performance? The authors may consider discussing this shortcoming.

This is an interesting idea and we agree with the reviewer that a comparison of lake and peatland model results would be an ideal evaluation of our methane scheme using extreme cases of water table depth. However, we do not see the possibility to perform such study, as explained below.

220

In our model configuration, the production of methane is considered to take place in mineral soils and does not include peatlands as definition: the layer of soil with > 30 cm of organic rich material (peat) accumulation. A mask containing the distribution of peatlands should be needed to introduce this feature. In addition, as carbon decomposition slows down in permanently anoxic areas of the soil column, the prescribed mask of peatlands should contain added soil C in order to describe deep peat layers characterized by a slow decomposition timescale. These steps are currently been taken for the global context with the JSBACH model and are still pending work for high horizontal-resolution domains such as the regional one presented in this work.

225

The scheme to model wetland areas using the TOPMODEL approach considers the topographic profile, which is provided as a prescribed compound topographic index in the model domain, and methane emissions take place in areas where the water table is located at or above the soil surface. In this context, the model does not explicitly simulate the location of “lakes” (inland open water bodies) but rather a dynamic change in the horizontal distribution and accumulation of water at or above the surface, which in turn may consider implicitly inland water bodies at different scales: lakes, wetlands, ponds, etc. With this model, it is not possible to discriminate at this coarse resolution, the type of water bodies, but rather it provides an average portion of the grid cell area where inundation can take place, and only the methane production and ultimately emissions, are linked to the carbon content and environmental conditions of the soil. If by definition there is no consideration of peatlands in our model, in the end all goes down to the available organic carbon in the soil for the production of methane. As requested by the reviewer, we discuss this shortcoming in the revised manuscript.

230

235

240

In the current manuscript, the authors “decreased or increased [the parameters] by a fixed value” (line 343). Could the authors use a Monte-Carlo approach instead to assess the parameter sensitivity?

245 The purpose of the parameter permutation is to know, to which parameter the model is most sensitive, as this identifies which parameter need to be better constrained to reduce model uncertainty. The purpose of a Monte-Carlo approach is the identification of the uncertainty of a model given a known probability distribution function of parameter values for a combination of parameters. MC approaches are not primarily designed to identify model sensitivities to specific parameters, even though some approaches such as LHS allow interpreting MC approaches in terms of model sensitivities; however only at very high computational costs. One-at-a-time schemes (OAT) as the one applied here directly target the model sensitivity, are computational cost efficient, and are deemed fully sufficient for the purpose (Saltelli et al. 2000). The identification of compensating effects between parameters or non-linear effects, which would require an MC approach area, is beyond the scope of this paper. We therefore consider an MC approach to assessing model sensitivity as unnecessary.

The authors mention “reported values in the literature”. Could they specifically discuss/show the observational constraints on the individual parameters?

260 We thank the reviewer for this comment. We improved the description of our selection of parameters for the sensitivity study in the revised ms, especially those that are obtained from observational constraints. The selected parameters are those that are prescribed in the model and are considered uncertain. Specifically, the selected values for  $\phi$  (snow porosity) and  $f_{CH4anox}$  (fraction of anoxic decomposed carbon that becomes methane) were those kept within ranges of values previously discussed in the published literature, whereas for the other four selected parameters (see below) we chose a range of values around the defined values for the control simulation.

265 Thus, the selected parameters are characterized by at least one of the two criteria: 1) it is a parameter with large uncertainty because it is not provided in current published literature or its values are still controversial as reported in published literature, and 2) it is possible to test a range of values based on reported values in literature. The last criterion is only true for two of the selected parameters ( $\phi$  and  $f_{CH4anox}$ ) as mentioned above. As given in the discussion ms, the six selected parameters for our sensitivity studies are:

In the TOPMODEL scheme:

- 1)  $\chi_{min\_cti}$ , minimum compound topographic index threshold value. This parameter fulfills criterion 1 since it is a model parameter that is exclusively part of the TOPMODEL scheme, therefore there is no literature reference and rather is a given value that has to be adjusted.

275 In the plant-mediated transport scheme:

- 2)  $d_r$ , root diameter. This is a highly uncertain value in literature with only few reported values. Few studies have reported the diameter of vascular plants in boreal ecosystems. In Wania et al., 2010 (cited in discussion ms and after Schimmel, 1995) the authors report a diameter for *Eriophorum angustifolium* of 3.95 mm, while for *Carex aquatilis* a value of 3.8 mm. Chapin and Slack (1979) reported a diameter for *Eriophorum vaginatum* of 0.8 mm, while Wang et al., 2016 reported a value of 1 mm for the same species. For our model set up, we use a value of 2 mm in the control run considering an average value between those reported in the literature. For the sensitivity study, we selected higher root diameters experiments: 5 and 8 mm.
- 3)  $R_{fr}$ , principal fraction of the pore-free soil volume occupied by roots. This is also a highly uncertain value that is not reported in literature; therefore, we assume in our control experiment a fraction of 40 % (i.e., in a certain volume of soil, 40 % is occupied by plants roots). For the sensitivity studies, we decreased and increased this reference value by 50 % of the control value, i.e., 20 % and 60 % respectively.

290 In the diffusion of gas through snow:

- 4)  $h_{snow}$ , snow depth threshold. The studies of Pirk et al., (2016) and Smagin and Shnyrev (2015) (both cited in the discussion ms) measured  $CH_4$  emissions through snowpacks under different conditions. These studies evidence the transport of gas through snow layers as thick as 1.4 m. However, regarding the thinner snowpack the authors only show results from layers 10 cm thin. For our purpose, the lower limit of snow thickness is simply a model metric that allows us to differentiate between emissions in the presence or absence of snow. We selected thinner snow layers to test the model response, and the changes on this threshold thus mainly deter-

mine the timing of the emissions, which ultimately influences the magnitude of the total emissions through snow by allowing an earlier or later release of gas trapped in the soil.

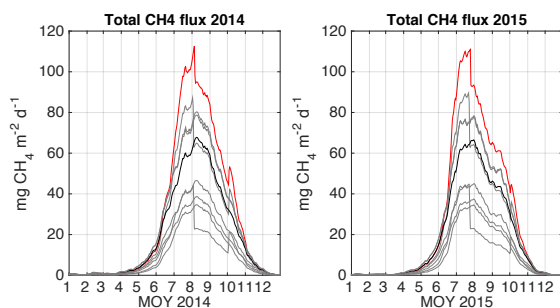
300 5)  $\phi$ , snow porosity. This parameter has been previously reported in literature and is derived from snow density measurements, which ultimately controls the amount of gas that can be diffused through the snow layer. This was discussed in the ms. Based on observations, Pirk et al., (2016) measured methane emissions through snow with densities that ranged between ca. 250 kg m<sup>-3</sup> (at the surface of the snowpack) to 420 kg m<sup>-3</sup> (at about 80 cm depth of the 1.4 m snowpack). According to our model results, the snow depths in the model domain did not exceed 30 cm during the peak of the snow accumulation (shown in Figure S4c of the discussion ms), thus is unlikely to find dense snowpacks. We chose a maximum density of 330 kg m<sup>-3</sup> that corresponds to a porosity of 0.64 as our control value and tested for the sensitivity experiments less dense snowpacks with increasing porosities of 0.71 (for a density of 263 kg m<sup>-3</sup> characteristic of aged snow) and 0.86 (for a density of 128 kg m<sup>-3</sup> for fresh snow).

310 In the overall methane module:

315 6)  $f_{\text{CH4anox}}$  or the fraction of anoxic decomposed carbon that becomes methane. This is a highly uncertain parameter in literature with some reported values in literature. In the discussion ms, we thoroughly discussed it (Lines 882 to 914), therefore we refrain to include here this discussion. However, we summarize by arguing that despite there are some values reported in literature, these are still uncertain and in our sensitivity tests we chose those values that have been reported and are characteristic of specific field conditions.

320 Line 406-408: Why do the authors only show one adjacent cell? What is the justification to compare a neighboring grid cell to the ground-based observations? To demonstrate the spatial heterogeneity the authors could consider using more than just two grid cells.

325 Thank you for this suggestion. Our intention to show a neighboring grid cell was to demonstrate the spatial heterogeneity in the model results. Showing other grid cells in the model domain indeed can complement this. We believe that the maps showing spatial variability in flux rates provide already a good overview on the overall spatial variability. This larger scale variability is a superposition of many environmental factors, the most important of these being inundation fraction and coverage fraction of C3 grasses. The closer analysis for these two cells that the reviewer refers to was mainly performed to emphasize that even moderate variations in these factors (and others, such as e.g. soil depth) can lead to systematic differences in simulated fluxes. As we see it, extending this kind of analysis also to other cells would not add to this message, but rather confuse the reader by providing too much information. We suggest, however, to extend the discussion related to the spatial heterogeneity in the modeled methane emissions by showing results of mean total methane fluxes in the eight grid cells surrounding grid cell A.



The figure on the left (now Fig. S8 in rev. MS) shows the time series of the total CH<sub>4</sub> fluxes at daily resolution for the eight grid cells surrounding grid cell A (shown in black). One of those surrounding grid cells is grid cell B (red line).

350 In the tables below, the mean±std. of the total methane fluxes during summer (June, July and August) from grid cell A (given as values in black at the center cell of each table), and the surrounding eight grid cells for 2014 (left table) and 2015 (right table). Left side grid cell

from the center cell, corresponds to the values for grid cell B (values in red).

June, July and August in 2014			June, July and August in 2015		
25.4 ± -7.1	56.0 ± -12.1	23.7 ± -3.7	25.2 ± -8.3	56.9 ± -14.7	24.9 ± -4.8
72.8 ± -15.9	48.6 ± -5.5	27.8 ± -4.0	75.5 ± -18.3	50.1 ± -7.3	28.2 ± -4.8
57.2 ± -6.8	57.9 ± -6.9	33.4 ± -4.7	59.2 ± -8.7	59.5 ± -10.4	34.3 ± -5.7

355

In line 464-465, the authors mention the “parameter adjustment”, but do not elaborate how exactly the parameter for the TOPMODEL was adjusted. Did the authors use an objective (cost) function to optimize this parameter?

360

There was no optimization of these parameters based on a cost function. The parameter adjustment for the TOPMODEL was also done in the same fashion as for the sensitivity studies: by varying each of the parameters of the TOPMODEL and analyzing the response by comparing the output to the chosen remote sensing data. This model parameter adjustment can only be done in this way within the current model structure. A more sophisticated optimization of parameters falls into a model data assimilation type, which is not implemented in this model configuration and goes beyond the scope of this work.

365

The authors demonstrate in their sensitivity analysis that the threshold TOPMODEL parameter and “allocation-of-decomposition-to-CH<sub>4</sub>” are the most important parameters determining the magnitude of simulated methane emissions. In my opinion, the authors should strengthen these results throughout the manuscript. It appears as if their results indicate that methane emissions mainly depend on methane production dynamics (i.e., fCH<sub>4</sub>anox) and on inundation as “on-off” switch of methane emissions.

370

The threshold TOPMODEL parameter and the allocation of C decomposition to methane are the parameters that, under the current model configuration, settings and for the selected groups of parameters for sensitivity tests, the most influential to the simulated methane emissions. This test was aimed to identify which of the most selected uncertain parameters have the highest influence to the results and with that, identify where the model is more sensitive and where it needs further improvements and evaluations, i.e. especially in those processes where the most influential parameters play a role in the model as in this case in the hydrology and carbon decomposition.

375

The methane emissions in our process-based model, not only depend on the methane that is produced based on the available carbon decomposed in the soil, but also depend on the available volumetric soil pore space, moisture, soil temperature and ice content in the soil as driving processes. Indeed, once methane is available in the soil to be emitted to the atmosphere, the inundated areas simulated with the TOPMODEL approach, determine the magnitude of the emissions. Our discussion regarding the sensitivity studies is based solely on the parameters chosen for the sensitivity experiments, and those are the threshold parameters in TOPMODEL and the fraction of available carbon to be decomposed into methane. We will improve this discussion to emphasize this result in this section.

380

385

Transport pathways and methane oxidation appear to be less important (merely changing the timing of emissions). Are these modelling results supported by observations in the field? The authors may consider discussing this in more detail.

390

The methane transport pathways are the result of the process-based methane calculations in the model according to, among others, the changes methane and oxygen concentrations in the soil and in the soil pore space that varies in relation to the freezing and thawing soil cycles, influencing directly the methane concentration in the soil.

395

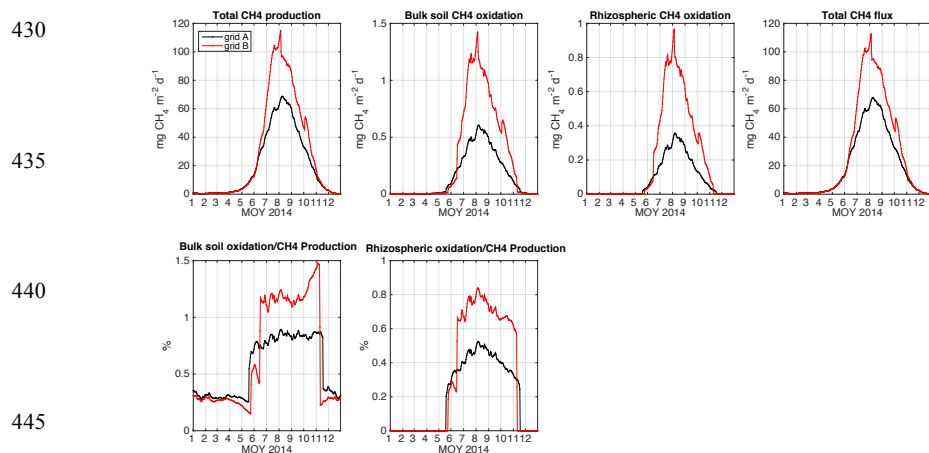
The timing of the emissions is linked to the changes mostly in the soil physical state and speed of transport processes by their definition, e.g. diffusion of gas in air is faster than in water, resistance to molecular gas diffusion through the exodermis of plants, all in a process-based design. The model still lacks of a proper hydrology representation that allows inundation without having to set the soil moisture to saturated conditions, and that overall has an impact in the e.g. diffusion and oxidation of the methane. In the parts of the grid cell that are not water saturated because inundation cannot take place, the methane processes are not taken into account. Thus, the still not well-represented methane processes are not less important, but are only part of the limitations of the current model configuration

400

and these results hint to the next steps to improve the model.

405 As presented in the discussion manuscript, some field studies have conducted experiments to measure independently the different pathways of methane emissions into the atmosphere. Through isotopic quantification of  $\delta^{13}\text{C}$ , Knoblauch et al., 2016 (cited in discussion ms) measured the amount of methane emitted through plants; Kwon et al., 2016 using chambers in the Chersky floodplain, also measured the gas emitted through plants. These studies were discussed in the discussion manuscript, and we demonstrated that, in agreement to field studies, the most dominant methane transport pathway from the total annual emissions (ca. 70 – 90 %), is through vascular plants when they are present. In the case of ebullition, this is a more difficult process to measure in field studies, because of its episodic nature. Despite some studies have attempted to measure methane emitted exclusively through ebullition (Tokida et al., 2007; Jammot et al., 2015 both cited in discussion ms), for models it is difficult to evaluate this process against observations.

415 In the case of methane oxidation, in our model configuration the oxygen content is explicitly taken into account, enabling two process-based oxidation processes: bulk soil methane oxidation and rhizospheric methane oxidation. After methane is produced in the soil (from available decomposed carbon), the bulk soil methane oxidation can take place considering the available oxygen in the soil pore spaces. The other oxidation pathway considers the available oxygen in plants. Only part of the oxygen in the soil is available for methane oxidation, and this discrimination relates to the amount of carbon dioxide produced during heterotrophic respiration, which has a maximum value of 40 % of the total oxygen content in the soil. An additional 10 % of the available oxygen is assumed to be unavailable because it is used in other processes (e.g. respiration by microbes). This leads to only 50 % of the total oxygen in the soil to be available for  $\text{CH}_4$  oxidation. The methane processes in the model (oxidation and emission) take place in the inundated area, and this also restricts the magnitude of the oxidation. The daily methane oxidation rates for the two oxidation pathways for grid cells A and B in 2014 are shown in the figure below.



450 The bulk soil  $\text{CH}_4$  oxidation accounts for about 1 % of the total methane production during the growing season for grid cell A and B, and an even smaller percentage (average 0.6 % for grid cell A and B during summer) for the rhizospheric  $\text{CH}_4$  oxidation. These leads to most of the methane that is produced to be emitted to the atmosphere through the different transport pathways. Past observational and laboratory studies have estimated the methane oxidation in boreal and tundra soils. Whalen and Reeburgh (2000) showed that about 55 % of the  $\text{CH}_4$  diffusing from the saturated boreal soils, were oxidized while reaching the surface. Through bottle incubations, Knoblauch et al. (2016) measured the volumetric  $\text{CH}_4$  oxidation potential of soil and moss samples collected from ponds of the Lena Delta. The fraction of produced  $\text{CH}_4$  that is oxidized before it is emitted was then calculated following three different approaches. Their results show a mean fraction of produced  $\text{CH}_4$  that was oxidized be-

460 tween 61 to 78 % estimated from a stable isotope approach, while slightly different values were found  
in samples from pond areas without vascular plants: up to 90 % of the CH<sub>4</sub> that was produced, was  
completely oxidized following a potential methanogenesis approach, and between 63 % to 94 % cal-  
culated from diffusive CH<sub>4</sub> fluxes into the bottom water.

465 Berestovskaya et al. (2005), measured CH<sub>4</sub> oxidation rates of different soil samples from the Russian  
Arctic tundra and found that generally the rates of methane oxidation exceeded those to the rates of  
methane production especially at temperatures of 5 degC. For this to happen, methane-oxidizing bac-  
teria rapidly consumes the methane released from the freshly thawed tundra soils and the methane  
already deposited in the unfrozen soil, and this takes place even before methanogens produce new  
methane.

470 Based on these scarce observations in boreal soils, the oxidation processes in our model are still ro-  
bust and need to be revisited in order to improve the contribution of the methane oxidation processes  
into the total methane emissions. We discuss this in more detail in the revised ms.

475 It is important noting that the process-based model presented in this manuscript explicitly considers  
physical drivers such as soil moisture, inundated area, soil temperature and substrate availability for  
methane production and emissions, and is potentially one of the few models that include explicitly  
methane oxidation processes. However, despite our efforts of improving the process-based representa-  
tion, intrinsic model shortcomings are still present, and those are related to setting a fixed criterion in  
the soil moisture to allow the accumulation of water above the surface, which leads to a loss in the  
connection to the soil temperature. This has been clearly stated in our manuscript. As such, a one-to-  
one comparison between the model results and observations can be hardly expected. Still, we demon-  
strated advances in the process-model based approach which lead to methane emissions results that  
480 are comparable in temporal variation in magnitude to those measured on site.

Line 61-62: Perhaps the authors could mention another important permafrost thaw effect on methane  
emissions here: increasing surface wetness due to surface subsidence of ice-rich soils (see for example  
Christensen et al., 2004; Johnston et al., 2014, Helbig et al., 2017).

485 OK, we mention now this process in the revised manuscript. Thanks for this suggestion.

Line 94-100: Wintertime methane emissions have also been reported by Helbig et al. (2017) for a bo-  
real peat landscape in northwestern Canada, where they found winter emissions to contribute about 25  
% to the annual budget.

490 Thank you for adding this citation that we overlooked because by the time our manuscript was sub-  
mitted, this paper was still not published, but now it will be added.

Line 121: Could the authors discuss here the most important “shortcomings in the parameterization”  
of the state-of-the-art methane models?

495 The biggest limitations for modeling methane emissions in boreal regions are related to the complex  
network of processes with highly variable influences that are difficult to disentangle with temporally  
and spatially scarce field measurements. The available published literature is also scarce and focused  
only on fine scale site-level studies or at very coarse global scale. Several models that attempt to sim-  
ulate methane emissions from soils are rather coarse and not well documented or evaluated, which  
leads the process-based principle remaining rather incomplete. These shortcomings are well docu-  
mented in the cited paper of Xu et al., 2016. According to the methane models intercomparison exer-  
cise WETCHIMP (Bohn et al., 2015; cited in the discussion manuscript) the authors conclude that  
process-based methane models are limited by the following factors: availability of a valid and highly  
resolved wetland map, account for methane emissions and uptake in dry non-wetland areas, limited  
soil thermal physics that do not contain freeze and thaw processes, lack of a snow scheme and conse-  
quently, gas transport in the presence of snow cover, lack of peat soils.

500 From our work presented in this manuscript and our model development efforts in this topic, we have  
taken into account some of this shortcomings and improved our model tool, however still limitations  
exist. We still conclude that in boreal regions influenced by permafrost, process-based modeling for  
methane emissions is challenged by the lack of the observational measurements that can contribute  
510 e.g. to understand better the dynamics of soil moisture and temperature, wetlands distribution, as well  
as the distribution and temporal variation of roots in vascular plants. Additionally, the land surface  
models that serve as framework have intrinsic limitations in their design, e.g. in the case of JSBACH,

515 the hydrology scheme does not allow the accumulation or horizontal redistribution of water and other  
tools such as TOPMODEL had to be implemented. Still after the inclusion of the TOPMODEL ap-  
proach, the final methane emissions are restricted exclusively to the areas where standing water takes  
place, leaving out the dry areas to come into play, and TOPMODEL does not feedback the soil ther-  
mal physics. Finally, the carbon decomposition scheme in our JSBACH model version is only de-  
pendent on 15-day mean of air temperature and precipitation, which leads to an absence of permafrost  
carbon in this model version.

520 This piece of discussion is completed in the revised ms to clarify better out statement of L121.

Line 133: Perhaps the work by Cresto-Aleina et al. (2013, 2016) on microtopography effects on sur-  
face water and methane emission dynamics could be mentioned here too.

525 OK, we will add this citation and process as suggested.

Line 500-501: Only mineral soils are considered for the methane modelling? How common are organ-  
ic soil in the study area? I would assume that at least top-soils in the floodplain would be organic-rich.  
How would “considering” organic soils change the results?

530 The lacking representation of organic soils is a shortcoming JSBACH has in common with many oth-  
er land surface models. The authors are only aware of two peatland-enabled versions of the LPJ  
(Lund-Potsdam-Jena) model in the published literature. In addition, a small number of further model-  
ling studies have been published, where organic layers were considered, though mainly for their ther-  
mal properties (e.g. Ekici et al., 2014, cited in discussion ms). This lacking representation is mainly  
due to the difficulties of coupling sub-gridscale hydrology and carbon cycle in a holistic way. The  
535 reviewer is right that organic soils are common in the study area. From measurements in the Chersky  
floodplain reported in Kwon et al., 2016, the soil layer has a top organic peat layer about 15-25 cm  
thick on top of alluvial material composed of silty clay. In the model configuration, only mineral soils  
are considered and indeed the organic carbon pools might be depressed in contrast to the organic car-  
bon in a peat layer. This was discussed earlier above in this response.

540 Line 577-579: The authors may consider supporting this statement with information on  
the exact magnitude of interannual variability.

545 We calculated the magnitude of the interannual variability of the fluxes from eddy covariance and the  
model by comparing the standard deviation of the monthly values from 2014 to those in 2015. We  
summarize these results in the new Fig. 6 of the revised ms.

550 The statement in the discussion ms is now supported by showing that largest interannual variability in  
the model grid cell A takes place in May and July with 7.9 and 5.5 mg CH<sub>4</sub> m<sup>-2</sup> d<sup>-1</sup> when compared  
the standard deviations from the monthly fluxes between 2014 and 2015, while for grid cell B, the  
largest variability between the two years took place in June and July (10.9 and 5.6 mg CH<sub>4</sub> m<sup>-2</sup> d<sup>-1</sup>,  
respectively). Still, the largest interannual variability was observed in June for the Eddy covariance  
data with 12.6 mg CH<sub>4</sub> m<sup>-2</sup> d<sup>-1</sup> difference in their monthly standard deviation between both years.

Line 589-592: What is the uncertainty in the eddy covariance flux measurements?

555 Could the authors quantify uncertainties due to random errors, gap-filling, u\*-threshold, and footprint  
heterogeneity? An uncertainty quantification of eddy covariance fluxes would further strengthen the  
model-observation comparison.

The uncertainty analysis for the eddy-covariance flux data consists of random and systematic errors  
and is assessed based on well-established concepts (Aubinet et al., 2012).

560 Random errors linked to the turbulent sampling error and instrument error are given as standard out-  
put of the flux processing software TK3 (Mauder and Foken, 2015) for each 30 min flux value. Foot-  
print uncertainties are not quantified, since there are no major transitions in biome types within the  
core areas of the flux footprints. Random errors are combined and considered as independent varia-  
bles.

565 Systematic errors can occur due to unmet assumptions and methodological challenges, instrument  
calibration and data processing. Instruments are calibrated in regular intervals, and in comparison to a  
second eddy-covariance tower close by (~ 600 m) no systematic offset in the frequency distributions  
of wind speed, sonic temperature, and methane mixing ratios between towers was observed. The

570 standardized software TK3 (Mauder and Foken, 2015) contains all the required processing steps for  
the flux data processing, as well as conversions and corrections, and yielded good agreement in a re-  
cent comparison with EddyPro (Fratini and Mauder, 2014). The post-processing quality control and  
flagging system scheme was based on stationarity and a well-developed turbulence scheme proposed  
by Foken and Wichura (1996) followed by additional tests applied to flag implausible data points in  
the resulting flux time series. Data coverage of methane fluxes was 86 % during the growing season  
and 67 % during the winter (Kittler et al., 2017).

575 The gap-filling method is based on a moving window that is centered in the gap and a 10-day window  
length, i.e. 5 days before and 5 days after the gap. The uncertainties were quantified as standard de-  
viation for the corresponding window, similar to the gap-filling uncertainties for the CO<sub>2</sub> flux via the  
MDS routine (Reichstein et al., 2005).

580 No u\*-threshold was applied to the flux dataset, since we determined the stationarity of the signal and  
integral turbulence characteristics also for nighttime conditions. This information facilitates identify-  
ing datasets with regular turbulent exchange also during stable stratification, therefore producing few-  
er gaps compared to a bulk exclusion of data during stable nighttime stratification through the u\*-  
filter method. Random errors decrease with averaging and were calculated according to Rannik et al.  
(2016).

585 Averaged over both years (2014 and 2015) the CH<sub>4</sub> flux uncertainty based on 30 min data is 5.1±8.8  
nmol m<sup>-2</sup> s<sup>-1</sup> (7±12.1 mg CH<sub>4</sub> m<sup>-2</sup> d<sup>-1</sup>). This result is not considering gap-filling techniques to the  
quality-checked signal (bulk uncertainty). The mean value considering also gap-filling is: 7.4±8.3  
nmol m<sup>-2</sup> s<sup>-1</sup> (10.2±11.5 mg CH<sub>4</sub> m<sup>-2</sup> d<sup>-1</sup>).

590 For a fen ecosystem, it has been reported an uncertainty of 4.7±3.8 nmol m<sup>-2</sup> s<sup>-1</sup>. This result considers  
quality-checked data without applying a gap-filling technique (Jammot et al., 2017).

595 After considering monthly averaging of the gap-filling and with a quality checked signal, the uncer-  
tainties of the CH<sub>4</sub> fluxes measured from EC for 2014 and 2015 are reduced to 0.35±0.22 mg CH<sub>4</sub> m<sup>-2</sup>  
d<sup>-1</sup>. Monthly uncertainty values are now added in Fig. 5c of the revised ms as error bars of the mean  
monthly values. Details on data uncertainty assessment as outlined above, are now provided in a new  
Appendix A on “Details on in-situ flux observations”. References cited in this section are listed at the  
end of this response.

Line 691-711: I am not sure how this section contributes to the research questions of this manuscript?  
Perhaps the authors could mention differences in environmental characteristics of grid-cell A and B  
600 briefly in the manuscript and move figure 9 to the supplementary material?

We will shorten this section and instead merge it with the discussion of methane fluxes, in this way  
we could move figure 9 to the supplementary material. This suggestion certainly will make the manu-  
script more focused on the main aim. Thanks for this suggestion.

605 Line 808-810: The impact of cooler early summer temperatures on soil warming and methane emis-  
sions has been demonstrated recently using multi-year methane observations in a boreal peat land-  
scape (see Helbig et al., in press). The authors may consider discussing their modelling results in rela-  
tion to these observations.

610 We thank the reviewer for making us aware of this new publication. We add it in the revised ms and  
cite it accordingly. Helbig et al., 2017 shows that between years 2013 and 2016, during May of each  
year the one in 2014 was colder compared to the other years. This finding was based on a meteorolog-  
ical record of an area in northwestern Canada. As a result of temperature shifts, soil temperatures varied  
and influenced the year-to-year methane fluxes, specially variations in spring soil temperature  
were influential. The findings of Helbig et al. are in good agreement with our model observations re-  
615 garding the interannual variability in air and soil temperature and their influence in methane emis-  
sions. We will complete our model results with this nice comparison.

Line 847-851: The authors may consider starting the discussion mentioning the parameters that actu-  
ally made a difference and not with the parameters that did not change the results. It should be high-  
620 lighted what process/parameter matters in the model.

Thank you for this suggestion. We will re-structure the discussion based on this suggestion.

Line 991-992: Few studies have shown that non-inundated upland areas may take up methane (e.g.,

625 Flessa et al., 2008). As far as I understand, such uptake is not considered in the current work. How  
could uptake in the drier areas of the model domain change simulation results? There are large areas  
in the model domain that appear to be characterized by upland landscapes and thus potential methane  
uptake (see Fig. 1).

630 Indeed atmospheric CH<sub>4</sub> uptake should not be neglected when considering a regional CH<sub>4</sub> budget,  
especially when the majority of areas are predominantly aerobic. With plot-based observations in dry  
areas of the Chersky floodplain, the CH<sub>4</sub> emissions were negative, indicating uptake (average of -3  
635 mg CH<sub>4</sub> m<sup>-2</sup> d<sup>-1</sup> during summer of 2014) and this value was considerably smaller compared to that of  
the CH<sub>4</sub> emissions measured in wet plots (on average 332 mg CH<sub>4</sub> m<sup>-2</sup> d<sup>-1</sup> in summer 2014) (see re-  
sponse above for figure of results). Based on this result and the consideration of an inundated fraction  
of 20 % during summer in the model grid cell A (Fig. 9d in discussion manuscript), about 66.4 mg  
CH<sub>4</sub> m<sup>-2</sup> d<sup>-1</sup> (in wet plots: 332 mg CH<sub>4</sub> m<sup>-2</sup> d<sup>-1</sup> \* 0.2 = 66.4 mg CH<sub>4</sub> m<sup>-2</sup> d<sup>-1</sup>) are emitted and 2.4 mg  
640 CH<sub>4</sub> m<sup>-2</sup> d<sup>-1</sup> are loss by uptake (oxidized) (given by the dry plots results: -3 mg CH<sub>4</sub> m<sup>-2</sup> d<sup>-1</sup> \* 0.8 = -  
2.4 mg CH<sub>4</sub> m<sup>-2</sup> d<sup>-1</sup> equivalent to 8.7 % of the total methane emissions), leading to the net CH<sub>4</sub> emis-  
sion of 64 mg CH<sub>4</sub> m<sup>-2</sup> d<sup>-1</sup> according to chamber measurements. The mean CH<sub>4</sub> emission in grid cell A  
during June-July-August 2014 (Fig. 5a of discussion manuscript) is 48.6 mg CH<sub>4</sub> m<sup>-2</sup> d<sup>-1</sup> in the inun-  
dated areas. The mean methane soil and plant oxidation for the same period of time, given by the  
645 model for grid cell A, is 0.63 mg CH<sub>4</sub> m<sup>-2</sup> d<sup>-1</sup> (0.3 % of the total emission) which is low compared to  
the uptake estimation for the chamber measurements in dry areas. However, these are only represent-  
ing oxidation processes in saturated soils, which are not predominant in contrast to dry soils. As men-  
tioned before, by not considering non-inundated areas in the modeling of methane processes, the me-  
thane uptake is ultimately underestimated because the conditions for methane oxidation are limited.

650 Line 1134-1141: The authors may consider not to introduce a new concept (e.g., anaerobic microsites)  
at the very end of the conclusions. I would recommend to only refer here to what has been shown in  
the manuscript so far.  
OK, we improve this section in the revised manuscript.

655 Line 1252-1255: What would happen if the model would run with the old order of processes?  
Shouldn't this be part of the uncertainty analysis?

660 The old order of processes was presented in the paper by Kaiser et al., 2017; there, it was shown that  
the order of processes was selected based on the velocity that they physically can exhibit, with ebulli-  
tion first and the slowest transport at last which was plant mediated transport due to the resistance of  
the plants exodermis. Observational evidences however, as discussed here and in the manuscript,  
show that in the presence of vascular plants, wetland annual methane emissions are mainly from the  
transport of gas through plants. Due to the structure of the model, it is not possible to run parallel pro-  
cesses and instead, a sequential flow of processes has to be computed. For this reason, the solution to  
improve the individual share of the transport processes was to re-arrange the processes by expected  
665 priority. We do not think this should be part of the sensitivity studies for this manuscript since this is a  
purely computational design and not due to the inherent processes in the model.

670 Fig. 1: Why did the authors use such a large study area, if ground-based observations were only avail-  
able for a very small fraction of the model domain? How can the model performance be evaluated for  
the other non-floodplain grid cells that appear to be characterized by different landscape characteris-  
tics?

We agree with the reviewer that a smaller study area could have been shown, especially for the area  
near the grid cell where ground-based observations take place.

675 Plot level model simulation have been performed in the past, particularly with a similar version of the  
model presented in this manuscript for a site in Samoylov (Kaiser et al., 2017). Model development  
for methane emissions has not only focused on the improvement in the mechanisms represented in the  
model for the production and transport of methane, but also in the scaling with the intention of under-

standing better the contribution of CH<sub>4</sub> processes over larger spatial scales. Regional scales still pose a challenge but certainly models need to be aimed to be applied to larger scales rather than only plot level. After a plot level application, we improved the description of some processes in the model and aim to test it in a rather larger, but still, regional spatial scale.

Thus, the intention of selecting a larger regional domain is two-fold: 1) to test and apply the process-based methane model in a larger than site-level domain and 2) to identify the heterogeneity in the methane processes linked to different soil and vegetation conditions, this is important since sub-grid soil heterogeneity is still not represented in the model, and is also particularly relevant for large-scale inundation evaluation.

We agree with the reviewer that no observational data is available to evaluate more than one model grid cell, and indeed one should be careful with the interpretation of the non-floodplain areas of the model domain, however, our contribution here is also aimed to be used for even larger domains and for future predictions, so testing such model already in larger scale and been showing its computational capability and overall realistic performance is a step forward towards that aim. As more observational efforts will be done in the future, in other areas near the Kolyma region and Chersky floodplain for our own practical purposes, the model will be able to be evaluated for those other areas. Also, an intercomparison between JSBACH results and atmospheric inverse modeling at the regional scale is in preparation. Until then, we still believe in the value of our scientific contribution to evidence the applicability of a refined process-based methane model.

Fig. 6: Why do the authors compare the mean grid-cell soil temperature profile to measured wet and dry soil temperature profiles? Physical soil properties differ drastically between wet and dry soils and consequently strongly determine soil temperature dynamics (see end of discussion). Wouldn't it be therefore necessary to at least model soil temperature dynamics of the inundated and non-inundated land surface separately?

We present these data in Fig. 6 (now Fig. 8 in revised MS) to show the existing model physical state that was used for the calculation of methane emissions in the model. We agree with the reviewer that ideally, the model should be able to produce results separately for the dry and for the wet soil areas. However and unfortunately, this is not possible with the current model configuration and this is due to the basic model structure of JSBACH. Each model grid cell is subdivided into tiles that only serve to describe different vegetation types, however the soil properties remain the same for the entire grid cell and average soil state variables are considered. Thus, the soil temperature dynamics actually represent the entire grid cell and these are independent of the TOPMODEL interactions, i.e. inundated and non-inundated areas. This is obviously a shortcoming in this version which was presented in the discussion ms and which is true for many other land surface models. In order to represent sub-grid heterogeneity of soil properties the model configuration would need to be completely restructured which we hope can be done in the near future with the new developments of the JSABCH 4.0. We improved also new Fig. 8 to include only the measured soil temperature from only the wet site, to keep consistency to the mostly wet site EC measured fluxes.

Fig. 7: Methane emissions increase considerably in the model at sub-zero soil temperatures.

In contrast, measured methane emissions appear to be quite insensitive to soil temperature below 0°C. The authors mention this mismatch in lines 655-659. Perhaps the authors can discuss this mismatch between temperature-emission responses in more detail. How is it possible that such cold simulated soil temperatures result in emissions of > 30 mg CH<sub>4</sub> m<sup>-2</sup> day<sup>-1</sup>?

We agree with the reviewer that wintertime processes are still not well captured with our current model configuration. This goes down basically to the soil moisture that had to be artificially modified to allow the accumulation of water at the soil surface according to the topographic profile. The results presented in Fig. 7 (now Fig. 8 in revised MS) show that, the high model methane emissions mentioned by the reviewer, take place mostly during October and May (grey circles and triangles for grid cells A and B, respectively) and this reflect the gradual transition of the emissions as the soil starts to freeze towards December and also as it starts to melt before summer. Comparing with the observations, this result seems implausible, however, we think is not also impossible to happen. In the work of Zona et al. (2016), the authors demonstrated the emissions of methane during the zero curtain period. In their Figure 3, panel B, high methane emissions take place still at subzero temperatures (on av-

735 average  $7.8 \text{ mg CH}_4 \text{ m}^{-2} \text{ d}^{-1}$  at  $-5 \text{ degC}$ ) between September and December in 2014, while in panel A,  
the methane fluxes behave more similarly to our observations in the Chersky floodplain (barely  
changing  $< 0 \text{ degC}$ ). Still the magnitude of the observed emissions is not as large as what we observe  
with JSBACH and here the model parameters and schemes might play the role. The zero curtain period  
740 presented in Zona et al. reflects the release of  $\text{CH}_4$  still in autumn, due to the production of  $\text{CH}_4$  in  
sub-soil warm layers. To investigate if the results of our model reflect somehow this process as well,  
still other schemes in the model must be revisited and improved such as: Q10 and water impact in  
carbon decomposition, and processes such as soil freezing under moisture limitation and thermal soil  
response.

Fig. 8: Here, an uncertainty estimate for the measured cumulative methane emissions would help in-  
745 interpreting the comparison between simulated and measured fluxes.

In order to include uncertainty estimates to the cumulative methane emissions presented in Fig. 8  
(now Fig. 11e in revised ms), we calculated the monthly cumulative fluxes in panel e and added the  
error bars as standard deviation of the monthly cumulative fluxes. Despite our discussion regarding  
the total cumulative fluxes when comparing the eddy covariance record to the model grid cells results,  
750 we observe that the uncertainty in the monthly fluxes is larger in all of the data sets during October  
2014 and generally decreases toward April 2015. The uncertainty ranges are also generally larger in  
the eddy covariance data and this is due to the high intrinsic signal daily variability.

Fig. 11: I am not sure how this figure contributes to the research questions. The seasonality of differ-  
755 ent methane emission pathways is already shown in Fig. 10. How does a representation of the spatial  
distribution of the methane emissions add to the manuscript?

As suggested by the reviewer, we moved former Fig.11, on total model domain methane emissions  
from the different pathways, to the supplementary material of the revised ms (Fig. S5).

#### Technical comments

760 Line 149: Remove “done”.

OK

Line 150: Remove “are”.

OK

Line 196: Please define what “hospitable and inhospitable” land means in this context.

765 We have completed this paragraph by adding the following lines: “A prescribed fraction of each grid  
cell is used to discriminate between land hospitable and inhospitable to vegetation. In JSBACH, each  
grid cell has a designated fraction where vegetation cover types across tiles can be assigned, hence is  
the fraction hospitable to vegetation. The remaining fraction of the grid cell is then associated to a  
land cover type that represents areas where vegetation does not grow, such as rocky surfaces and des-  
770 erts; hence it is considered inhospitable to vegetation (Reick et al., 2013).”

Line 534: What do the authors mean with “visually”? They state in the previous sentence that differ-  
ences are not statistically significant.

775 We refer here to the time shift in the mean methane emissions signal when the sensitivity experiments  
are compared. However, indeed the statistical analysis showed that there is no significant difference  
between the results of the sensitivity tests for the individual and total emissions. We rephrased this  
sentence to avoid confusion, it now reads: “A time shift is seen however, in the  $\text{CH}_4$  emissions from  
mid-October until mid-November (Fig. 3, column 4 of row e), with the larger emissions through snow  
taking place earlier if  $h_{\text{snow}}$  is thinner.

780 Nevertheless, this temporal shift in the  $\text{CH}_4$  emissions through the snow is not observed in the total  
 $\text{CH}_4$  emissions.”

Fig. 3: Please clarify what the inset figures show.

785 Thank you for pointing this out. Now we added the following sentence to the caption: “The inset fig-  
ures in some of the panels are zooms to periods of time where larger difference between signals is  
depicted.”

### References added to the revised ms:

- 790 Aubinet, M., T. Vesala, and D. Papale (2012), *Eddy Covariance - A practical guide to measurement and data analysis*, 449 pp., Springer, Dordrecht; Heidelberg; London; New York, doi:10.1029/2002JD002055.
- 795 Berestovsakaya, Y.Y., I.I. rusanov, I.V. Vasil'eva and N.V. Pimenov (2005), The processes of methane production and oxidation in the soils of the Russian Arctic tundra, *Microbiology*, 74(2), 221-229, 10.1007/s11021-005-0055-2.
- Chapin III, F.S. and M. Slack (1979), Effect of defoliation upon root growth, phosphate absorption and respiration in nutrient-limited tundra graminoids, *Oecologia*, 42, 1, 67-79, 10.1007/BF00347619.
- 800 Davidson, S. J., Santos, M. J., Sloan, V. L., Reuss-Schmidt, K., Phoenix, G. K., Oechel, W. C., and Zona, D.: Upscaling CH<sub>4</sub> fluxes using high-resolution imagery in Arctic tundra ecosystems, *Remote Sensing*, 9, 1227, 2017, 10.3390/rs9121227.
- 805 Foken, T., and B. Wichura (1996), Tools for quality assessment of surface-based flux measurements, *Agr Forest Meteorol*, 78(1-2), 83-105, doi:10.1016/0168-1923(95)02248-1.
- Fratini, G., and M. Mauder (2014), Towards a consistent eddy-covariance processing: an intercomparison of EddyPro and TK3, *Atmos Meas Tech*, 7(7), 2273-2281, doi:10.5194/amt-7-2273-2014.
- 810 Jammet, M., Crill, P., Dengel, S., and Friborg, T.: Large methane emissions from a subarctic lake during spring thaw: mechanisms and landscape significance, *Journal of Geophysical Research: Biogeosciences*, 120, 2289-2305, 2015, 10.1002/2015JG003137.
- 815 Jammet, M., S. Dengel, E. Kettner, F. J. W. Parmentier, M. Wik, P. Crill, and T. Friborg (2017), Year-round CH<sub>4</sub> and CO<sub>2</sub> flux dynamics in two contrasting freshwater ecosystems of the subarctic, *Biogeosciences*, 2017, 14, 5189-5216, doi:10.5194/bg-14-5189-2017.
- 820 Kittler, F., M. Heimann, O. Kolle, N. Zimov, S. Zimov, and M. Göckede (2017), Long-term drainage reduces CO<sub>2</sub> uptake and CH<sub>4</sub> emissions in a Siberian permafrost ecosystem, *Global Biogeochem. Cy.*, 31, 1704-1717, doi:10.1002/2017GB005774.
- Mauder, M., and T. Foken (2015), *Eddy-Covariance Software TK3*, doi:10.5281/zenodo.20349.
- 825 Rannik, U., O. Peltola, and I. Mammarella (2016), Random uncertainties of flux measurements by the eddy covariance technique, *Atmos Meas Tech*, 9(10), 5163-5181, doi:10.5194/amt-9-5163-2016.
- Reichstein, M., et al. (2005), On the separation of net ecosystem exchange into assimilation and ecosystem respiration: review and improved algorithm, *Glob Change Biol*, 11(9), 1424-1439, doi:10.1111/j.1365-2486.2005.001002.x.
- 830 Reick, C., T. Raddatz, V. Brovkin, V. Gayler, (2013), Representation of natural and anthropogenic land cover change in MPI-ESM, *Journal of Advances in Modeling Earth Systems*, 5, 459-482, 10.1002/jame.20022.
- 835 Saltelli, A., Chan, K. & Scott, E. M. (2000), *Sensitivity Analysis. Wiley Series in Probability and Statistics*, John Wiley & Sons, Ltd.
- 840 Tokida, T., Mizoguchi, M., Miyazaki, T., Kagemoto, A., Nagata, O., and Hatano, R.: Episodic release of methane bubbles from peatland during spring thaw, *Chemosphere*, 70, 165-171, 2007, 10.1016/j.chemosphere.2007.06.042.
- Wang, P., L. Mommer, J. van Ruijven, F. Berendse, T. C. Maximov, M. M. P. D. Heijmans, 2016,

Seasonal changes and vertical distribution of root standing biomass of graminoids and shrubs at a Siberian tundra site, *Plan Soil*, 10.1007/s11104-016-2858-5.

845

Whalen, S.C. and W.S. Reeburgh (2000), Methane oxidation, production, and emission at contrasting sites in a Boreal Bog. *Geomicrobiology Journal*, 17, 237-251.

**References recommended by reviewer (and added also to the revised ms).**

850 Christensen TR, Johansson T, Åkerman HJ et al. (2004) Thawing sub-arctic permafrost: Effects on vegetation and methane emissions. *Geophysical Research Letters*, 31, L04501.

855 Cresto-Aleina F, Brovkin V, Muster S, Boike J, Kutzbach L, Sachs T, Zuyev S (2013) A stochastic model for the polygonal tundra based on Poisson – Voronoi diagrams. *Earth System Dynamics*, 4, 187–198.

Cresto-Aleina F, Runkle BRK, Brücher T, Kleinen T, Brovkin V (2016) Upscaling methane emission hotspots in boreal peatlands. *Geoscientific Model Development*, 9, 915–926.

860

Flessa H, Rodionov A, Guggenberger G et al. (2008) Landscape controls of CH<sub>4</sub> fluxes in a catchment of the forest tundra ecotone in northern Siberia. *Global Change Biology*, 14, 2040–2056.

865 Helbig M, Boike J, Langer M, Schreiber P, Runkle BRK, Kutzbach L (2013) Spatial and seasonal variability of polygonal tundra water balance: Lena River Delta, northern Siberia (Russia). *Hydrogeology Journal*, 21, 133–147.

870 Helbig M, Chasmer L, Kljun N, Quinton WL, Treat CC, Sonnentag O (2017) The positive net radiative greenhouse gas forcing of increasing methane emissions from a thawing boreal forest-wetland landscape. *Global Change Biology*, 23, 2413–2427.

875 Helbig M, Quinton WL, Sonnentag O (2017) Warmer spring conditions increase annual methane emissions from a boreal peat landscape with sporadic permafrost. *Environmental Research Letters*, 12, 115009, doi: 10.1088/1748-9326/aa8c85.

Johnston CE, Ewing S a, Harden JW et al. (2014) Effect of permafrost thaw on CO<sub>2</sub> and CH<sub>4</sub> exchange in a western Alaska peatland chronosequence. *Environmental Research Letters*, 9, 85004.

880

Liljedahl AK, Boike J, Daanen RP et al. (2016) Pan-Arctic ice-wedge degradation in warming permafrost and influence on tundra hydrology. *Nature Geoscience*, 9, 312–318.

885 Parmentier FJW, van Huissteden J, van der Molen MK, Schaepman-Strub G, Karsanaev SA, Maximov TC, Dolman AJ (2011) Spatial and temporal dynamics in eddy covariance observations of methane fluxes at a tundra site in northeastern Siberia. *Journal of Geophysical Research*, 116, G03016.

890 Sachs T, Giebels M, Boike J, Kutzbach L (2010) Environmental controls on CH<sub>4</sub> emission from polygonal tundra on the microsite scale in the Lena river delta, Siberia. *Global Change Biology*, 16, 3096–3110.

895

## Anonymous Referee #2

Thank you very much for your comments to our discussion manuscript. Below we address one by one the comments made during this review. All answers are in blue font.

Overall:

The ms has its focus on regional scale methane dynamic and the modelling of year round dynamics, which is certainly relevant and highly needed. In general there are quite few year round measurements of methane dynamics in the arctic region, which also explains why the modelling studies are even fewer and regional budgets are poorly constrained. Further, the understanding of drivers and exact transport mechanisms in the top soil and soil – snow- atmosphere still in most (not all) cases relies on an interpretation of a net emission, rather than independent quantification of the individual components adding up the net CH<sub>4</sub> emission. For that reason the focus of the current ms is important and timely. Despite that the ms is well written and in general well references, I'm a bit reluctant about the qualities of the ms, because I basically find that it tries to accomplish too much and not in a fully convincing way. As pointed out by reviewer 1, also I have a serious problem with the differences in scaling which are used in the different components of the study. In my perspective, the very coarse spatial scale of the model does not compare well with the highly advanced model approach of partitioning the production and transport of CH<sub>4</sub> in the soil and snow. The ms simultaneously tries to solve the issues of the spatial /temporal methane dynamics of the large Siberian wetlands, the process pathways and comparing all the modelling output to relatively few and very local measurements near Chersky. I basically don't think that the available measurements are well suited to verify the model output of the processes leading to the net CH<sub>4</sub> emission at the surface, and the differentiation of pathways of CH<sub>4</sub> during different periods of the year.

In agreement with reviewer 1, we detailed further our approach for the scaling between the model output at grid cell level and the available observations, especially those from Eddy covariance measurements. These are also added in this response below.

We agree with the reviewer 2, and also highlighted by reviewer 1, that the observational data to validate our model output is few. On the other hand, boreal wetlands, especially those in permafrost regions as in far Northeast Siberia are quite understudied due to the difficulty to reach those places and perform measurements all year round. The data presented in this manuscript shows a synergistic and unique study between the first year-round greenhouse gas emission measurements and summer chamber fluxes in a site of the Kolyma (Chersky) floodplain and a process-based methane model embedded in a land surface model. Site level comparisons are achieved by comparing the two years of continuous Eddy covariance methane flux measurements and summer flux chamber measurements to the model grid cell output. Many fluxes simulated by models in other world regions cannot be adequately evaluated due to the lack of measurements on the study site and have to rely in measurements done in other areas, or from data that has been collected during different periods of time, e.g. only summer measurements. In contrast, our study benefits greatly from the simultaneous temporal and spatial (at grid cell scale possible) synergy where the model development has directly benefited from the year-round greenhouse gas fluxes observations. Finally, it is not our aim to be able to evaluate all model grid cells but rather demonstrate that a process-based methane model can achieve in an Arctic tundra region and this is already a scientific contribution per se to the scientific community.

In my opinion the ms could benefit from being divided into two; one with focus on the annual budget for Siberian and one focused on the process modelling of the different pathways for methane through the soil/snow pack. The later one could benefit from some kind of lab or micro cosmos comparison, where processes could be studied more precisely than what is mostly the case in the field.

We appreciate this suggestion made by the reviewer. The reviewer suggests to have one ms focused solely in the annual methane budget for a larger study region, i.e. Siberia. In fact, we plan to work on such a larger scale (but still high-resolution, process-based) study in the future. However, at this point our intention is mainly to provide a first proof-of-concept of the applicability of our modeling framework at a still relatively small regional domain, and we believe that this manuscript needs a strong focus on the background description of the used model configuration. Such description has not been published elsewhere. The reviewer also suggests to have such process modeling description supported by e.g. micro cosmos experiments, in a separate ms. We agree that such a study would be an excellent

955 addition to the study we already completed; however, developing micro cosmos experiments is out of the scope of our current project and this step could be done for future investigations in order to refine the current model configuration. Instead of splitting our work into two separate manuscripts, we therefore suggest instead to improve the flow of the current ms: we shortened the revised ms and moved the extra useful information to the supplementary material, and clarify further the issues mentioned through this review in the new revised ms.

960 Regardless of the approach, the issues of differences in scales should be discussed much more detailed and qualified than it is done in the present version of the ms. From my perspective the output of the model and the assessment of the advances in the new “improved” version is not credible as it appears now, despite that the output is in the same ballpark as the measured data, and a number of other studies.

965 As mentioned earlier, we refined the analysis for the comparison between the methane fluxes from eddy covariance and those from the model, regarding the difference in scales, this also helps to sustain better our results presented in the ms. The difference in scales between EC data and model output is also a comment made by reviewer #1. Our answer to this concern is (same as for Rev. #1):

970 We agree that the comparison between model methane fluxes and those from observations, specifically from eddy covariance, is a challenge. In our manuscript, we use a scaling factor for the chamber data by considering chamber measurements that were done under exclusively wet and under exclusively dry summer conditions. We then make use of the total fraction of inundated areas in the model grid cell (IF) modeled with the TOPMODEL approach to scale the total chamber fluxes. This scaling approach takes into consideration that the model methane fluxes represent the emissions from only the

975 portion of the grid cell that is inundated, i.e. with water at or above the soils surface.

In the case of the eddy covariance fluxes, following the concerns of the reviewer, we re-evaluated our approach for this comparison. In the revised version of this manuscript we include now a thorough analysis of the footprint area of the eddy covariance fluxes as part of a new Appendix A on “Details on in-situ flux observations”. This appendix also includes details on the eddy covariance flux data

980 uncertainty assessment and more detailed results on the chamber measurements, as requested below also by the reviewer.

In this new appendix, we analyze the type of vegetation and its coverage in the footprint area of the EC tower, from remote sensing images as a metric to identify wet and dry areas. It has been recently shown in the literature that the type of vegetation in tundra landscapes is a good indicator of

985 the spatial distribution and variation of CH<sub>4</sub> fluxes (Davidson et al., 2017) and it is also expected that the majority of the CH<sub>4</sub> fluxes are emitted from wetlands in tundra ecosystems (Helbig et al., 2017).

In the Chersky floodplain, areas with dominant cotton grasses, specifically *Eriophorum angustifolium*, are indicators of predominant wet soils, while tussocks, specifically *Carex appendiculata* in our study area, and shrubs are indicators of predominant dry soil conditions. It is important noting that *C. appendiculata*, can be also found in wet areas, but is predominant in dry areas.

990 For the model, the vegetation distribution per grid cell is too coarse to consider this metric similar as that for the remote sensing data in the EC footprint area, however the total abundance of C3 grasses in the grid cell A is 33.3 % as given for the model (with the rest of the grid cell dominated by deciduous shrubs and extra tropical evergreen trees), but there is no discrimination between cotton grasses and tussocks.

995 The footprint of the eddy covariance tower in the Chersky floodplain covers an approximate area of 400 m x 400 m, similar to that one depicted in Fig. 1 of Kittler et al. 2016 (cited in discussion ms) (see new Appendix A at the end of the revised ms for footprint area for the EC tower used in this manuscript). The remote sensing analysis revealed that cotton grasses are present in about 26 % of the footprint area, which would translate into the same portion of the footprint area as fully wet zones during the “wet months”: after spring melt in June and until August when most annual precipitation in the region takes place, covering most of the growing season. As will be shown below in this response,

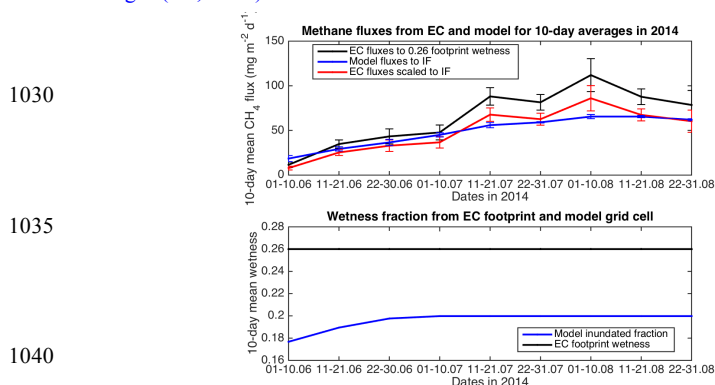
1000 CH<sub>4</sub> fluxes measured by chambers (footprint of 60 cm x 60 cm) revealed that during the growing season in dry soil areas of the Chersky floodplain that are characterized by a water table below the surface, the emission of methane during the growing season is negligible with even some atm. CH<sub>4</sub> up-

1005

take by soil (i.e. negative CH<sub>4</sub> flux rates) (data shown in new Appendix A). Under this consideration, and as confirmed recently by Helbig et al., 2017, the majority of the CH<sub>4</sub> fluxes measured by the EC tower would represent fluxes from fraction of wetland in the footprint area, i.e. 26 %.

1010 In case of the model grid cell where the location of the EC tower falls (grid cell A in Fig. 1 of the discussion ms), the IF for June-July-August during 2014 shows growing inundation values from 17.7 % to 19.9 % (for 10-day mean values for those three months) representing the percentage of total wet areas in the grid cell area. These values are slightly smaller than the 26 % wetness area in the EC footprint, and denote the area of the grid cell where the model methane emissions take place (i.e., no

1015 emissions in dry areas, in agreement to the chamber measurements).  
 With this basis and to make a closer comparison between EC flux measurements and model data for the growing season months, we scaled linearly the 10-day mean EC methane fluxes to the IF from the model, and calculated the standard deviation of the 10-day mean. In the next figure, we show: TOP panel, the original 10-day mean EC methane flux measurements that would represent the emissions of a 26 % wet area between June and August 2014 (black line), the 10-day mean EC methane fluxes scaled to the 10-day mean IF from the model for the same period of time (red line) and 10-day mean model methane emissions for grid cell A, which imply emissions from the IF from the model (blue line). Error bars in all lines are one standard deviation of the 10-day mean flux values. The BOTTOM panel shows the 10-day mean IF from the model used to scale the EC fluxes (blue line), and the constant wetness percentage of the footprint area calculated from the vegetation coverage remote sensing images (i.e., 26 %).



We observe that the scaled EC methane fluxes decreased as a lower IF is considered within the footprint, and those new calculated fluxes become closer to those from the model, and in most cases the latter fall within the 10-day standard deviation of the EC fluxes.

1045 Unfortunately, it is not possible to obtain a temporal varying wetness area for the EC footprint all year, based on our approach of only considering the vegetation cover, thus wouldn't be appropriate to scale all of the EC fluxes for 2014 and 2015 to the IF from the model without any reference for spring and winter wet footprint areas. However, from this analysis we learn that: 1) considering the vegetation cover as indicator of soil wetness, the EC footprint area holds a very similar area to that of the model grid cell through which the majority of the methane is emitted to the atmosphere and 2) the net offsets between methane flux model and EC data can largely be attributed to differences in wetness levels.

1050 Summarizing, we assume that for both the model grid cell and the eddy covariance footprint, methane emissions are not spatially homogeneous, but bound to the distribution of wet (inundated) areas. Accordingly, a meaningful agreement between model and observations can only be obtained if two factors are fulfilled: (i) the fraction of wet surfaces agrees between both data sets, and (ii) the flux rates from wet surfaces agree between both datasets. Through correcting the offsets in inundated fraction, we could demonstrate that the flux rates between model and eddy covariance observations agree very well, emphasizing the sound setup of the model algorithms and parameter settings. We add the analysis presented here into the new Appendix A to complement the discussion on scaling fluxes for com-

parison between EC and model data.

**Specific:**

1065 L48 -> 66: Maybe a matter of taste, but I'm in general against using these "horror scenarios" which draw lines between the carbon pool of the Arctic soils and potential increase of GHGs. I think we now know that no indications are found that something very dramatic is happening in foreseeable future, and it doesn't add to the understanding of the ms. Consider rephrasing.

1070 Thank you for this suggestion. We will consider rephrasing these lines. However, we think it is still important to mention them, such as that changes in air temperature, soil topography and projected shifts in precipitation in Arctic tundra ecosystems will influence in the future the soil hydrologic regime in permafrost areas which in turn will affect future emissions of CO<sub>2</sub> and CH<sub>4</sub> into the atmosphere from Arctic terrestrial ecosystems. This projected scenario is part of current literature discussions, which draw the framework of studies like ours presented in this manuscript.

1075 L187: Despite that you are obviously aware of the complications of the comparison between scale I'll encourage you to address specifically how the scaling issue between 0,5\_ modelling grid and EC footprint or chambers is dealt with.

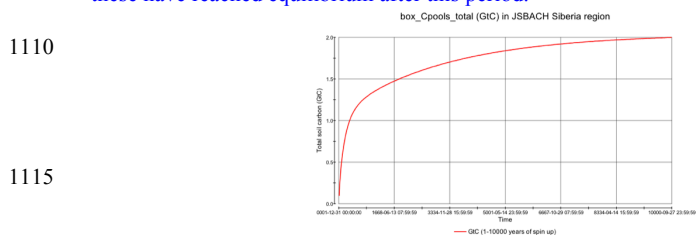
We have added the response to this important suggestion above.

1080 L218: Again please justify, why 11 soil layers are needed, when the horizontal scale is this coarse. The coarse horizontal resolution in the model does not influence the need for a refined vertical discretization of soil processes. In particular, a fine vertical resolution is required to find numerically stable solutions of the gas diffusion equation.

1085 L323: Spun up for 10.000 years? Please justify further, climate (or C – pools) can not be assumed to have remained constant for this period of time.

1090 Thank you for this question. The idea behind the so called spin up approach is to initialize state variables, such as temperature, moisture or carbon content based on the process representation (the differential equations) and environmental conditions during a pre-industrial time when we can neglect a human-induced disturbance of ecosystems and climate. This is important in prognostic modelling in order to reliably isolate effects of anthropogenic actions and related climate change on ecosystems. Usually, soil carbon pools have a mean residence time of less than 1000 years in the aerobic case and hence, this slowest carbon pool will reach a steady state with pre-industrial climate after 1000 years of iteration. For example, for a temperate terrestrial ecosystem we would assume a stable climate over 1000 years round 1700-1800 and substitute the pre-industrial climate by an observation-based climatology from 1901-1930. Climate variations in the past (e.g. little ice age) are usually neglected because future climate change will be much stronger.

1095 Soil organic matter in permafrost regions is additionally stabilized by soil freezing, even in the active layer, i.e. the OM is either frozen over long time periods in permafrost or the decomposition season is reduced to a few months. That is an additional stabilization which leads to much higher effective mean residence times and hence we need to spin-up the model longer to reach the pre-industrial steady state, usually 10000 years are valid (McGuire et al., 2016; Chadburn et al., 2017). In Chadburn et al. (2017) it was shown that such approach leads to soil organic matter pools comparable to observations at several Arctic stations. At the Cherskii site, we unfortunately do not count with observed carbon stocks. In the following figure however, we show the total carbon (sum of woody, green and reserve) in the soil at the end of this spin up period for the entire model domain and it can be seen that these have reached equilibrium after this period.



L403: I understand that the numbers can be compared, but please argue why the field site measurements can be assumed to be averaging the full 0,5x0,5\_ modelling pixel.

1120 In this context, we approach a scaling factor considering the wet and dry areas of the grid cell vs. the wet and dry plots in the chamber sites (model grid cell and chamber plots heterogeneity). This was documented in the discussion manuscript. Briefly, to obtain the total flux from chamber measurements, the values measured from fully wet sites and fully dry sites were scaled to the daily-inundated fractions as given from the model, leading to Eq. 8 of the discussion manuscript. Taking this approach  
1125 in consideration, the final fluxes from chamber measurements represent the CH<sub>4</sub> emissions per m<sup>2</sup> per day under heterogeneous (wet and dry) soil conditions, similar to those at grid cell scale.

L445: Differences seems to be substantial please comment.

1130 The differences in the wetland extent from the model compared to those from the high-resolution remote sensing data might seem substantial (~ 6 %), however, it is important noting the following:

- No other remote sensing data exclusive for this area at such high resolution (150 m) has been available for the Boreal Arctic region such as that one used for our study (Reschke et al., 2012; cited in discussion ms). Other available wetland extent remote sensing products are only at global scale with spatial resolutions in the order of 25 km. By having a better-resolved reference wetland extent, ensures that the uncertainties in the model wetland extent are limited mostly to the model technique and spatial resolution used to simulate wetlands. In addition, high latitude wetlands still pose a challenge in remote sensing, due to the long periods of darkness during the year.
- The addition of the TOPMODEL scheme in the land surface model JSBACH allows the representation of standing water following the topographic profile of the region of interest. Without this scheme, it is not possible at all with this model to allow accumulation of water at the soil surface. Furthermore, this is not an exclusive characteristic of the JSBACH model, as most land surface models lack of an explicit and fully functional hydrology model where also the dynamics of inland waters, such as runoff, are possible to be simulated. From the modeling point of view and within the inherent limitations of the model structure, the possibility of simulating wetland extent in a land surface model and having a remote sensing data with sufficient resolution is an excellent combination of first steps achievements to improve process-based modeling for greenhouse gases at high latitudes. For this reasons, we argue that a 6 % difference between the remote sensing wetland data and the modeled data provides a first good approximation.

1140  
1145  
1150 L470: I basically don't understand how a threshold can be set for proportion of flooded area in a pixel – what is the rational? Theoretically the whole pixel could be inundated –I assume?

1155 The proportion of flooded area in a pixel follows exclusively the topographic profile and the location of the water table, in a way that if there is enough water content in the soil (basically close to saturation) it will be possible to accumulate water at the surface and only if the topography structure allows it. For this reason, not all the pixel could be inundated. The sequence of the TOPMODEL scheme in our model configuration follows the next steps: 1) selection of soil layer where the water table will be positioned according to the soil water content, 2) by defining a water table threshold, the model locates the position of the water table, 3) a fixed TOPMODEL parameter defines the dependence of flooding on the water table variation in a way that the lower the value of this parameter means that larger areas with the same water table will be flooded (parameter  $f$  of equation 1, exponential decay of transmissivity with depth, in the discussion manuscript), 4) a fixed threshold in the TOPMODEL scheme limits the area of floodability ( $\chi_{\min\_eti}$ , given in L242-245 in the discussion ms), this is used to avoid the occurrence of running water and is dependent on soil types. This TOPMODEL parameter is used in the general TOPMODEL scheme to allow runoff, which in our model configuration should not be taken into account. The lower the value the larger the flooded area e.g., limits of the horizontal extent of the inundated area. We find this level of detail on the model configuration can only be added in the supplementary material of our manuscript and we will consider doing so.

1170

L532: What effect of the snow would you have expected in this context?  
As shown in the sensitivities exercise, by describing thinner snow layers (3 and 1 cm) than the value in the control simulation (5 cm) allows only in a temporal shift of the emissions without affecting the magnitude of the total annual CH<sub>4</sub> emissions. The intention of doing this test is to analyze the response of the model exclusively to this parameter and our hypothesis (thinner snow layers allows faster diffusion of gas than thicker layers with constant density values) has been confirmed.

1175

L630: there seems to be significant difference in measured and modelled soil temperatures, please comment.

1180

The effect of having higher soil moisture in the soil pores influences the soil thermal regime in organic-rich soils both during summer and winter. When the soil pores are predominantly filled with water, the water promotes a high thermal capacity, and when pores are predominantly filled with air, the thermal soil capacity decreases and more energy is required to heat the soil. Also, near-surface vegetation in these tundra environments, such as mosses and lichens (Porada et al., 2016) plays an important role as effective thermal insulator but also would help to insulate the surface soil layers from the warm surface temperatures from atmospheric influence during summer. As well, snow cover serves as thermal insulator, and a further snow layer evaluation from the model and measurements in the site needs to be done as measurements become available.

1185

Besides the need to consider the previous factors, our results evidence the effect of the soil moisture variation, which in general is quite low, to the soil thermal regime. The soil hydrology, as mentioned extensively in the manuscript, poses still limitations in our current model configuration and it requires further improvements, also hopefully based, on available soil moisture measurements in this study region, which at the moment are unavailable.

1190

L665: probably why also both absolute values and seasonal pattern seems distinctly different  
It is unclear to us what this comment from the reviewer is referring to. We ask for a further clarification in a way that a suitable response can be given from our side.

1195

L710 -723: that differentiation between ebullition and diffusion seems unfounded, and it is hard to see how you verify the different pathways, please elaborate.

1200

In our methane module, emissions of methane via ebullition and diffusion are explicitly modeled and are based in fundamental principles of gas motion. Diffusion of a gas is a molecular motion process and its speed relies on the medium where it takes place: it is slow in water and faster in air. It works independently of a water table with the net movement of molecules following a concentration gradient from high to low concentrations in order to achieve equilibrium. In the case of ebullition, this takes place when a certain volume of water gets saturated with a specific gas and oversaturation allows the formation of bubbles that, due to pressure effects, are released through available pathways, such as interstitial water in the soil. While diffusion is a continuous but rather slow molecular process, ebullition is fast and highly sporadic. These are well known physical processes in gas dynamics, and an excellent review on the explicit diffusion and ebullition processes for methane in soils is provided in Le Mer and Roger (2001), *Eur. J. Soil Biol.* Vol. 37, doi: 10.1016/S1164-5563(01)01067-6.

1205

Para 3.4.3: could this be merged with the sensitivity study in 3.2? seems to be fundamentally alike.

1210

This recommendation by the reviewer is unclear. Section 3.2 is about presenting the results of the sensitivity experiments, while section 3.4.3 contain results on the environmental controls related to the methane fluxes and their temporal variation. Thus, these sections are not alike and therefore cannot be merged as suggested. Perhaps there was some confusion in the number of sections that the reviewer is referring. We ask for a clarification on this comment to better assess a response.

1215

Fig. S5b: legend does not seem to match.

1220

Ok, panels a and b were inverted and this is now corrected. Thank you for identifying this mistake. This is now Fig. S6).

1225

L916-920: the conclusions here seem somewhat unfounded due to the previously mentioned scaling issues.

The lines the reviewer here is referring to are part of the discussion and not of the conclusion section (starting in L1098 of discussion ms). Related to the lines referred here from the discussion, we wrote:  
1230 “We simulated for the first time year-round methane emissions in a Northeast Siberian region centered on the city of Chersky, including emissions during the non-growing season. Our results showcase the ability of the improved JSBACH-methane model to reproduce seasonality in the CH<sub>4</sub> emissions when compared to fluxes measured by eddy covariance and chambers in a study site near Chersky.”

1235 In these lines of the discussion, we refer also explicitly to the ability of the model to reproduce the seasonality of the methane emissions (lower in winter, higher in summer months) independent of their magnitude, which we presented and discussed accordingly in the discussion ms. Regarding the scaling between EC measurements and model results for the comparison of their magnitude, we hope that with the clarification above this argument is adequately answered.

#### 1240 **References added to the revised ms:**

Chadburn, S.E., et al., (2017), Carbon stocks and fluxes in the high latitudes: using site-level data to evaluate Earth system models, *Biogeosciences*, 14, pag. 5143-5169, doi:10.5194/bg-14-5143-2017.

1245 Davidson, S. J., Santos, M. J., Sloan, V. L., Reuss-Schmidt, K., Phoenix, G. K., Oechel, W. C., and Zona, D.: Upscaling CH<sub>4</sub> fluxes using high-resolution imagery in Arctic tundra ecosystems, *Remote Sensing*, 9, 1227, 2017, 10.3390/rs9121227.

1250 Helbig, M., Quinton, W.L., Sonnentag O., (2017) Warmer spring conditions increase annual methane emissions from a boreal peat landscape with sporadic permafrost. *Environmental Research Letters*, 12, 115009, doi: 10.1088/1748-9326/aa8c85.

1255 McGuire, A.D. et al., (2016), Variability in the sensitivity among model simulations of permafrost and carbon dynamics in the permafrost region between 1960 and 2009. *Global Biogeochemical Cycles*, 30(7), pag. 1015-1037, doi:10.1002/2016GB005405.

Porada, P., A. Ekici and C. Beer (2016), Effects of bryophyte and lichen cover on permafrost soil temperature at large scale, *The Cryosphere*, 10, 2291-2315, 10.5194/tc-10-2291-2016.

#### 1260 **List of relevant changes in revised manuscript.**

In addition to the responses made by two anonymous reviewers presented above, in the revised ms the following major changes were done.

- 1) Former Appendix A (on details of the revised model configuration) was moved as part of the section 2 of supplementary material. The Appendix only contains now the new section on “Details on in-situ flux observation program” (Appendix A) located at the end of the revised ms.
- 1270 2) The section 1 of the supplementary material contains the detailed information of the TOPMODEL scheme originally included in the discussion ms in section 2.2
- 3) We removed former section 3.3.4 and merged it to discussion (section 4.2)
- 1275 4) Former section 3.3.3 “Winter emissions” is merged to 3.4.2 “Impact of snow on the seasonal distribution of CH<sub>4</sub> emissions”. This information is now contained in section 3.4.2 "Impact of snow on the winter and seasonal variation of CH<sub>4</sub> emissions". In that context, former Fig. 11 (now Fig. 10) is shortened (removed former panels a, f, g) because it was redundant information that is shown in current Fig. 9.

## Year-round simulated methane emissions from a permafrost ecosystem in Northeast Siberia

Karel Castro-Morales<sup>1\*</sup>, Thomas Kleinen<sup>2</sup>, Sonja Kaiser<sup>1</sup>, Sönke Zaehle<sup>1</sup>, Fanny Kitzler<sup>1</sup>, Min Jung Kwon<sup>1§</sup>, Christian Beer<sup>3,4</sup> and Mathias Göckede<sup>1</sup>

<sup>1</sup> Max Planck Institute for Biogeochemistry, Jena, Germany

<sup>2</sup> Max Planck Institute for Meteorology, Hamburg, Germany

<sup>3</sup> Department of Environmental Science and Analytical Chemistry, Stockholm University, Sweden

<sup>4</sup> Bolin Centre for Climate Research, Stockholm University, Stockholm, Sweden

<sup>§</sup> Present address: Korea Polar Research Institute, Incheon, Republic of Korea

\*Correspondence to: Karel Castro-Morales ([kcastro@bgc-jena.mpg.de](mailto:kcastro@bgc-jena.mpg.de))

### Abstract

Wetlands of northern high latitudes are ecosystems highly vulnerable to climate change. Some degradation effects include soil hydrologic changes due to permafrost thaw, formation of deeper active layers, and rising topsoil temperatures that accelerate the degradation of permafrost carbon and increase in CO<sub>2</sub> and CH<sub>4</sub> emissions. In this work we present two years of modeled year-round CH<sub>4</sub> emissions to the atmosphere, from a northeastern Siberian region in the Russian Far East. We use a revisited version of the process-based JSBACH-methane model that includes four CH<sub>4</sub> transport pathways: plant-mediated transport, ebullition and molecular diffusion in the presence or absence of snow. The gas is emitted through wetlands represented by grid cell inundated areas simulated with a TOPMODEL approach. The magnitude of the summertime modeled CH<sub>4</sub> emissions is comparable to ground-based CH<sub>4</sub> fluxes measured with the eddy covariance technique and flux chambers in the same area of study, whereas wintertime modeled values are underestimated by one order of magnitude. In an annual balance, the most important mechanism for transport of methane into the atmosphere is through plants (61 %). This is followed by ebullition (~35 %), while summertime molecular diffusion is negligible (0.02 %) compared to the diffusion through the snow during winter (~4 %). We investigate the relationship between temporal changes in the CH<sub>4</sub> fluxes, soil temperature, and soil moisture content. Our results highlight the heterogeneity in CH<sub>4</sub> emissions at landscape scale and suggest that further improvements to the representation of large-scale hydrological conditions in the model, will facilitate a more process-oriented land surface scheme and better simulate CH<sub>4</sub> emissions under climate change. This is especially necessary at regional scales in Arctic ecosystems influenced by permafrost thaw.

**Keywords:** methane, permafrost, carbon cycle, Arctic, wetlands, winter emissions.

Karel 27/2/2018 11:32

**Deleted:** Methane emissions to the atmosphere from natural wetlands are estimated to be about 25 % of the total global CH<sub>4</sub> emissions. In the Arctic, these areas are highly vulnerable to the effects of global warming due to atmospheric warming amplification, leading to ...oil hydrologic changes du ... [1]

Karel 27/2/2018 11:45

**Deleted:** -

## 1. Introduction

During the last 30 years, atmospheric temperatures at northern high-latitudes have risen more than the global average (Schuur et al., 2015; Serreze et al., 2000). In consequence, many permafrost areas in these regions have experienced expedited thawing rates in recent years. Permafrost in northern high-latitude ecosystems contains twice as much carbon as the current carbon pool in the atmosphere and about half of global soil organic carbon (Hugelius et al., 2014; Tarnocai et al., 2009). About two-thirds of the terrestrial Arctic is classified as wetlands (Liljedahl et al., 2016; Hugelius et al., 2014) and permafrost underlies most of them. Wetlands globally contribute about 25 % of the total CH<sub>4</sub> emissions (using bottom-up approaches between 2003-2012) from natural sources into the atmosphere, and from that, nearly 4 % is emitted from wetlands at northern high-latitudes > 60 °N (Saunois and al., 2016). The degradation of freshly available carbon from permafrost thaw is expected to contribute strongly to a positive carbon-climate feedback in Arctic ecosystems (e.g. Beer, 2008). Changes in air temperature, soil topography and projected shifts in precipitation in Arctic tundra ecosystems (Kattsov and Walsh, 2000; Lawrence et al., 2015) influence the soil hydrologic regime in permafrost areas. Also, thawing permafrost will induce changes in the surface wetness due to surface subsidence of ice-rich soils (Christensen et al., 2004; Helbig et al., 2017b). These changes will therefore also influence the magnitude of future emissions of CO<sub>2</sub> and CH<sub>4</sub> into the atmosphere from Arctic terrestrial ecosystems (Hugelius et al., 2014; Lawrence et al., 2015; Schuur et al., 2008). Drier soil columns will enhance methane oxidation and increase CO<sub>2</sub> emissions (Kittler et al., 2016; Kwon et al., 2016; Lawrence et al., 2015; Liljedahl et al., 2016; Sturtevant et al., 2012), also leading to changes in plant community structure (Christensen et al., 2004; Kutzbach et al., 2004; Kwon et al., 2016). Thus, it is imperative to improve our understanding of the effects of climate change in permafrost wetlands, specifically their contribution to greenhouse gases into the atmosphere. Freeze and thaw soil processes are critical mechanisms that modulate the seasonality of CH<sub>4</sub> emissions in permafrost ecosystems of the Arctic (Panikov and Dedysh, 2000). Most of the annual CH<sub>4</sub> emissions from Arctic wetlands take place during summer (growing season). In spring, the rising air and soil temperatures promote the melt of snow and ice in the soil, stimulating the microbial production of gas within the mostly anoxic active layer (i.e. the surface soil layer that thaws during summer and freezes again during autumn). During this season, episodic releases of large amounts of CH<sub>4</sub> in the form of bursts have been evidenced in wetlands (e.g. Friborg et al., 1997; Song et al., 2012), peatlands (e.g. Tokida et al., 2007) and lakes (e.g. Jammet et al., 2015) of northern high-latitudes. During late autumn, CH<sub>4</sub> emis-

Karel 26/2/2018 10:26

Deleted: of these areas

Karel 2/3/2018 11:54

Deleted: propagate

Karel 2/3/2018 11:54

Deleted: to

Karel 23/2/2018 18:23

Deleted:

Karel 2/3/2018 16:12

Deleted: However,

Karel 2/3/2018 16:12

Deleted: during spring

Karel 2/3/2018 16:12

Deleted: , which is mostly anoxic

Karel 2/3/2018 16:13

Deleted: E

Karel 2/3/2018 16:13

Deleted: during spring

Karel 2/3/2018 16:14

Deleted: as well as in

sions still take place when the active layer starts to freeze gradually from the top and ice begins to fill the soil pore spaces, i.e. the so-called zero curtain period. Through this period, the remaining CH<sub>4</sub> in the soil that was produced during the growing season, or in the deeper warm soil layers is squeezed out of the soil. This remaining gas is emitted to the atmosphere via molecular diffusion, and via the “pressure pumping” phenomenon due to advection enhanced by wind (Bowling and Massman, 2011; Massman et al., 1997), through the forming layer of snow (Mastepanov et al., 2008, 2013; Zona et al., 2016). Previous studies have reported that the late autumn CH<sub>4</sub> emissions in Arctic tundra ecosystems account for up to 50 % of the annual CH<sub>4</sub> flux released in the form of gas bursts (Mastepanov et al., 2008; Zona et al., 2016).

Soil and vegetation at northern high-latitudes remain covered by snow during most of the year (October to May). Snow is an effective thermal insulator between the soil and the atmosphere, and it is a porous medium that allows the diffusive exchange of gases. Only few observational efforts have previously been made to constrain gas fluxes through the snow in tundra and permafrost environments during the long and cold Arctic winter. CH<sub>4</sub> emissions have been measured using flux chambers and eddy covariance (EC) towers in various snow-covered areas, e.g. in boreal forest soils (Kim et al., 2007; Whalen and Reeburgh, 1992), boreal peat landscapes bogs and fens (Helbig et al., 2017b; Panikov and Dedysh, 2000; Rinne et al., 2007; Smagin and Shnyrev, 2015), and in subalpine soils (Mast et al., 1998; Wickland et al., 1999). Also, in the Alaskan tundra (Zona et al., 2016) and in the Zackenberg valley in northern Greenland (Mastepanov et al., 2008; Pirk et al., 2016). In boreal peat bogs of West Siberia, cold season CH<sub>4</sub> emissions contribute from 3.5 to 11 % of the annual CH<sub>4</sub> fluxes (Panikov and Dedysh, 2000). In other Arctic permafrost tundra ecosystems, however, winter CH<sub>4</sub> emissions were one to two orders of magnitude lower than the emissions during summer, and only accumulate in the snowpack in the presence of layers of ice blocking their exit route to the atmosphere (Pirk et al., 2016). Wickland et al. (1999) concluded that in snow-covered subalpine wetland soils, CH<sub>4</sub> fluxes accounted for 25 % of the annual fluxes, similarly to the recent results shown in a boreal peat landscape of northwestern Canada (Helbig et al., 2017b). However, there are still large uncertainties in cold season CH<sub>4</sub> emissions from wetlands and permafrost ecosystems of the Arctic tundra, particularly related to projected changes in vegetation phenology due to climate warming which might also lead to changes in snow cover, e.g. more shrubs will tend to hold more snow during winter (Blanc-Betes et al., 2016; Domine et al., 2015). A thicker snow layer will insulate more the soil column during autumn and winter, preserving the heat of the active layer after the preceding growing (zero

- Karel 2/3/2018 16:09  
**Deleted:** “
- Karel 2/3/2018 16:09  
**Deleted:** ”
- Karel 2/3/2018 16:16  
**Deleted:** ,
- Karel 2/3/2018 16:17  
**Deleted:** and still
- Karel 2/3/2018 16:17  
**Deleted:** layers,
- Karel 2/3/2018 16:20  
**Deleted:** Since there are numerous technical limitations to measuring
- Karel 2/3/2018 16:21  
**Deleted:** season in the Arctic, a few observational efforts have previously been made to constrain these emissions. These studies have found evidence for the continuation of CH<sub>4</sub> fluxes through snow during the freeze-in period and wintertime in Arctic tundra and permafrost environments. U
- Karel 2/3/2018 16:27  
**Deleted:** measurements with
- Karel 2/3/2018 16:28  
**Deleted:** , CH<sub>4</sub> emissions have been recorded from snow-covered areas,
- Karel 23/2/2018 18:30  
**Deleted:** in Western Siberia
- Karel 23/2/2018 18:27  
**Deleted:** , boreal fens (Rinne et al., 2007)
- Karel 2/3/2018 16:30  
**Deleted:** Other relevant wintertime studies from
- Karel 2/3/2018 16:30  
**Deleted:** Arctic permafrost and wetland areas include
- Karel 2/3/2018 16:35  
**Deleted:** extent to which
- Karel 2/3/2018 16:35  
**Deleted:** contribute to the annual CH<sub>4</sub> budgets from Arctic
- Karel 2/3/2018 16:35  
**Deleted:** is largely unknown. Also,
- Karel 2/3/2018 16:36  
**Deleted:** in Arctic tundra
- Karel 2/3/2018 16:37  
**Deleted:** more
- Karel 2/3/2018 16:38  
**Deleted:** continuing to contribute to preservation
- Karel 2/3/2018 16:38  
**Deleted:** of

curtain period) season. This will further impact the extent of subsequent wintertime CH<sub>4</sub> productions and emissions.

210 Numerical models have made much progress to better simulating the magnitude and temporal and spatial variability of CH<sub>4</sub> emissions in boreal regions. Methane models include the traditional theoretical and empirical approaches that describe the mechanistic understanding of the processes involved in the production, oxidation and transport of CH<sub>4</sub> in terrestrial ecosystems (e.g. Grant, 1998; Riley et al., 2011; Walter and Heimann, 2000). Previous studies have also  
215 improved the scaling representation from plot to regional areas in specific locations, and also to global frameworks (Bohn et al., 2015; Lawrence et al., 2015; Melton et al., 2013; e.g. Riley et al., 2011; Ringeval et al., 2011; Tagesson et al., 2013; Wania et al., 2010). There are still many shortcomings in land surface models for boreal regions because a complex network of processes and a wide range of spatial and seasonal variation characterize these areas. These  
220 are particularly related to the inability of accounting for methane emissions and uptake in dry non-wetland areas, capturing shifts in vegetation cover (e.g. Chen et al., 2015), representing soil thawing and freezing cycles due to a poor soil thermal physics representation (e.g. Schuldt et al., 2013; Zhu et al., 2014), varying wetland extents and water tables (Bohn et al., 2015), accounting for microtopography effects on surface water and methane emissions dynamics (Cresto Aleina et al., 2013, 2016), upscaling to larger areas or for coupling to earth system models (e.g. Mi et al., 2014; Xu et al., 2015). Also, the majority of models lack a snow scheme that interacts with gas transport and a descriptive representation of peat soils (Xu et al., 2016). Special challenges exist for regional scale model simulations in wetland-dominated areas influenced by climate change, such as in Arctic permafrost ecosystems,  
230 mostly because of the lack of observational constraints sufficient to understand the processes in these areas and to evaluate model outputs.

The aim of this work is to analyze the performance of an improved process-based methane model, designed for Arctic tundra and wetlands underlain by permafrost, when applied to a regional domain in Northeast Siberia. Our intention is to evaluate the potential of a refined process-based methane model as a proof of concept, for its application to larger than site level scales. Also, a regional scale application will allow the identification of spatial heterogeneities in CH<sub>4</sub> emissions in boreal regions. To address these objectives, we simulate year-round CH<sub>4</sub> emissions during 2014 and 2015 with the process-based JSBACH-methane model (Kaiser et al., 2017) in a region dominated by low-lying wetland areas and continuous permafrost in the Russian Far East. This model includes freeze and thaw soil cycles associated with explicit methane production, oxidation and transport. The latter takes place through distinct

Karel 26/2/2018 10:34

Moved (insertion) [5]

Karel 26/2/2018 10:34

Moved (insertion) [4]

Karel 26/2/2018 10:39

Moved (insertion) [6]

Karel 26/2/2018 10:07

Moved down [3]: In this work, we simulate year-round CH<sub>4</sub> emissions during 2014 and 2015 in a region dominated by low-lying wetland areas and continuous permafrost in the Russian Far East. For this, we use the JSBACH-methane model that includes freeze and thaw soil cycles associated with explicit methane production, transport, and oxidation processes (Kaiser et al., 2017).

Karel 26/2/2018 10:15

Deleted: Although to this day numerical models have made much progress towards better simulating the magnitude and temporal and spatial variability of CH<sub>4</sub> emissions from terrestrial ecosystems, there are still many shortcomings in their parameterizations (Xu et al., 2016). The key schemes of these models are based on traditional theoretical and empirical approaches that describe the mechanistic understanding of the processes involved in the production, oxidation and transport of CH<sub>4</sub> in terrestrial ecosystems. [2]

Karel 26/2/2018 10:33

Deleted: , especially for

Karel 26/2/2018 10:33

Deleted: at regional scales

Karel 26/2/2018 10:34

Deleted: that are primarily

Karel 26/2/2018 10:42

Deleted: Models of the emissions of ... [3]

Karel 26/2/2018 10:34

Moved up [4]: (e.g. Schuldt et al., ... [4])

Karel 26/2/2018 10:34

Moved up [5]: (e.g. Chen et al., 2015)

Karel 26/2/2018 10:39

Moved up [6]: (e.g. Mi et al., 2014; ... [5])

Karel 26/2/2018 21:11

Formatted: Subscript

Karel 26/2/2018 10:07

Moved (insertion) [3]

Karel 26/2/2018 10:57

Deleted: In this work,

Karel 26/2/2018 10:57

Deleted: w

Karel 26/2/2018 10:53

Deleted: For this,

Karel 26/2/2018 10:53

Deleted: we use the JSBACH-metha ... [6]

Karel 26/2/2018 11:00

Deleted: t, and oxidation processes

320 pathways: plant-mediated, ebullition, and diffusion. In this work, we use an improved version  
of the model that explicitly simulates CH<sub>4</sub> emissions to the atmosphere in the presence of  
snow during the non-growing season, and also contains a revised representation of CH<sub>4</sub>  
transported by plants including the description of relevant features of vascular plants based  
on the volume of roots in the soil pore space. We present and analyze the year-round tem-  
325 poral variation of the CH<sub>4</sub> emissions and their relationship to the environmental controls at a  
regional (model domain) scale. The model performance was assessed by comparison of the  
simulated CH<sub>4</sub> emissions against year-round EC measurements and summertime chamber  
flux measurements in the same study area. Because temporal variation in the amount of inun-  
dated area is essential for the estimation of CH<sub>4</sub> emissions from wetlands (Prigent et al.,  
2007), our model also includes a representation of inundated areas using a TOPMODEL ap-  
330 proach. We evaluate the modeled horizontal extent of the inundated areas against the wetland  
area from a high-resolution remote sensing product.

## 2. Methods

### 2.1. Site description

The target region of this study is located in Northeast Siberia, Sakha Republic. The model  
335 domain is centered on the town of Chersky and to the west is dominated by low-lying wet-  
land areas of the Kolyma River floodplain and to the east by dry upland tundra (Fig. 1a). This  
is a region of continuous permafrost and active layer depths that range between 20 and 180  
cm. Winter spans from October to May, with daily air temperatures that remain well below  
the freezing point and average daily temperatures of about 13 °C during July (Dutta et al.,  
340 2006). In this region prevail dry climate conditions, with a mean annual precipitation of 218  
mm (60 % as snow and 40 % as rain; Dutta et al., 2006). At the Kolyma River floodplain, the  
soil profile has a top layer of organic material (~15-25 cm thick) that is located above alluvial  
mineral soils, i.e. silty clay (Kittler et al., 2016; Kwon et al., 2016). In this area, the vegeta-  
345 tion is heterogeneous and representative of wet tussock tundra. There, the water-logged areas  
are covered by the tussock-forming sedges (*Carex appendiculata* and *Carex lugens*), and cot-  
ton grasses (*Eriophorium angustifolium*) (Kwon et al., 2016). During the spring snowmelt  
(May and June), large sections of the Kolyma floodplain usually become inundated, and dur-  
ing summer, the extent of surface water recedes due to evapotranspiration and drainage to the  
river channels located nearby. However, most areas remain inundated throughout the year  
350 (Kwon et al., 2016) and microtopographic structures typical of polygonal tundra landscapes  
are sparse in this region. The eastern part of the model domain has more elevated slopes and  
drier soils with tundra vegetation dominated by grasslands and forests, i.e. dwarf evergreen

Karel 26/2/2018 10:58

Deleted: (Kaiser et al., 2017).

Karel 26/2/2018 10:53

Deleted: .

Karel 26/2/2018 10:56

Deleted: The aim of this work is to improve our understanding of year-round CH<sub>4</sub> emissions in an Arctic region dominated by wetlands underlain by permafrost. With this purpose, we simulated CH<sub>4</sub> emissions differentiated among distinct pathways: plant-mediated, ebullition, and diffusion. We ... [7]

Karel 2/3/2018 12:00

Deleted: drivers

Karel 21/2/2018 14:59

Deleted: eddy covariance

Karel 29/11/2017 13:49

Deleted: done

Karel 2/3/2018 12:00

Deleted: of study

Karel 29/11/2017 13:50

Deleted: are

Karel 2/3/2018 16:45

Deleted:

Karel 2/3/2018 12:01

Deleted: at the Russian Far East (

Karel 2/3/2018 12:01

Deleted: of Sakha)

Karel 2/3/2018 16:45

Deleted: to the west

Karel 2/3/2018 16:46

Deleted: is characterized by the presence

Karel 2/3/2018 16:46

Deleted: The long

Karel 2/3/2018 16:46

Deleted: w

Karel 2/3/2018 16:46

Deleted: , while the

Karel 2/3/2018 16:46

Deleted: are

Karel 2/3/2018 16:47

Deleted: D

Karel 2/3/2018 16:47

Deleted: prevail in this region

Karel 26/2/2018 11:21

Deleted: loam

Karel 2/3/2018 16:47

Deleted: , such as

Karel 2/3/2018 16:47

Deleted: ,

Karel 2/3/2018 16:47

Deleted: like

Karel 2/3/2018 16:48

Deleted:

and deciduous shrubs, *Sphagnum* mosses, and lichens, and few trees (Dutta et al., 2006; Merbold et al., 2009). Loess soil deposits originating from the accumulation of aeolian and alluvial sediments characterize the soil in this region.

## 2.2. Model configuration

The model results presented in this work were obtained with a regional configuration in offline mode of the land-surface component of the MPI-ESM (Max Planck Institute for Meteorology Earth System Model), the so-called Jena Scheme for Biosphere Atmosphere Coupling in Hamburg (JSBACH) model. We used a JSBACH version that has been extended from the version of the CMIP5 activity (e.g. Brovkin et al., 2013; e.g. Raddatz et al., 2007; Reick et al., 2013). Modifications include the addition of a multilayer hydrology scheme (Hagemann and Stacke, 2015) and the representation of permafrost physical processes (Ekici et al., 2014). The model domain covers an area of 7 degrees in longitude (158° E to 165° E) and 3 degrees in latitude (66.5° N to 69.5° N). Using a horizontal resolution of 0.5° (Fig. 1b), this results in a model domain with 14×6 equally spaced grid cells. The vertical structure in the model domain comprises 11 non-equidistant soil layers with thicknesses that increase from 6.5 cm at the top to 23.2 m at the bottom, reaching a maximum column depth of 40.5 m.

This vertical refinement is necessary to achieve numerically stable solutions for the gas diffusion equation. In the model domain, the root zone is confined to the top five layers (maximum depth of 1.1 m) with maximum and mean root depths of 0.88 m and 0.42 m respectively. The soil ice content is restricted to the top six layers (maximum depth of 2.0 m), with bedrock located from the 6<sup>th</sup> layer downwards.

In JSBACH, each grid cell has defined fractions for different types of vegetation that are assigned across a maximum of 11 non-equal tiles, hence a hospitable fraction to vegetation, that represents the sub-grid scale heterogeneity of vegetation cover. The remaining fraction of the grid cell where vegetation is not assigned, is then associated to a land cover type that represents areas inhospitable to vegetation such as rocky surfaces and deserts (Reick et al., 2013).

In our model domain, only four land cover types were present (ordered by dominance in the model domain): 1) C3 grasses, 2) deciduous trees, 3) evergreen trees and 4) deciduous shrubs (see Fig. S1 for the spatial distribution of the cover types in the model domain).

The model configuration contains the basic JSBACH modules with components from the Biosphere-Energy-Transfer-Hydrology model, BETHY (Knorr, 2000). The vegetation carbon is categorized into three groups: wood, green, and reserve. The soil carbon and decomposition model Yasso07 (Tuomi et al., 2009, 2011) takes care of the transport and decomposition of carbon into the soil. It simulates the breakdown of litter and soil organic matter based on

Karel 2/3/2018 16:49

Deleted: but

Karel 2/3/2018 12:03

Deleted: A prescribed fraction of each grid cell is used to discriminate between hospitable and inhospitable land (Reick et al., 2013).

Karel 2/3/2018 16:58

Deleted: The hospitable part is then subdivided into a maximum of 11 tiles each of which is assigned a land cover type to represent the sub-grid scale heterogeneity of vegetation cover.

Karel 2/3/2018 17:00

Deleted: These tiles may have different sizes.

Karel 2/3/2018 17:00

Deleted: D

Karel 2/3/2018 17:00

Deleted: E

Karel 2/3/2018 17:00

Deleted: D

Karel 27/2/2018 11:50

Deleted: their

measurements of soil carbon and litterbag experiments, and has been previously implemented into JSBACH (Goll et al., 2015; Thum et al., 2011). In Yasso07, soil litter is divided into three classes: non-woody, woody, and humus. The non-woody class is subdivided into four pools representing groups of chemical compounds with an independent decomposition rate determined by changes in air temperature and precipitation, thus it has no relation to plant species (Goll et al., 2015; Tuomi et al., 2009).

Most of the CH<sub>4</sub> emissions into the atmosphere from Arctic terrestrial ecosystems are from wetland areas, thus the representation of the wetland extent in CH<sub>4</sub> models is of relevance.

We use a TOPMODEL (TOPographic MODEL) approach (Beven and Kirkby, 1979; Kleinen et al., 2012; Stocker et al., 2014) to determine the fraction of any grid cell that is inundated implying it has a water table at or above the soil surface. We obtain a grid cell mean water table position from the soil hydrology scheme (Hagemann and Stacke, 2015) determined from the saturation state of the soil layers: the lowest soil layer that is not completely frozen or completely saturated contains the grid cell mean water table, with the exact location within the layer given as the layer fraction that is saturated. Details on the TOPMODEL scheme in JSBACH are shown in section 1 of supplementary material.

The position of the local water table depth  $z_i$  is used to define the grid cell wetland area (Eq. S1), i.e. the grid cell wetland area is defined where  $z_i \geq 0$  and it is subject to a minimum CTI (compound topographic index) threshold value  $\chi_{\min, \text{cti}}$  that limits the maximum possible areas that can be flooded following the approach of Stocker et al. (2014), with lower values leading to larger wetland areas. In this configuration, the constant prescribed value of  $\chi_{\min, \text{cti}}$  and the exponential decay of transmissivity with depth  $f$  (Eq. S1) are tunable parameters of the TOPMODEL module used to expand or reduce the fraction of inundated surface areas in a model grid cell. Within the inundated fraction of the grid cell, a constant relative soil moisture saturation of 0.95 is assumed. The decomposition of soil organic matter is reduced to 35 % of the aerobic decomposition in line with Wania et al. (2010).

The CH<sub>4</sub> production and emission processes in the model are tightly linked to the volumetric soil porosity to allocate gas transport (Kaiser et al., 2017). This model configuration contains a permafrost module to explicitly simulate soil freeze and thaw processes coupled to the hydrological and thermal regimes in the soil column (Ekici et al., 2014). This is a relevant process in permafrost regions where changes in the soil ice content drive the seasonal changes in the volumetric soil pore space, and changes in the soil moisture ultimately determine whether the soil pores are filled with water or air.

Karel 26/2/2018 11:25

Deleted:

Karel 2/3/2018 17:01

Deleted:

Karel 3/3/2018 10:47

Deleted: In this model, the standard

Karel 3/3/2018 10:47

Deleted: was extended to 11 vertical layers to resolve a grid cell mean water table position. This is

Karel 3/3/2018 10:47

Deleted: by

Karel 3/3/2018 10:29

Deleted: The position of the mean water table in the grid cell is used in a TOPMODEL (TOPographic MODEL) approach (Beven and Kirkby, 1979; Kleinen et al., 2012; Stocker et al., 2014) to define the fraction of the grid cell with a water table at or above the soil surface. With the implementation of this hydrological scheme, JSBACH now has a dynamic wetland module that allows modeling the water table and the fractional area of inundation at a grid cell scale (Kleinen et al., 2012).

Karel 2/3/2018 17:10

Deleted: The main input parameter for TOPMODEL is the so-called compound topographic index, CTI (Kirkby, 1975). CTI represents a topographic profile that is used to define how likely a landscape point is to become water saturated and is defined as  $\gamma_i = \ln(\alpha_i / \tan \beta)$ , where  $\alpha_i$  is a dimensionless index used to determine the source contributing area at point  $i$ , and  $\tan \beta$  is the local slope. Based on statistical information of the CTI, areas in a landscape with similar CTI values will have similar hydrological responses allowing a simplification of the hydrological calculations in the model. In this work, the CTI values were generated from the CEH-UK high-resolution global dataset of topographic index values (Marthews et al., 2015). The distribution of CTI values within a model grid cell was estimated with gamma function ... [8]

Karel 3/3/2018 10:54

Deleted: located at or above the surface. Consequently,

Karel 3/3/2018 10:56

Formatted: Font:(Default) Times New Roman

Karel 3/3/2018 10:56

Deleted:  $\leq z_i$ ,

Karel 2/3/2018 17:12

Deleted: CTI

Karel 3/3/2018 10:56

Deleted: defined to

Karel 3/3/2018 10:57

Deleted:

Karel 2/3/2018 17:14

Deleted: a

### 2.2.1. Methane module

In this work, the JSBACH-methane configuration presented in Kaiser et al. (2017) underwent several modifications. Besides being coupled to TOPMODEL and the soil carbon Yasso07 components, the CH<sub>4</sub> module itself acquired several extensions: i) a refined description of plant-mediated transport, ii) allowance of gas transport via diffusion through the snow during the non-growing season, and iii) change in the order of transport processes. Details on each of these changes are listed in [section 2 of the supplementary material](#).

In the process-based JSBACH-methane module, the equilibrium between the concentrations in free atmosphere, soil air, and soil moisture is assumed for the initialization of the methane and oxygen concentrations in the soil. During each model time step, CH<sub>4</sub> is produced in the soil column depending on the soil hydrological conditions (i.e. ice content and soil moisture), soil temperatures, soil pore space, and the available decomposed carbon. The fraction of CH<sub>4</sub> produced from the total carbon decomposition under anaerobic conditions for mineral soils ( $f_{CH_4anox}$ ) is prescribed as 0.5 (i.e. 50 % of the anaerobically decomposed carbon is used to produce CH<sub>4</sub>). Since this setting is highly uncertain, the model response to a range of  $f_{CH_4anox}$  values is tested in sensitivity experiments as part of this work. [T](#)

[The JSBACH-methane module contains two explicitly modeled CH<sub>4</sub> oxidation processes:](#) bulk soil oxidation and rhizospheric oxidation of methane (plant oxidation). These oxidation pathways interact iteratively in the model with the methane transport processes, reducing the methane pool when oxidation takes place. [Only part of the oxygen in the soil is available for methane oxidation, and this discrimination relates to the amount of carbon dioxide produced during heterotrophic respiration, which uses up to a maximum value of 40 % of the total oxygen content in the soil. An additional 10 % of the available oxygen is assumed to be unavailable because it is used in other processes such as respiration by microbes. This leads to only 50 % of the total oxygen in the soil to be available for CH<sub>4</sub> oxidation.](#)

To facilitate the interaction between the CH<sub>4</sub> and TOPMODEL modules, the ice-free pores of the soil column are [prescribed at a saturation level of 95 % in the fraction of the grid cell that was determined as inundated. This concept mimics the lateral distribution of water that creates water-logged conditions,](#) depending on the topographic profile. However, the soil temperatures, ice content and available carbon for CH<sub>4</sub> production are not [changed in the model](#) during this process. Thus, CH<sub>4</sub> emissions from a grid cell happen under a combination of soil temperatures, ice content, and available carbon decomposition characteristic of an unsaturated soil column on the one hand, and ice-free soil pores with soil moisture at 95 % saturation on the other. Ultimately, the methane production, oxidation, and transport processes only take

Karel 26/2/2018 19:19

Deleted: Appendix A

Karel 2/3/2018 17:18

Deleted: .

Karel 2/3/2018 17:19

Deleted: T

Karel 2/3/2018 17:19

Deleted: are contained in the JSBACH-methane module

Karel 23/2/2018 17:58

Formatted: Subscript

Karel 2/3/2018 17:21

Deleted: in this new model version

Karel 2/3/2018 12:04

Deleted: ed

Karel 2/3/2018 12:04

Deleted: to

Karel 2/3/2018 12:05

Deleted: with moisture to justify the accumulation of water at or above the soil surface

Karel 2/3/2018 12:05

Deleted: influenced

place in the saturated portion of the grid cell (Fig. S2). The transport of the gases to and from the atmosphere is distributed across four explicitly modeled transport processes: plant-mediated transport, ebullition, and molecular diffusion without snow and through the snow.

Karel 2/3/2018 17:23

Deleted: see schematic in

The transport pathways follow a sequential order based on the expected priority with their efficiency based upon prevailing soil moisture content (set to constant 95 % saturation in the inundated areas) taking into account the ice-corrected volumetric soil porosity, which in turn depends on the soil temperature.

Karel 27/2/2018 11:56

Deleted: The efficiency of each transport process is

Karel 2/3/2018 17:25

Deleted: which is

Karel 27/2/2018 11:56

Deleted: and takes

Karel 2/3/2018 17:26

Deleted: aerenchyma system

Karel 2/3/2018 12:05

Deleted: space

The plant-mediated transport in the model only takes place in areas with C3 grasses and follows Fick's first law, including the diffusion of gas between the roots of plants and the surrounding soil pores. In wetland ecosystems, many plants have developed an efficient aerenchyma system that functions as a transport mechanism of gases between the atmosphere and their roots. Plants need oxygen for metabolic processes and the root exodermis is an efficient barrier that keeps the oxygen inside the plant roots and, at the same time, slows down the diffusion of gas from the soil into the roots; thus, the gas flow is restricted by the thickness of the exodermis tissue. In the JSBACH-methane module, the root exodermis has a pre-

scribed diffusivity value of 80 % of the total diffusivity of the same gas in water, for the gas transport from soil into the plant. Ebullition takes place when excess gas that has not been dissolved in the available soil pore liquid water forms bubbles that are rapidly transported upwards from their source in the deep soil layers through the water and into the atmosphere, successfully bypassing the oxic areas in the soil. Diffusion is the molecular transfer of gas from high to low concentration gradients between soil layers and the atmosphere following Fick's second law. In this model version, diffusion is now also allowed to take place through a layer of snow using a simplified formulation that does not take into account the enhanced advection of gas in the snowpack due to wind, i.e. pressure pumping.

Karel 2/3/2018 12:06

Deleted: , for the gas between the plant and the surrounding soil pores

Karel 27/2/2018 11:54

Deleted: In combination with a shallow root zone and few gas transporting roots therein, in the original JSBACH-methane model, plant-mediated transport was the slowest emission process and therefore took place only after ebullition and molecular diffusion. For the configuration of this work this condition was modified (see Appendix A for further details).

Karel 2/3/2018 12:06

Deleted: ,

Karel 2/3/2018 12:06

Deleted: and i

Karel 2/3/2018 17:30

Deleted: it

Karel 2/3/2018 12:07

Deleted: . The latter is

Karel 2/3/2018 12:08

Deleted: amounts are

Karel 2/3/2018 17:33

Deleted: The detailed description of how these processes and transport pathways are modeled in JSBACH-methane can be found in

Karel 27/2/2018 12:00

Deleted: .

Karel 2/3/2018 17:36

Deleted: were also used to drive the model

Karel 2/3/2018 17:36

Deleted: .

Between the model time steps, the amount of gas is constant, whereas the gas concentrations change in relation to the varying ice-free pore space. Further details on how these schemes are included in the model are shown in the supplementary material, and for more details the reader is also referred to Kaiser et al. (2017).

### 2.2.2. Experimental set up and sensitivity experiments

The model was forced with the daily reanalysis atmospheric data CRUNCEPv7 (The Climate Research Unit from University of East Anglia, analysis of the National Centers for Environmental Prediction reanalysis atmospheric forcing version 7.0) from 1901-2015 with a spatial resolution of 0.5° (Viovy and Ciais, 2016). Prescribed annual means of atmospheric CO<sub>2</sub> values (<https://www.esrl.noaa.gov/gmd/ccgg/trends/global.html>), were also used to drive the

655 model. The model was spun-up for 10,000 years of simulation by repeating cycles of atmospheric data from 1901-1930 (~330 cycles) to equilibrate the soil carbon pools and ensure pre-industrial steady state (Chadburn et al., 2017; McGuire et al., 2016). The total carbon (woody, green and reserve) after spin up in the entire model domain showed little change over the last 500 years of the spin up period. The methane module was de-activated during  
660 this procedure. After that, simulations were initialized with reanalysis data from 1931 until 2015 (85 years). To allow equilibration of the soil carbon pools to the hydrology as well as equilibration of CH<sub>4</sub>, a model adjustment period of 850 years (10 cycles using the 85 years of reanalysis data) was added. After this period, the subsequent output of the model was stored and used for data analysis. In this simulation, we used prescribed reference values for parameters in the TOPMODEL and methane modules that represent the control simulation. A description of the most relevant prescribed parameters and variables in the control simulation is outlined in Table 1.

To evaluate the robustness of the model and identify the parameters to which the model is most sensitive, a set of sensitivity experiments was done following a cost efficient parameter-permutation approach (Saltelli et al., 2000). Six model parameters that are prescribed in the model and are involved in the newly modified code for this model version were selected. These parameters are either not provided in published literature, the published values are largely uncertain due to the nature of method used to obtain these values, or the measured values cover a wide range of options characterizing different conditions in nature. The selected parameters are:  $\chi_{\min\_cti}$  for the evaluation of TOPMODEL,  $d_r$  and  $R_{fr}$  for the evaluation of plant-mediated transport,  $h_{\text{snow}}$  and  $\phi$  for evaluation of the transport via diffusion through the snow, and the fraction of anoxic decomposed carbon that becomes CH<sub>4</sub> ( $f_{\text{CH}_4\text{anox}}$ ) for the evaluation of the methane production. For each parameter, reference values from the control simulation were decreased or increased for one parameter at a time, by a fixed value (shown together with the results in Table 2), resulting in a total of 12 independent sensitivity simulations.

The values for the parameters  $\chi_{\min\_cti}$ ,  $d_r$  and  $R_{fr}$  and  $h_{\text{snow}}$  are highly uncertain. The first one is a parameter that is part of the TOPMODEL parameterization, whereas the rest are highly uncertain or absent in published literature, therefore we decided to choose extreme values with respect to their values in the control simulation. The selected values for  $\phi$  and  $f_{\text{CH}_4\text{anox}}$  were kept within ranges reported in the literature. The snow porosity is derived from measurements of snow and ice, and ultimately controls the amount of gas that can diffuse through the

Karel 26/2/2018 19:25

Deleted:

Karel 2/3/2018 18:24

Deleted: Among other modules,

Karel 2/3/2018 18:24

Deleted: t

Karel 2/3/2018 18:25

Deleted: 11<sup>th</sup> cycle was stored

Karel 2/3/2018 18:26

Deleted: subsequent

Karel 23/2/2018 14:32

Deleted:

Karel 23/2/2018 14:32

Deleted: was done to test s

Karel 23/2/2018 14:34

Deleted: selected

Karel 23/2/2018 14:47

Deleted: whose value is prescribed and are involved in the newly modified parts of the code for this model version: the simulation of inundated areas (TOPMODEL module), diffusion of methane through plants and snow, and the allocation of soil carbon under anaerobic conditions for methane production.

Karel 23/2/2018 14:38

Deleted:

Karel 23/2/2018 15:00

Deleted: Specifically,

Karel 23/2/2018 15:00

Deleted: t

Karel 23/2/2018 15:04

Deleted: of previously

Karel 23/2/2018 15:04

Deleted: values

snow layer. Different snow densities lead to different snow porosities: 330 kg/m<sup>3</sup> ( $\phi=0.64$ ) for wind packed snow), 263 kg/m<sup>3</sup> ( $\phi=0.71$ ) for settled snow and 128 kg/m<sup>3</sup> ( $\phi=0.86$ ) for fresh damp new snow. These values were tested to reflect the effect of gas diffusion through less to more porous snow layers. All  $\phi$  values were calculated with  $\rho_{ice} = 910 \text{ kg/m}^3$ .

The parameter  $f_{CH4anox}$  is highly uncertain in literature. In our model, a setting of  $f_{CH4anox} = 1.0$  would imply that all of the decomposed soil carbon would become CH<sub>4</sub> under anaerobic conditions. The value used in the reference simulation is 0.5. In the context of the sensitivity experiments, we decrease  $f_{CH4anox}$  to 0.1 (i.e. 10 % of the decomposed carbon will become CH<sub>4</sub> and 90 % will be oxidized), and to 0.3 (i.e. 30 % of the decomposed carbon will become CH<sub>4</sub> and 70 % will be oxidized).

Each sensitivity simulation consisted of a re-initialization from the conditions in the control simulation from the last time step on 31 December 1999. This was to allow the model to adjust to the parameter change for 13 years before the year of result analysis (i.e. 2014). In order to keep consistency in the treatment of our simulations, the same re-initialization procedure was done for a reference simulation by re-initializing the control simulation from the restart conditions on 31 Dec 1999, as in the sensitivity experiments, but without changing any parameter (i.e. maintaining the same parameters as in the control simulation). The results from the sensitivity experiments were compared to the results from the reference simulation. The temporal resolution of all the model simulations is 30 min, with hourly output averaged for analysis into daily and monthly values.

### 2.3. Observational data

#### 2.3.1. Wetland product

Methane emissions to the atmosphere in the model occur largely from areas with a water table at or above the surface. These fractions of “inundated” areas in each model grid cell represent the horizontal extent of wetlands (including lakes, peatlands, or temporally inundated areas). As described in Section 2.2, in our study the inundated fraction for each grid cell is estimated through the TOPMODEL approach. For evaluation, we compared the spatial distribution of the inundated areas per grid cell to the wetland extent remote sensing product from ENVISAT ASAR (European Space Agency’s ENVISAT with an Advanced Synthetic Aperture Radar operating in Wide Swath mode C-band). The ENVISAT ASAR WS-wetland product (EAWS) was tested for operational monitoring in northern Russia, where small-scale ponds and an overall high soil moisture level are common surface features (Reschke et al., 2012). The backscatter of the EAWS product for high latitudes has a higher spatial and tem-

Karel 23/2/2018 15:13

Formatted: Superscript

Karel 23/2/2018 15:04

Deleted: , whereas for the other four parameters tested we chose extreme values with respect to the defined values in the control simulation

Karel 23/2/2018 15:26

Moved (insertion) [2]

Karel 23/2/2018 15:26

Deleted: A value of

Karel 23/2/2018 15:27

Deleted: would mean

Karel 23/2/2018 15:27

Deleted: .

Karel 27/2/2018 12:02

Deleted: ,

Karel 2/3/2018 18:35

Deleted: is

Karel 2/3/2018 18:35

Deleted: for each grid cell

Karel 27/2/2018 12:02

Deleted: To evaluate the performance of TOPMODEL in our model configuration,

poral resolution (150 m and 2 to 3 days, respectively) than other commonly used wetland products (e.g. Prigent et al., 2007), which have spatial resolutions of the order of kilometers. Thus, the EAWS product is able to capture small water bodies like tundra ponds and wetland patches that remain almost unchanged throughout the year and are associated with permafrost areas. The spatial coverage of the EAWS product includes most of northern Russia and is subdivided into 10 mosaics, each with different coverage areas. It is freely available as GeoTIFF images, each representing a 10-days-mean in a wetland map during July and August in 2007 (i.e. 01-10 July, 11-20 July, 21-31 July, 01-10-August, 11-20 August, 21-31 August, all in 2007; Reschke et al., 2012).

For the evaluation of the modeled wetland extent, each 10-days-mean image of the EAWS product was mapped to the same grid of georeferenced rectangular cells of the JSBACH domain. From the total 84 model grid cells, 35 model grid cells fall into the area coverage of the EAWS images (Fig. 1b). The wetland fraction from the EAWS remote sensing product ( $w_{rs}$ ) in percentage was calculated as the ratio of pixels flagged as wetland (ID = 1) to the total number of pixels contained in the grid cell. In the model, the spatial wetland fraction ( $w_{mod}$ ) is represented as the fraction of the total grid cell area that is inundated (i.e. with a water table at or above the soil surface). To facilitate a direct comparison against  $w_{rs}$ , the  $w_{mod}$  values from the control simulation were averaged to the same 10-days-mean in 2007 as the remote sensing data.

### 2.3.2. Chamber measurements

To evaluate the performance of the methane model, we compared the total modeled methane fluxes ( $F_{mod}$ ) to the total methane fluxes measured with flux chambers ( $F_{ch}$ ) in the Kolyma River floodplain (Fig. 1b, see also Kwon et al., 2016). In this study, chamber fluxes from an undisturbed control area were considered for model evaluation purposes. The chamber flux measurements were done during the early to mid-growing season (15 June to 20 August) in 2014. As additional ancillary variables, water table depth, vegetation cover, and soil temperature were also measured. For further details on the gas measurements, calculations, and discussion of the chamber flux results the reader is referred to Kwon et al. (2016).

The surface area of each chamber along the control transect is  $0.36 \text{ m}^2$ , therefore even all 10 chambers combined can only represent a very small fraction of the surface area of a single model grid cell ( $2.5 \times 10^9 \text{ m}^2$ ). However, since both  $F_{mod}$  and  $F_{ch}$  are normalized to a unit area ( $\text{CH}_4/\text{m}^2/\text{day}$ ), it is possible to directly compare  $F_{ch}$  to  $F_{mod}$ . For the model evaluation exercise, we extracted the daily  $F_{mod}$  corresponding to the same dates of the chambers flux measurements, and only the emissions from that model grid cell where the chamber plots were ge-

Karel 2/3/2018 18:36

**Deleted:** This product has been previously evaluated against other land cover and wetland products.

Karel 2/3/2018 18:37

**Deleted:**

Karel 2/3/2018 18:37

**Deleted:** in our

Karel 2/3/2018 12:12

**Deleted:** about

ographically positioned (grid cell A, Fig. 1b). We also show the results from an adjacent grid cell (grid cell B, Fig. 1b) to demonstrate the spatial heterogeneity between the model grid cells for a region close to the chamber flux measurements. This specific 2<sup>nd</sup> grid cell was chosen to highlight the fact that even areas that appear similar in overall ecosystem structure can produce deviating CH<sub>4</sub> flux rates, for example influenced by environmental factors such as soil depth, inundation fractions or C3 grass coverage.

Due to the heterogeneous topographic characteristics in the study site, the microsites of the chamber plots within the control area include water-saturated (average water table during the growing season > 10 cm below the surface, observed in 8 chamber plots) and unsaturated characteristics (dry soil conditions, i.e. water table < 10 cm below the surface, observed in 2 chamber plots, Kwon et al., 2016). Thus, the total  $F_{ch}$  from the chamber plots was averaged separately for the wet plots ( $F_{ch\_wet}$ ) and for the dry plots ( $F_{ch\_dry}$ ). This heterogeneity in the data finds its equivalent in the model grid cell heterogeneity as estimated by TOPMODEL, where on average only a portion of the grid cell area is inundated and the rest remains dry during a specific period of time. Thus, to obtain the total  $F_{ch}$  the chamber flux measurements,  $F_{ch\_wet}$  and  $F_{ch\_dry}$  were scaled to the daily-inundated fractions  $w_{mod}$  for the selected model grid cell  $g$ :

$$F_{ch} = F_{ch\_wet} \cdot w_{mod} + F_{ch\_dry} \cdot (1 - w_{mod}) \quad (1)$$

At two of the chamber sites, temperature sensors (hereinafter referred to as redox systems) continuously recorded the soil temperature profile at three soil depths (4, 16, and 64 cm). The redox systems are located in a site dominated by dry soils and a site dominated by wet soils, and thus these temperature measurements reflect the important influence of soil water levels on the soil thermal regime across the seasons.

### 2.3.3. Eddy covariance measurements

The model results were also compared to ecosystem-scale methane fluxes measured by an EC tower situated in the Chersky floodplain near the north end of the chamber plot transect in a control area (Tower 2 at 68.62° N and 161.35° E in Fig. 1 of Kittler et al., 2016). The observation height is at 5.11 m a.g.l., and fluxes are available at 30 min intervals. For details on the instrumental setup, raw data collection, and EC data post-processing, the reader is referred to Kittler et al. (2016; 2017). The analysis of uncertainties in the EC data is presented in Appendix A. The field of view (“footprint area”) of an EC system with the given sensor height above the ground normally extends up to several hundred meters in the main wind direction at any given time, changing with atmospheric turbulence conditions. (Fig. 1 of Kittler et al.,

Karel 2/3/2018 12:13  
Formatted: Superscript

Karel 2/3/2018 12:15  
Formatted: Subscript

Karel 26/2/2018 19:26  
Deleted: 8

Karel 21/2/2018 14:59  
Deleted: eddy covariance

Karel 21/2/2018 14:53  
Moved (insertion) [1]

Karel 5/3/2018 10:32  
Deleted: the

Karel 21/2/2018 14:53  
Moved up [1]: near the north end of the chamber plot transect in the control area (Tower 2 in Fig. 1 of Kittler et al., 2016)

Karel 21/2/2018 14:54  
Deleted: This tower is located at 68.62° N and 161.35° E,

Karel 21/2/2018 14:54  
Deleted: and has an instrument

Karel 21/2/2018 14:54  
Deleted: of

Karel 2/3/2018 12:15  
Deleted: at an elevation of 6 m a.s.l. The data

Karel 21/2/2018 15:02  
Deleted: eddy covariance

Karel 15/12/2017 09:06  
Deleted: g

Karel 21/2/2018 14:59  
Deleted: eddy-covariance

Karel 2/3/2018 12:16  
Deleted:

Karel 21/2/2018 15:18  
Deleted: see e.g.

2016). The position of the EC tower falls within the area of model grid cell A (shown in Fig. 1b) and far away from the grid cell borders; thus, it is assumed that all the CH<sub>4</sub> fluxes measured with the EC system fall within the area of grid cell A. To improve this comparison due to the difference of spatial scale between the EC footprint and model grid cell areas, for the former we analyzed the vegetation composition within the footprint using highest resolution land cover maps based on WorldView-2 remote sensing imagery. For this analysis, we aggregated vegetation classes to differentiate between areas of predominant wet soils or wetlands (dominated by the cotton grass *Eriophorum angustifolium*) and dry soils (dominated by shrubs and the tussock *Carex appendiculata*). We then compared the extent of the wetlands to the inundated fractional area of the model grid cell considered as the corresponding model wet area. It has been recently shown in the literature that the type of vegetation in tundra landscapes is a good indicator of the spatial distribution and variation of CH<sub>4</sub> fluxes (Davidson et al., 2017), and it is also expected that the majority of the CH<sub>4</sub> fluxes are emitted from wetlands in tundra ecosystems (Helbig et al., 2017a). About 26 % of the fluxes measured by the EC tower were emitted from wetland areas within the footprint, i.e. from wet soils with cotton grasses. Within the entire model grid cell A, the inundated fraction is between 17.7 % and 19.9 % (10-day mean values in summer months) during the summer of 2014, while C3 grasses cover 33.3 % of the area (with no explicit separation between cotton grasses and tussocks). To investigate the EC methane fluxes for a smaller wetland area similar to that one in the model grid cell, it is possible to linearly scale the 10-day mean EC methane fluxes to the inundated fraction from the model, resulting in CH<sub>4</sub> fluxes that might be closer to those from the model. Results of this scaling approach for fluxes in summer 2014 are shown in Appendix A.

### 3. Results

#### 3.1. Evaluation of inundated areas

Within the context of this analysis, fractions of inundation are given as the percentage of the total grid cell area that holds water at or above the surface. The first comparison between remote sensing ( $w_{rs}$ ) and simulated ( $w_{mod}$ ) wetland extents, using an initial TOPMODEL configuration, showed that the model mostly overestimated the extent of inundated fractions. For example, in the predominantly wet sections north of the model domain ( $> 68.5^\circ N$ ), the averaged  $w_{rs}$  is 9 % whereas  $w_{mod}$  was simulated at 15 %. However, in drier areas ( $< 68.5^\circ N$ )  $w_{rs}$  is on average 1.2 % whereas the model did not predict inundation in those grid cells. Since modeled methane emissions only take place in the inundated areas of a grid cell, it was necessary to modify the prescribed TOPMODEL parameters to improve  $w_{mod}$  towards  $w_{rs}$ . To

Karel 21/2/2018 15:18  
Deleted: , for an example of a footprint  
Karel 21/2/2018 15:02  
Deleted: eddy covariance  
Karel 21/2/2018 15:00  
Deleted: emissions  
Karel 21/2/2018 15:00  
Deleted: eddy covariance

Karel 21/2/2018 15:08  
Formatted: Font:Italic  
Karel 21/2/2018 15:09  
Formatted: Font:Italic

Karel 21/2/2018 16:30  
Formatted: Subscript  
Karel 21/2/2018 16:30  
Formatted: Subscript

Karel 22/2/2018 13:34  
Formatted: Subscript

Karel 22/2/2018 13:35  
Deleted: .

Karel 2/3/2018 21:08  
Deleted: fractions

Karel 2/3/2018 21:08  
Deleted: based on the original

Karel 2/3/2018 21:09  
Deleted: .

Karel 2/3/2018 21:10  
Deleted: .

achieve this, the initially prescribed maximum threshold for inundation ( $\chi_{\min\_cti}$ ) was modified in a similar fashion than for the sensitivity experiments through a step change of the parameter value and subsequent analysis of results, until the horizontal extent of inundated areas in the model decreased compared to the results of the initial configuration. Changes in this value have an effect only on wet areas. In Fig. 2 the latitudinal distribution of the percent difference between  $w_{\text{mod}}$  and  $w_{\text{rs}}$  for 01-10 August 2007 after parameter adjustment (i.e.  $\chi_{\min\_cti}=12$ ) is depicted. We show only the results corresponding to one EAWS image because the results are similar for the other five available GeoTIFF images. The distribution of modeled grid cell inundated areas during the same period of time is shown in the inset of Fig. 2: model grid cells with more than 1 % of inundated area are found from the northwest to the southeast part of the model domain, and also include some grid cells in the western and northern parts. The spatial distribution of the modeled inundated areas throughout the year does not vary considerably because the inundated fraction in the model takes into account the accumulation of liquid and frozen water. However, the fraction of inundation within each grid cell varies in relation to drier or wetter conditions. After parameter adjustment through step change tests, the comparison between  $w_{\text{mod}}$  and  $w_{\text{rs}}$  resulted in a mean difference of  $-1\pm 8\%$  and a median of 2 % integrated over all the six 10-days-mean periods. However, some outlier values result in considerable single-pixel differences between  $w_{\text{mod}}$  and  $w_{\text{rs}}$ , ranging from +19 % in the southernmost areas ( $< 68.5^\circ \text{ N}$ ) to  $-23\%$  in the northernmost areas ( $> 69^\circ \text{ N}$ ). The best agreement between model and EAWS product is observed between latitudes  $68.5^\circ$  and  $69^\circ \text{ N}$  (Fig. 2).

During the process of optimization between  $w_{\text{mod}}$  and  $w_{\text{rs}}$ , the parameter  $f$  was not modified because this would influence both the inundated and dry areas of a grid cell. The best value for  $\chi_{\min\_cti}$  that resulted in a closer agreement between  $w_{\text{mod}}$  and  $w_{\text{rs}}$  is applied in the configuration of the control and reference simulations of this work. We exemplify the effect on the modeled methane emissions due to changes in the  $\chi_{\min\_cti}$  value, and include this parameter in the sensitivity experiments shown in the following section.

### 3.2. Sensitivity experiments

We investigated the impact of different values for selected model parameters (shown in column two of Table 2) on the individual transport processes and total  $\text{CH}_4$  emissions. We compared the results from the reference simulation at daily resolution in 2014 to six pairs of sensitivity experiments (Fig. 3, with pairs of sensitivity experiments shown as panels within rows a through f). The annual mean model domain  $\text{CH}_4$  emissions for each experiment are

Karel 27/2/2018 09:57

Deleted: so that

Karel 2/3/2018 21:14

Deleted: for the selected value of

Karel 2/3/2018 21:14

Deleted: (

Karel 2/3/2018 21:14

Deleted: i.e.

Karel 2/3/2018 21:12

Deleted: since

Karel 2/3/2018 21:16

Deleted: a change of this parameter would

Karel 2/3/2018 21:17

Deleted: chosen

Karel 2/3/2018 21:19

Deleted: used

Karel 2/3/2018 21:19

Deleted: for

Karel 2/3/2018 21:17

Deleted: in

Karel 2/3/2018 21:20

Deleted: of

Karel 2/3/2018 21:20

Deleted: 3.2

Karel 2/3/2018 21:20

Deleted: To

Karel 2/3/2018 21:21

Deleted: of

Karel 2/3/2018 21:21

Deleted: , w

also summarized in Table 2. From all the sensitivity experiments, a significant difference in model output between the reference simulation and the simulations with modified settings was found only for parameters  $\chi_{\min\_cti}$  and  $f_{CH4anox}$  (for both variables  $n=365$  and  $p<0.01$  after a nonparametric Wilcoxon rank-sum test; see also Fig. 3, all panels in row a and f).

The prescribed threshold parameter  $\chi_{\min\_cti}$  in the TOPMODEL module sets the maximum possible area in the grid cell that can be flooded. A higher  $\chi_{\min\_cti}$  value leads to a larger wetland extent in already inundated areas within the model grid cell. Consequently, our results show that a change in  $\chi_{\min\_cti}$  has a large effect on the CH<sub>4</sub> emissions: describing  $\chi_{\min\_cti} = 13$  leads to nearly 1.5 times higher CH<sub>4</sub> emissions during summer and autumn compared to the results using the reference value of 12, and about two times higher than the results with the lower  $\chi_{\min\_cti}$  test value of 11 (Fig. 3, row a). The effect of varying  $\chi_{\min\_cti}$  in the resulting model mean inundated fraction is shown in Fig. S3 of the supplementary material. With the higher  $\chi_{\min\_cti}$  value (i.e. 13), the annual average of the inundated fraction in the model domain (0.054) increases by 54 %, whereas with the lower  $\chi_{\min\_cti}$  value (i.e. 11) the annual average inundated fraction in the model domain (0.024) decreases by 35 %, both with respect to the annual average of the inundated fraction in the model domain from the reference simulation (0.0367).

The  $f_{CH4anox}$  parameter is a prescribed fixed value used to define the fraction from the total decomposed soil organic matter that will be allocated for CH<sub>4</sub> production (i.e. anoxic carbon mineralization), with the rest becoming CO<sub>2</sub>. As in many other land surface models, only mineral soils are considered in our model configuration (limitation further discussed below in Sect. 4.3). For a  $f_{CH4anox}$  value of 0.5 (control) the resulting mean summertime CH<sub>4</sub> emissions in the model domain were five times higher than the emissions with lower  $f_{CH4anox}$  values (0.1 or 0.3) (Fig. 3, row f).

The remaining parameters tested in this sensitivity test (Table 2) show that with the chosen values, the simulated CH<sub>4</sub> emissions are not significantly different from each other. The  $d_r$  parameter associated with the plant-mediated transport pathway shows that the difference between the simulated CH<sub>4</sub> emissions is not statistically significant through the year between fine plant roots of 2 mm (as defined in the reference simulation) and thicker roots of 8 mm (Fig. 3, row b). A small variation can be noted for ebullition and diffusion mostly during July (Fig. 3, column 1 and 2 of row b). The difference in emissions due to an increase in the soil root volume from 20 % to 60 % is also not statistically significant (Fig. 3, row c).

Karel 2/3/2018 21:23

Deleted: predefined

Karel 26/2/2018 11:16

Deleted: I

Karel 23/2/2018 15:26

**Moved up [2]:** A value of  $f_{CH4anox} = 1.0$  would mean that all of the decomposed soil carbon would become CH<sub>4</sub> under anaerobic conditions. The value used in the reference simulation is 0.5.

Karel 26/2/2018 11:16

Deleted: , this is considered for mineral soils only

Karel 23/2/2018 15:29

Deleted: In the context of the sensitivity study, we tested the effect on the simulated CH<sub>4</sub> emissions by decreasing

Karel 23/2/2018 15:29

Deleted: to 0.1 (i.e. 10 % of the decomposed carbon will become CH<sub>4</sub>, whereas 90 % will be oxidized), and to 0.3 (i.e. 30 % of the decomposed carbon will become CH<sub>4</sub> whereas 70 % will be oxidized). The

Karel 23/2/2018 15:32

Deleted: responded evidently to changes in the value of  $f_{CH4anox}$ : with

Karel 23/2/2018 15:34

Deleted:

Karel 23/2/2018 15:33

Deleted: the largest  $f_{CH4anox}$  value of 0.5,

Karel 23/2/2018 15:34

Deleted: the summer CH<sub>4</sub> emissions were five times higher than the summer emissions with the lower  $f_{CH4anox}$  value of 0.1

Karel 2/3/2018 21:26

Deleted: within

Karel 2/3/2018 21:26

Deleted: is

Karel 2/3/2018 21:27

Deleted: study

For the selected parameters associated with the emissions of CH<sub>4</sub> through the snow, the porosity of snow  $\phi = 0.64$  used in the reference simulation ( $\rho_{\text{snow}}$  of 330 kg/m<sup>3</sup> for wind packed snow), has a mean tortuosity  $\tau = 0.77$ , calculated with Eq. S6 (suppl. material). The tortuosity value decreases with denser snow, thus for  $\phi = 0.71$  corresponds a  $\tau = 0.79$  ( $\rho_{\text{snow}} = 263$  kg/m<sup>3</sup> for aged settled snow), whereas for  $\phi = 0.86$  means a  $\tau = 0.85$  ( $\rho_{\text{snow}}$  of 128 kg/m<sup>3</sup> for fresh damp new snow). Our sensitivity results from these experiments show that the differences between the winter CH<sub>4</sub> emissions through a layer of fresh damp snow, or through a wind packed snow layer, are not statistically significant (Fig. 3, row d).

Finally, the fixed limiting snow depth, which discriminates between ordinary CH<sub>4</sub> transport via diffusion and diffusion through the snow, was also tested. In the reference simulation, this switch happens at a fixed  $h_{\text{snow}} \geq 5$  cm. In the sensitivity experiments, we decreased  $h_{\text{snow}}$  to 3 and 1 cm. The results show that differences between the individual and total CH<sub>4</sub> emissions through various  $h_{\text{snow}}$  values are not statistically significant (Fig. 3, row e). A time shift is seen however, in the CH<sub>4</sub> emissions from mid-October until mid-November (Fig. 3, column 4 of row e), with larger emissions through snow taking place earlier if  $h_{\text{snow}}$  is thinner. Nevertheless, this temporal shift in the CH<sub>4</sub> emissions through the snow does not influence the total CH<sub>4</sub> emissions. The regionally aggregated CH<sub>4</sub> transport via ebullition, diffusion and plants during the same months is reduced as  $h_{\text{snow}}$  becomes thinner, thus compensating for the shift in the emissions in the presence of snow and maintaining a mass balance in the annual total emissions.

### 3.3. Evaluation of modeled emissions with eddy covariance and chamber measurements

#### 3.3.1. Evaluation of year-round modeled total CH<sub>4</sub> emissions

The methane emissions from EC measurements used here to evaluate the modeled CH<sub>4</sub> emissions at grid cell scale spans from April 2014 until September 2015, while data from chamber measurements are restricted to the period of June to August 2014. The modeled total CH<sub>4</sub> emissions used for this comparison correspond to the grid cell where both the EC tower and the chambers are geographically located (grid cell A, Fig. 1b). Also, we show the modeled total CH<sub>4</sub> emissions from the neighboring grid cell to the west (grid cell B, Fig. 1b) and further discuss their association with environmental variables and prescribed parameters in the model. The EC data presented here has been subject to a thorough quality check, and gap-filling was subsequently applied to produce a continuous time series (see Appendix A for details also on uncertainties analysis). For the year-round data evaluation it is not possible to

- Karel 23/2/2018 15:35  
Deleted: corresponds to a
- Karel 23/2/2018 15:35  
Deleted: , characteristic of
- Karel 23/2/2018 15:35  
Deleted: and
- Karel 26/2/2018 19:26  
Deleted: 6
- Karel 23/2/2018 15:37  
Deleted: We tested two other values of  $\phi$ , and by doing so simulated the properties of other types of snow:  $\phi = 0.71$  corresponds to a settled snow type with  $\rho_{\text{snow}}$  of 263 kg/m<sup>3</sup>, and  $\phi = 0.86$  corresponding to fresh damp new snow with a lower  $\rho_{\text{snow}}$  of 128 kg/m<sup>3</sup> (both  $\phi$  values were calculated with  $\rho_{\text{ice}} = 910$  kg/m<sup>3</sup>). The tortuosity value also decreases with denser snow, thus the corresponding  $\tau$  values are 0.79 and 0.85 for aged and fresh snow, respectively
- Karel 2/3/2018 21:47  
Deleted:
- Karel 29/11/2017 14:20  
Deleted: Our
- Karel 29/11/2017 14:20  
Deleted: the
- Karel 29/11/2017 14:26  
Deleted: Visually
- Karel 29/11/2017 14:26  
Deleted: an effect is seen
- Karel 2/3/2018 21:48  
Deleted: the
- Karel 29/11/2017 14:26  
Deleted: in time and being of a large ... [9]
- Karel 2/3/2018 21:49  
Deleted: is not observed in
- Karel 2/3/2018 21:53  
Deleted: To evaluate the model per ... [10]
- Karel 2/3/2018 21:52  
Deleted: M
- Karel 21/2/2018 15:03  
Deleted: eddy covariance
- Karel 2/3/2018 21:52  
Deleted: are
- Karel 2/3/2018 21:53  
Deleted: available
- Karel 21/2/2018 15:01  
Deleted: eddy covariance
- Karel 26/2/2018 19:34  
Deleted: show
- Karel 26/2/2018 19:34  
Deleted: (section 3.3.4)
- Karel 26/2/2018 19:34  
Deleted: .

1065 apply the suggested linear scaling approach between the EC flux and model flux data, based  
on the vegetation type as indicator of wetland areas in the EC footprint and the inundated  
fraction predicted in the model (section 2.3.3). This is due to the lack of year-round vegeta-  
tion coverage from remote sensing data that would otherwise allow obtaining a temporal var-  
ying wetness area for the EC footprint. However, the results shown in Appendix A from the  
1070 suggested scaling approach for data in summer 2014 serve as a demonstration that: 1) the ar-  
eas with wet soils within the EC footprint and the model grid cell, translated into the areas  
where the majority of the CH<sub>4</sub> emissions take place, show only minor differences, and 2) the  
offset between methane fluxes from EC and from the model can be largely attributed to these  
differences in the extent of wetland areas. In the course of this manuscript we will consider  
1075 the EC fluxes as representative for the processes within the entire model grid cell, therefore  
allowing a direct comparison to the modeled CH<sub>4</sub> fluxes.  
Despite the large spatial scale of the modeled emissions, the monthly mean of the CH<sub>4</sub> emis-  
sions from the EC and chamber measurements agree well with the monthly model results for  
the grid cells A and B and for 2014 and 2015. Positive correlations between the measured and  
modeled CH<sub>4</sub> fluxes, with correlation coefficients (R<sup>2</sup>) higher than 0.95, are observed in all  
1080 comparisons except for the correlation between the chamber measurements and the results  
from grid cell B (R<sup>2</sup>=0.85; Fig. 4). Fig.5a and b display box plots of the monthly mean CH<sub>4</sub>  
emissions for summer months (June, July, and August) from each data set: both grid cells (A  
and B), EC data for 2014 and 2015, and chamber flux measurements for 2014 only. In 2014,  
the median of the CH<sub>4</sub> emissions from grid cell B is consistently higher than the rest of the  
1085 other compared datasets, and this is followed by the EC fluxes (Fig. 5a). The same is ob-  
served in 2015 (except for the lack of chamber flux measurements during that year; Fig. 5b).  
During both years, the median of the modeled CH<sub>4</sub> emissions from grid cell A is generally  
lower than the rest of the compared data sets (Fig. 5a and b).  
The time series of the monthly mean CH<sub>4</sub> emissions from the model grid cell A and B is  
1090 compared with the observational datasets in Fig. 5c. The shaded area around the mean values  
is one standard deviation calculated from the daily values; thus, it represents the range of var-  
iability in the emissions within each month. To analyze the contribution of uncertainties in  
the daily variability of the EC data, random (due to e.g. turbulent sampling or instrument er-  
ror) and systematic (e.g. instrument calibration or drift) errors in this data set were assessed.  
1095 The uncertainties in the EC data are given as error bars in the monthly averages in Fig. 5c and  
account on average for 0.35±0.22 mg CH<sub>4</sub> m<sup>-2</sup> d<sup>-1</sup> of the monthly emissions. These uncertain-

Karel 22/2/2018 13:56  
Formatted: Subscript

Karel 2/3/2018 22:00  
Deleted: Considering

Karel 21/2/2018 15:01  
Deleted: eddy covariance

Karel 2/3/2018 22:01  
Deleted: only

Karel 21/2/2018 15:01  
Deleted: eddy covariance

Karel 21/2/2018 15:01  
Deleted: eddy covariance

Karel 26/2/2018 12:35  
Deleted:

ties are smaller than the spread of the daily variability. A summary of the methods followed to account for these errors is presented in Appendix A.

For the two years of analysis, modeled CH<sub>4</sub> emissions of grid cell A underestimate the EC monthly values by 4.7±8.1 mg CH<sub>4</sub> m<sup>-2</sup> d<sup>-1</sup>. However, the modeled values from grid cell B are higher for most of 2014 and 2015 by as much as 6.1±10.5 mg CH<sub>4</sub> m<sup>-2</sup> d<sup>-1</sup>. During winter, the model CH<sub>4</sub> emissions from both grid cells are on average 3.7 mg CH<sub>4</sub> m<sup>-2</sup> d<sup>-1</sup> lower than the EC measurements (Fig. 5c). The modeled CH<sub>4</sub> emissions from both grid cells show large interannual variability. This is evidenced in Fig. 6, which compares the standard deviation of the monthly fluxes between the two years of analysis. In the model results, particularly grid cell B shows large interannual variability in summer months (10.9 mg CH<sub>4</sub> m<sup>-2</sup> d<sup>-1</sup> in June and 5.6 mg CH<sub>4</sub> m<sup>-2</sup> d<sup>-1</sup> in July).

Methane emissions from the chamber flux measurements are lower than the model results of both grid cells for June and July 2014 (on average by 16.6 mg CH<sub>4</sub> m<sup>-2</sup> d<sup>-1</sup> in June and 24.3 mg CH<sub>4</sub> m<sup>-2</sup> d<sup>-1</sup> in July), but also than the EC flux data (on average 15.3 mg CH<sub>4</sub> m<sup>-2</sup> d<sup>-1</sup> and 25.1 mg CH<sub>4</sub> m<sup>-2</sup> d<sup>-1</sup> in June and July, respectively). However, the results from grid cell A are in closer agreement with the chamber flux measurements, with the chamber data showing larger emissions by 8.2 mg CH<sub>4</sub> m<sup>-2</sup> d<sup>-1</sup> compared to results from grid cell A during August 2014. The shaded areas of the EC data evidence the largest spread in daily variability of all of the presented data sets, particularly in summer months. Thus, despite the disagreement between monthly mean values, there is an obvious overlap in the shaded areas between all data sets during 2014, while a larger disagreement is observed only during the summer of 2015 between results from grid cell B and EC data (Fig. 5c).

The root mean square error between the daily CH<sub>4</sub> fluxes from grid cell A and the observations, normalized to the mean of the measurements (NRMSE = RMSE / mean (CH<sub>4</sub>)<sub>obs</sub> x 100) is on average < 30 % from June to October for both years, while for spring and winter is on average 80 % with the maximum NRMSE during May in 2014 (107 %) and 2015 (104 %). Thus, the large variation of the measured daily fluxes in summer leads to a lower error when compared to the summertime modeled fluxes, whereas the lower magnitude and variation in wintertime fluxes leads to capture a larger error between modeled values and the observations.

### 3.3.2. Relationship between soil temperatures and CH<sub>4</sub> emissions

To examine the relationship between soil temperatures and CH<sub>4</sub> emissions, we first compared the modeled and measured soil temperature profiles. The temporal evolution of the vertical profiles of daily soil temperatures, measured with the redox systems, is shown in Fig. 7a for

Karel 26/2/2018 12:31

Deleted: Compared to the eddy covariance measurements,

Karel 26/2/2018 12:29

Deleted: the model

Karel 26/2/2018 12:31

Deleted: s

Karel 26/2/2018 12:29

Deleted: CH<sub>4</sub> emissions in grid cell A

Karel 26/2/2018 12:20

Deleted: , but

Karel 2/3/2018 22:06

Deleted: (Fig. 5c)

Karel 26/2/2018 12:20

Deleted: Averaged over both years, results from grid cell A are lower than the results from the eddy covariance measurements by 4.7±8.1 mg CH<sub>4</sub> m<sup>-2</sup> d<sup>-1</sup>. In contrast, CH<sub>4</sub> emissions from grid cell B are on average larger than the eddy covariance measurements by as much as 6.1±10.5 mg CH<sub>4</sub> m<sup>-2</sup> d<sup>-1</sup>.

Karel 21/2/2018 15:01

Deleted: eddy covariance

Karel 26/2/2018 11:37

Deleted: ; however, the interannual variability of the observations is even larger than the model data.

Karel 21/2/2018 15:02

Deleted: eddy covariance

Karel 2/3/2018 22:07

Deleted: (Fig. 5c)

Karel 26/2/2018 12:39

Deleted: -

Karel 26/2/2018 12:36

Deleted: D

Karel 26/2/2018 12:36

Deleted: from the model and observations from eddy covariance and chamber fluxes

Karel 26/2/2018 12:26

Deleted: monthly variability

Karel 26/2/2018 12:37

Deleted: as depicted by the shaded areas. It is furthermore important to note that (... [11])

Karel 26/2/2018 12:38

Deleted: A

Karel 26/2/2018 12:03

Deleted: the eddy covariance

Karel 26/2/2018 12:39

Deleted: However, the daily varia (... [12])

Karel 26/2/2018 12:33

Deleted:

Karel 23/2/2018 11:07

Deleted: -

Karel 26/2/2018 14:37

Deleted: 6

the wet plot and in Fig. 7b for the dry plot in 2015. The measured soil temperatures were only available from August to December in 2014, and behaved similarly in 2015 for the same months. The temperature values measured with the sensors at 4, 16, and 64 cm depth were linearly interpolated every 2 cm through the vertical soil column to construct the soil temperature profiles shown in Fig. 7a and b. For comparison, the modeled vertical profiles of the daily soil temperatures in 2015 for the top four soil layers (bottom depth of 3, 12, 29, and 58 cm) in grid cells A and B were also linearly interpolated every 2 cm (Fig. 7c and d). During winter and spring, the measured soil temperatures are not lower than  $-16\text{ }^{\circ}\text{C}$ , while the modeled temperature values are as low as  $-26\text{ }^{\circ}\text{C}$  within extended sections of the period from December to May. The measured values in the dry plot show abrupt temperature changes during the transition between freezing conditions ( $< 0\text{ }^{\circ}\text{C}$ ) and warmer conditions ( $> 0\text{ }^{\circ}\text{C}$ ) during mid-December and mid-May. This abrupt change is also seen in the wet plots with freezing conditions remaining for a shorter period of time; i.e. the change to and from warmer temperatures takes place only from the end of January until mid-May. Also, generally colder temperatures are observed in the top part of the soil column and gradually extend to deeper soil layers as the season progresses. In contrast, although the modeled soil temperatures reach lower values during winter, a smoother transition of temperature is evidenced from freezing to warmer conditions in spring, and to freezing conditions again in autumn. In the model results, the soil temperature remains homogeneous along the vertical profile. Measured temperatures above freezing conditions occur from mid-June until the end of September. As summer progresses, warmer soil temperatures extend from the surface to deeper soil layers (Fig. 7a and b). In the dry plot, however, the warmer conditions remain only in the top 16 cm of the soil column (Fig. 7b) due to lower soil moisture content and lower thermal conductivity compared to the wet plot. The model is able to capture the timing of the seasonal transition from spring to summer at the end of May, the duration of the summer conditions, and the magnitude of the temperature values. For grid cells A and B, the summer temperature profiles are more similar to the wet than to the dry plot. The average measured soil temperature in the range of the sensor's depths (top 64 cm) during summer (June, July, and August, 2015) in the dry plot was  $2.1\text{ }^{\circ}\text{C}$ , while in the wet plot for the same period the average measured soil temperature was  $4.7\text{ }^{\circ}\text{C}$ ; in the model, the average soil temperature in the top 58 cm is about  $4.9\text{ }^{\circ}\text{C}$  during summer of 2015. The modeled warm soil temperatures ( $> 5\text{ }^{\circ}\text{C}$ ) reach deeper soil layers in summer; however, this is not observed in the measured data. This could simply be due to the coarse vertical resolution of the data because of the large gap between sensors (from 16 to 64 cm depth). Thus, to evaluate the extent of the warm soil temperatures

Karel 26/2/2018 14:37

Deleted: 6

Karel 3/3/2018 11:07

Deleted: ; thus we show here only the vertical profiles for 2015

Karel 3/3/2018 11:08

Deleted: To construct the soil temperature profiles,

Karel 3/3/2018 11:08

Deleted: t

Karel 26/2/2018 14:38

Deleted: 6

Karel 3/3/2018 11:10

Deleted: in both 2014 and 2015

Karel 3/3/2018 11:57

Deleted:

Karel 26/2/2018 14:38

Deleted: 6

Karel 26/2/2018 14:38

Deleted: 6

Karel 3/3/2018 11:15

Deleted: between the

Karel 3/3/2018 11:15

Deleted: of the redox systems, with a large gap between

Karel 3/3/2018 11:15

Deleted: and

Karel 3/3/2018 11:16

Deleted: deeper

depicted in the model, this portion of the soil column needs to be better resolved vertically by the measurements.

A larger disagreement between measured and modeled soil temperatures, however, occurs during the transition from autumn to winter. The measured temperatures remain around  $-3$  °C in the top 64 cm from October to mid-December, until they change abruptly to around  $-10$  °C in the dry plot during mid-December (Fig. 7b), and in the wet plot towards the end of January (Fig. 7a). In contrast, the model results show a gradual transition between the seasons, with decreasing soil temperatures to values  $< 0$  °C starting in mid-October (Fig. 7c and d).

To investigate the effect on the CH<sub>4</sub> emissions due to the abrupt changes in the measured soil temperatures, we plotted the soil temperature at 12 cm (for model data) and at 16 cm (measured values for the wet plot) against the total CH<sub>4</sub> emissions for grid cells A and B and from EC measurements in 2014 (Fig. 8). The modeled soil temperatures represent the entire grid cell conditions, whereas the CH<sub>4</sub> emissions are only from the saturated and inundated portion of the grid cell (Fig. S2). Despite this disagreement, CH<sub>4</sub> processes in the model follow the seasonal variation in soil temperature. This relationship, however, is only possible to analyze on a qualitative basis. A positive non-linear correlation between soil temperatures and CH<sub>4</sub> emissions is observed in all comparisons. Fitted polynomial curves are plotted on top of each data set. During 2015 (and 2014, data not shown), the CH<sub>4</sub> emissions measured with EC drop faster with the changes of temperature until freezing conditions. Between  $-3$  and  $-14$  °C, little variation in the lowest CH<sub>4</sub> emissions is observed, whereas the change of modeled CH<sub>4</sub> emissions with respect to changes in soil temperature is more gradual within that range of sub zero temperatures. Lower methane emissions in the model compared to those in the EC data, take place in winter and are associated with even lower soil temperatures than the ones registered by the sensors in the redox systems.

### 3.4. Year-round modeled methane emissions

Domain means of the seasonal courses of CH<sub>4</sub> emissions from the different CH<sub>4</sub> transport pathways in 2014 and 2015 from the reference simulation, as well as the daily mean snow depth, are shown in Fig. 10. The results show a distinct seasonality for each of the individual methane emission pathways. Overall, the lowest CH<sub>4</sub> emissions occur between November and May. During these months, the timing of the CH<sub>4</sub> emissions through the snow is largely modulated by the changes of the snow depth, and accordingly, takes place predominantly in spring and autumn. The methane emissions via plants, ordinary molecular diffusion, and ebullition are mostly restricted to the period May through mid-November in areas when and

- Karel 3/3/2018 11:16 Deleted:
- Karel 26/2/2018 14:38 Deleted: 6
- Karel 26/2/2018 14:38 Deleted: 6
- Karel 26/2/2018 14:38 Deleted: 6
- Karel 3/3/2018 11:17 Deleted:
- Karel 3/3/2018 11:17 Deleted: that
- Karel 3/3/2018 11:17 Deleted: have on the CH<sub>4</sub> emissions
- Karel 3/3/2018 11:32 Deleted: average
- Karel 3/3/2018 11:32 Deleted: and dry
- Karel 21/2/2018 15:02 Deleted: eddy covariance
- Karel 26/2/2018 14:38 Deleted: 7
- Karel 2/3/2018 12:29 Deleted: ,
- Karel 21/2/2018 15:02 Deleted: eddy covariance
- Karel 3/3/2018 11:38 Deleted: low 0
- Karel 3/3/2018 11:39 Deleted: constant
- Karel 3/3/2018 11:39 Deleted: are
- Karel 3/3/2018 11:40 Deleted: despite the further decrease in soil temperature. In contrast
- Karel 3/3/2018 11:40 Deleted: , especially from autumn to winter
- Karel 3/3/2018 11:41 Deleted: in both years, until
- Karel 3/3/2018 11:41 Deleted: few
- Karel 3/3/2018 11:44 Deleted: The lower simulated soil temperatures in the model might explain the l... [13]
- Karel 26/2/2018 15:24 Formatted: Font:Not Bold
- Karel 3/3/2018 13:03 Deleted: <#>Winter emissions ... [14]
- Karel 26/2/2018 15:44 Formatted ... [15]
- Karel 3/3/2018 12:38 Deleted: variability

1295 | where  $h_{\text{snow}}$  does not exceed 5 cm (or it is absent). The magnitude of the CH<sub>4</sub> emissions through molecular diffusion is the least relevant among the four modeled transport pathways.

### 3.4.1. Summertime CH<sub>4</sub> transport pathways

1300 | From May to mid-November, CH<sub>4</sub> emissions take place only in the grid cells with inundated areas, with the highest flux rates simulated for the center west of the domain (Fig. S5). During this period  $h_{\text{snow}}$  is either absent or does not exceed 5 cm. Ebullition precedes the emissions through plants during late March 2014 and during early April 2015. In both years, the mean of the CH<sub>4</sub> emissions in the model domain through ebullition rise steadily, followed by a short but pronounced decrease to 3.5 mg CH<sub>4</sub> m<sup>-2</sup> d<sup>-1</sup>, the ebullition of CH<sub>4</sub> rises again to reach its maximum during mid summer with similar magnitude in both years (7.2 mg CH<sub>4</sub> m<sup>-2</sup> d<sup>-1</sup>). This maximum is achieved later in 2014 (9<sup>th</sup> of August) than in 2015 (16<sup>th</sup> of July) and during the same days than the peak of maximum gas transported through plants. The domain means of the CH<sub>4</sub> emissions through plants reached their maximum value of 15 mg CH<sub>4</sub> m<sup>-2</sup> d<sup>-1</sup> in both years. Similar to ebullition, right after the summer maximum of emissions, the emissions through plants start to decrease until mid-November. In contrast to 2014, a shoulder is shaped in the emissions through ebullition and plants, and to less extent in diffusion, during the end of August to mid September in 2015, indicating the continuation of CH<sub>4</sub> emissions even as the soil starts to freeze (Fig. 9). Annually, CH<sub>4</sub> transported by plants is the dominant pathway, contributing 61 % to the total domain mean annual CH<sub>4</sub> emissions. These emissions take place from May to mid-November in areas where  $h_{\text{snow}} < 5$  cm, and are restricted to areas where C3 grasses are present (Fig. S1 and the panels of the first column in Fig. S5). The gas transported through ebullition is 33.9 % in 2014 and 35.7 % in 2015 of the total annual CH<sub>4</sub> emissions.

1310 | Methane emissions through ordinary molecular diffusion also take place if  $h_{\text{snow}} < 5$  cm in the inundated portion of the grid cells (panels in the third column of Fig. S5). In the absence of snow during summer and early autumn, CH<sub>4</sub> emissions via diffusion in the model domain average about  $2.9 \times 10^{-3}$  mg CH<sub>4</sub> m<sup>-2</sup> d<sup>-1</sup> (similar in 2014 and 2015), while during late autumn, winter and early spring the emissions via this pathway are only possible if  $h_{\text{snow}} \geq 5$  cm. For those few grid cells with  $h_{\text{snow}} < 5$  cm during the non-growing season (November to May), the CH<sub>4</sub> emitted via molecular diffusion is two to three orders of magnitude lower (mean of  $3.4 \times 10^{-5}$  mg CH<sub>4</sub> m<sup>-2</sup> d<sup>-1</sup> for both years) than during the growing season (June to September) (Fig. 9). Methane transported via molecular diffusion during the growing season contributes only 0.02 % to the total CH<sub>4</sub> annual budget.

Karel 3/3/2018 12:38

Deleted: simply

Karel 26/2/2018 14:40

Deleted: 11

Karel 3/3/2018 12:48

Deleted: , reaching up to 5 mg CH<sub>4</sub> m<sup>-2</sup> d<sup>-1</sup> by mid June. Following

Karel 3/3/2018 12:48

Deleted: However,

Karel 3/3/2018 12:48

Deleted: t

Karel 3/3/2018 12:50

Deleted: After its maximum in 2014, ebullition of gas steadily

Karel 3/3/2018 12:52

Deleted: s

Karel 3/3/2018 12:50

Deleted: from mid-August until mid-November, while in 2015 the emissions via ebullition remain high during most of July and start to decrease steadily only in August, leveling up during the first part of September and after that continuing to decrease until

Karel 3/3/2018 12:55

Formatted: Subscript

Karel 3/3/2018 13:04

Deleted: 10

Karel 3/3/2018 13:00

Deleted: contributed

Karel 3/3/2018 13:01

Deleted: to

Karel 3/3/2018 12:57

Deleted: Annually, CH<sub>4</sub> transported by plants is the dominant pathway, contributing 61 % of the total domain mean annual CH<sub>4</sub> emissions. These emissions take place from May to mid-November in areas where  $h_{\text{snow}} < 5$  cm, and are restricted to areas where C3 grasses are present (Fig. S1 and panels of the first column in Fig. 11). The domain means of the CH<sub>4</sub> emissions through plants reached their maximum by 5<sup>th</sup> August in 2014 and by 16<sup>th</sup> July in 2015 with a maximum value of 15 mg CH<sub>4</sub> m<sup>-2</sup> d<sup>-1</sup> in both years (Fig. 10).

Karel 26/2/2018 14:40

Deleted: 11

1360 **3.4.2. Impact of snow on the winter and seasonal variation of CH<sub>4</sub> emissions**

1365 During early spring, late autumn and winter, methane emissions take place through a layer of snow  $\geq 5$  cm deep. The mean maximum accumulation of snow in the model domain takes place in spring: earlier in 2014 (0.23 m on 21<sup>st</sup> March) than in 2015 (0.17 m on 8<sup>th</sup> March). The spatial distribution of the spring snow depths in 2014 and 2015 (Fig. S4<sub>a</sub> and <sub>b</sub>) show deeper snow layers in the dryer southwestern part of the model domain. On average, the layer of snow starts to melt rapidly at the beginning of May in 2014 and at the end of April in 2015, reaching total snowmelt by 2<sup>nd</sup> June 2014 and 27<sup>th</sup> May 2015 (Fig. 9). The average CH<sub>4</sub> emissions through the snow in the entire model domain during January and February are 0.17 mg CH<sub>4</sub> m<sup>-2</sup> d<sup>-1</sup> in 2014 and 0.12 mg CH<sub>4</sub> m<sup>-2</sup> d<sup>-1</sup> in 2015. The CH<sub>4</sub> emissions fluctuate through the winter, and these changes are related to changes in the thickness of the snow cover. During the rapid snowmelt period in spring (March, April and May), the daily domain average CH<sub>4</sub> emissions to the atmosphere through the snow increase (Fig. 9) with domain mean average spring CH<sub>4</sub> emissions of 0.65 CH<sub>4</sub> mg m<sup>-2</sup> d<sup>-1</sup> and 0.43 mg CH<sub>4</sub> m<sup>-2</sup> d<sup>-1</sup> in 2014 and 2015, respectively. The maximum domain mean daily emissions of CH<sub>4</sub> outside the growing season are modeled during May, with 1.66 mg CH<sub>4</sub> m<sup>-2</sup> d<sup>-1</sup> in 2014 and 0.96 mg CH<sub>4</sub> m<sup>-2</sup> d<sup>-1</sup> in 2015, and these take place predominantly in the central part of the model domain (panels in the fourth column of Fig. S5). In the entire model domain, the emissions of CH<sub>4</sub> through snow contribute 4.7 % and 2.7 % to the total mean annual CH<sub>4</sub> emissions for 2014 and 2015, respectively. Although deeper spring snow layers are modeled in 2014 than in spring 2015 (Fig. 9) in the areas where CH<sub>4</sub> is emitted to the atmosphere (Fig. S4<sub>a</sub> and <sub>b</sub>), the total methane emissions through snow from January to mid-May amount to  $\sim 70$  mg CH<sub>4</sub> m<sup>-2</sup> in 2014, and only 66 % of that value in 2015 ( $\sim 46$  mg CH<sub>4</sub> m<sup>-2</sup>; Fig. 9). Integrated over the model domain during autumn, the snow starts to accumulate later in 2014 (9<sup>th</sup> October 2014) than in 2015 (30<sup>th</sup> September 2015), and the snow layer becomes rapidly deeper until December at a similar accumulation rate for both years (Fig. 9). As the snow accumulates, the emissions via ebullition and plants decline, but diffusion through snow rises as soon as the snow depth reaches 5 cm in some grid cells. From November to December, the mean CH<sub>4</sub> emissions through the snow in the domain amount to 37.3 mg CH<sub>4</sub> m<sup>-2</sup> in 2014, and 33 % less in 2015 (12.4 mg CH<sub>4</sub> m<sup>-2</sup>). The modeled CH<sub>4</sub> emissions through the snow only consider the ordinary molecular diffusion of CH<sub>4</sub> between the soil and the atmosphere, and the pressure pumping effects due to advection of gas by wind is not taken into account.

1385 At the grid cell level, in Fig. 11 we show the CH<sub>4</sub> emissions through the snow from the EC measurements and those from grid cell A and B simulated by the JSBACH model, all at daily

Karel 3/3/2018 12:58  
Deleted: [16]

Karel 2/3/2018 12:30  
Formatted: Font color: Auto

Karel 26/2/2018 15:18  
Deleted: c

Karel 26/2/2018 15:18  
Deleted: d

Karel 3/3/2018 13:31  
Deleted: 12a

Karel 3/3/2018 13:32  
Deleted: (Fig. 10 and Fig. 12g)

Karel 3/3/2018 13:32  
Deleted: (Fig. 12g)

Karel 3/3/2018 13:32  
Deleted: (Fig. 12a)

Karel 3/3/2018 13:14  
Deleted: 10

Karel 3/3/2018 13:32  
Deleted: (Fig. 12g)

Karel 26/2/2018 14:41  
Deleted: 11

Karel 3/3/2018 13:33  
Deleted: 12a

Karel 26/2/2018 15:19  
Deleted: c

Karel 26/2/2018 15:19  
Deleted: d

Karel 3/3/2018 13:14  
Deleted: 10

Karel 3/3/2018 13:33  
Deleted: 12a

1410 resolution. The time series of daily emissions are shown from the beginning of October 2014  
to the end of April 2015 (Fig. 11a) and in October 2015 (Fig. 11c). The difference between  
the model methane emissions for grid cells A and B, and EC data is shown in Fig. 9b and d  
for the same cold season periods. Comparable to the EC measurements, the winter emissions  
in the model drop abruptly at the end of October 2014, remaining low until March 2015. Dur-  
1415 ing October 2014, the model CH<sub>4</sub> emissions in grid cell B are higher, while the emissions  
from grid cell A are more similar to the EC measurements (Fig. 11a). This is also found in  
the first half of October 2015 (Fig. 11c). However, during this month the EC measurements  
show no clear trend, while the model CH<sub>4</sub> emissions show a decreasing trend over time. Dur-  
ing most of the winter in 2014/2015 (i.e. from November 2014 until April 2015), the modeled  
1420 CH<sub>4</sub> emissions from grid cells A and B remain lower than the EC measurements by on aver-  
age 2.8 mg CH<sub>4</sub> m<sup>-2</sup> d<sup>-1</sup>. During January, February and March in 2015 the mean model CH<sub>4</sub>  
emissions for grid cells A and B are 0.4 mg CH<sub>4</sub> m<sup>-2</sup> d<sup>-1</sup>, while the EC data show persistently  
higher values averaging 3.8 mg CH<sub>4</sub> m<sup>-2</sup> d<sup>-1</sup> for the same months (Fig. 11a). Model emissions  
start rising (2.0 mg CH<sub>4</sub> m<sup>-2</sup> d<sup>-1</sup>) to values similar to those in the EC data (2.8 mg CH<sub>4</sub> m<sup>-2</sup> d<sup>-1</sup>)  
1425 only in mid-April.

To investigate if the CH<sub>4</sub> emissions from the model during the entire wintertime are equiva-  
lent to the total winter emissions measured by EC, we calculated the cumulative sum of the  
modeled CH<sub>4</sub> emissions and EC from October 2014 to March 2015. The uncertainty as the  
standard deviation of the monthly cumulative fluxes is shown in error bars for each data set  
1430 (Fig. 11e). Our results show that, despite a higher earlier release of methane in grid cell A,  
the modeled total emissions released during that winter are not equivalent to those from the  
EC measurements, with the latter providing evidence for larger total CH<sub>4</sub> emissions in winter  
than predicted by the model. The cumulative uncertainties are also larger in the eddy covari-  
ance data and this is due to the large daily variability compared to the model results. In our  
1435 model, the emissions through the snowpack take only into account the molecular diffusion of  
gas, whereas the advection of gas due to wind as an additional transport pathway is not in-  
cluded.

### 3.4.3. Impact of environmental controls on CH<sub>4</sub> flux seasonality

Several systematic interannual differences between the timing and magnitude of the individu-  
1440 al CH<sub>4</sub> transport pathways in 2014 and 2015 were found in the model results. These include  
e.g. the maxima of the individual emissions, which occur a few days later in 2014 than in  
2015. To improve the interpretation of the temporal variability of CH<sub>4</sub> emissions through the  
different pathways, we analyze the temporal changes in soil temperatures within the root

1445 | zone (top five soil layers) as simulated by the model. It is important to note that because of  
the current structure of the model, the depicted soil temperature in Fig. 10b reflects the aver-  
age conditions of the entire grid cell, and not only the inundated portion with saturated soils  
where CH<sub>4</sub> emissions take place. Still, the analysis of the temporal changes in the mean grid  
cell soil temperatures gives an indication of the nature and magnitude of the seasonal changes  
that indirectly control the CH<sub>4</sub> emissions. The gradient of temperatures in the root zone for  
1450 | the entire domain between spring and summer is steeper in 2015 than in 2014 (Fig. 10b). The  
maximum soil temperatures are similar in both years (8.7 °C); however, this maximum was  
reached at the beginning of August in 2014 while in 2015 the maximum was reached at the  
beginning of July and remained high throughout August. During the rest of the year, the  
mean soil temperatures were 2 °C higher in 2014 compared to 2015 (-4.5 °C and -6.5 °C,  
1455 | respectively). The mean changes in temperature in the top five soil layers reflect the changes  
in the air temperature as given in the atmospheric forcing data. According to the mean air  
temperature in the model domain, the summer of 2014 was colder than the summer of 2015  
(by up to 10 °C for individual days during June, Fig. S6a). This leads to delayed warming of  
the soil, later high CH<sub>4</sub> production, and thus a later release of CH<sub>4</sub> into the atmosphere during  
1460 | summer in 2014 than in 2015, as shown in Fig. 10a. These findings are in good agreement  
with those recently presented in Helbig et al., (2017b). In a comparison of meteorological  
records of air temperature between 2013 and 2016 in northwestern Canada, the authors found  
that the coldest May of those years took place in 2014. As a result, during that year a shift in  
air temperature influenced the soil temperature, and with it the year-to-year methane fluxes,  
1465 | especially during spring.  
Figure 10c depicts the model domain mean relative soil moisture content in the top five soil  
layers for 2014 and 2015. As with soil temperature, the soil moisture reflects the average  
conditions of the entire grid cell and not just those in the inundated portion where the soil  
moisture is set to nearly saturation levels. Although these values are not linked to the area of  
1470 | the grid cell where CH<sub>4</sub> is transported and emitted, we can still show the temporal changes of  
soil moisture content in the non-saturated portion of the grid cell between years and seasons.  
These changes can be linked to changes in precipitation patterns (Fig. S6b) and soil tempera-  
tures. According to the mean precipitation from the CRU-NCEP reanalysis data, more precip-  
itation fell in the model domain during early July in 2014 compared to the same period in  
1475 | 2015 (Fig. S6b). This led to the top five soil layers becoming wetter on average in 2014 (Fig.  
10c) and potentially allowed higher thermal capacity in the soil during that period. In con-  
trast, more precipitation fell during most of August and September 2015 than for the same

Karel 26/2/2018 15:33  
Deleted: 2

Karel 26/2/2018 15:33  
Deleted: 2

Karel 26/2/2018 14:41  
Deleted: 5

Karel 26/2/2018 15:34  
Deleted: 2

Karel 3/3/2018 13:24  
Deleted: h

Karel 3/3/2018 13:43  
Deleted: 2

Karel 26/2/2018 14:41  
Deleted: 5

Karel 26/2/2018 14:42  
Deleted: 5

Karel 26/2/2018 15:34  
Deleted: 2

1490 periods in 2014 (Fig. S6b), leading to an increase in the relative moisture content towards end  
of summer and early autumn (Fig. 10c). These changes in soil moisture influence the soil  
temperature at the grid cell scale, and thus the soil temperature feedbacks to the CH<sub>4</sub> process-  
es. Therefore, it is possible to indirectly relate the effects of changes in grid cell scale soil  
moisture to the changes in the modeled CH<sub>4</sub> emissions.

1495 The mean relative soil ice content in the top five layers of the model domain (Fig. 10d) was  
higher in winter and spring of 2014 than in 2015, and this is a general observation for the en-  
tire domain. However, the air temperatures from the reanalysis data during that period were  
on average higher in 2014 than in 2015 (Fig. S6a). The ice content decreases at a fast rate  
during June in both years, however the complete loss of ice in the soil is reached earlier in  
June of 2015 than in 2014, and this is a reflection of colder temperatures in June 2014, delay-  
ing the complete melt of the more abundant ice in the soil during that year relative to the  
same month in 2015 (Fig. S6a). The soil ice content feeds back to the modeled available pore  
1500 space for CH<sub>4</sub> production, thus the ice content changes in the soil can be indirectly linked to  
the CH<sub>4</sub> emissions. The earlier reduction of ice content in the soil during June 2015 might  
have contributed to the earlier release of methane during that month, via ebullition, compared  
to 2014 (Fig. 9). The lower air and soil temperatures at the beginning of autumn in 2015 (Fig.  
S6a) led to higher ice content in the soil during October 2015 compared to 2014 (Fig. 10d).  
1505 The soil temperatures remain warmer in autumn of 2014, enabling more CH<sub>4</sub> to be emitted  
during November 2014 when the snow starts to accumulate in contrast to 2015 (Fig. 9 and  
10a).

#### 4. Discussion

##### 4.1. Sensitivity experiments

1510 Through the model sensitivity experiments we identified that changes to the values of the pa-  
rameters  $\chi_{\min\_cti}$  and  $f_{CH_4anox}$  caused statistically significant differences in the total CH<sub>4</sub> emis-  
sions ( $p < 0.001$ ). A significant increase in CH<sub>4</sub> emissions with increasing inundated surface  
area (TOPMODEL parameter  $\chi_{\min\_cti}$ ) highlights the importance of this approach to regulate  
the extent of the grid cell inundated areas. However, further investigations and improvements  
1515 in the TOPMODEL approach, as well as a better integration into the hydrology scheme of  
JSBACH, are needed in order to better constrain the modeled CH<sub>4</sub> emissions with JSBACH.

The results of our sensitivity experiments also provided evidence that the magnitude of the  
simulated CH<sub>4</sub> emissions responds strongly to changes in the parameter values of the fraction  
of anaerobic decomposed soil organic matter that becomes methane,  $f_{CH_4anox}$ . In soil systems

Karel 26/2/2018 14:42  
Deleted: 5

Karel 26/2/2018 14:45  
Deleted: .

Karel 26/2/2018 14:44  
Deleted: during

Karel 26/2/2018 14:43  
Deleted: most of the

Karel 26/2/2018 14:44  
Deleted: in 2015

Karel 26/2/2018 15:34  
Deleted: 2

Karel 26/2/2018 15:34  
Deleted: 2

Karel 26/2/2018 14:42  
Deleted: 5

Karel 26/2/2018 14:42  
Deleted: 5

Karel 3/3/2018 13:45  
Deleted: 12f

Karel 26/2/2018 14:42  
Deleted: 5

Karel 26/2/2018 15:34  
Deleted: 2

Karel 3/3/2018 13:46  
Deleted: 12g

Karel 3/3/2018 13:46  
Deleted: h

Karel 23/2/2018 16:09  
Deleted: .

Karel 26/2/2018 15:59  
Moved down [7]: Our sensitivity experi-  
that changes in the values of most of the se-  
lected parameters result in no significant dif-  
ferences in the modeled CH<sub>4</sub> emissions for the  
individual pathways or the total flux. Specifi-  
cally, varying the diameter of roots from finer  
to thicker, and varying the amount of availa-  
ble soil volume occupied by roots, di... [17]

Karel 3/3/2018 13:46  
Deleted: Our sensitivity experimen... [18]

Karel 26/2/2018 16:00  
Deleted: .

Karel 26/2/2018 16:00  
Deleted: C

Karel 27/2/2018 12:14  
Moved (insertion) [8]

Karel 27/2/2018 12:14  
Deleted: the

Karel 27/2/2018 12:15  
Deleted: value of

Karel 26/2/2018 16:00  
Deleted: . [19]

1575 where fermentation and methanogenesis are exclusive processes, i.e. without the presence of  
alternative pathways for respiration via terminal electron acceptors by other microbial groups  
that ultimately can suppress the production of CH<sub>4</sub>, the CO<sub>2</sub>:CH<sub>4</sub> ratio after anaerobic carbon  
1580 mineralization is normally 1:1 (Conrad, 1999), i.e.  $f_{\text{CH}_4\text{anox}} = 0.5$ . We used this value in the  
reference simulation because it was previously reported in the literature as characteristic of  
water-saturated polygon centers (Preuss et al., 2013), and it is similar to the value reported  
for unsaturated zones in boreal bogs (Whalen and Reeburgh, 2000). However, in wetland ar-  
1585 eas, CH<sub>4</sub> is still subject to oxidation after its production and the CO<sub>2</sub>:CH<sub>4</sub> ratio is expected to  
increase and to vary among types of wetlands (Bridgman et al., 2013). Thus, although the  
value of  $f_{\text{CH}_4\text{anox}}$  determines the fraction of CH<sub>4</sub> produced under anoxic conditions, this CH<sub>4</sub>  
still can undergo oxidation before it is emitted to the atmosphere. Furthermore,  $f_{\text{CH}_4\text{anox}}$  can be  
theoretically related to the fraction of CH<sub>4</sub> that is left after oxidation and before it is emitted  
1590 to the atmosphere ( $f_{\text{ox}} = 1 - f_{\text{CH}_4\text{anox\_left}}$ ). Values of  $f_{\text{ox}}$  have been previously reported as ranging  
between 0.6-0.7 for sites with vascular plants. On the other hand, it can be nearly equal to 1  
in sites with, for example, a layer of *Sphagnum* moss, where the majority of the produced  
CH<sub>4</sub> is oxidized, or in bottom soils in pond centers where slow molecular diffusion of CH<sub>4</sub>  
takes place through the water (Knoblauch et al., 2016). Under the latter conditions,  $f_{\text{ox}}$  can be  
approximated to > 0.9 (i.e. > 90 % of the produced CH<sub>4</sub> is oxidized before it is emitted to the  
1595 atmosphere). This value has been estimated in polygonal ponds without vascular plants, em-  
pirically supporting the relevance of CH<sub>4</sub> oxidation below the water table in these types of  
environments (Knoblauch et al., 2016). A lower CH<sub>4</sub> oxidation fraction occurs in the pres-  
ence of vascular plants that are effective at bypassing the aerobic areas in the soil. Under the-  
se conditions,  $f_{\text{CH}_4\text{anox\_left}}$  can increase moderately from 0.2 to 0.4 (i.e.  $f_{\text{ox}}$  is from 0.6 to 0.8,  
1600 meaning that 60 to 80 % of the produced CH<sub>4</sub> is oxidized in the soil column). Although cur-  
rent estimates for  $f_{\text{CH}_4\text{anox\_left}}$  from laboratory and on-site experiments are still scarce, they  
mostly agree that those are lower than our reference value of 0.5. This is expected because  
 $f_{\text{CH}_4\text{anox\_left}}$  excludes the portion of CH<sub>4</sub> that is oxidized directly after production, whereas  
 $f_{\text{CH}_4\text{anox}}$  is only the initially produced CH<sub>4</sub>. Still, our modeled CH<sub>4</sub> emissions might benefit  
from prescribing a spatially variable  $f_{\text{CH}_4\text{anox}}$  value linked to the distribution of vascular plants  
and soil wetness in the model domain.

1605 As for the rest of the selected parameters for the sensitivity exercise, no significant differ-  
ences were observed in the modeled CH<sub>4</sub> emissions for the individual pathways or the total  
flux. Specifically, varying the diameter of roots from finer to thicker, and varying the amount  
of available soil volume occupied by roots, did not cause significant differences in modeled

Karel 27/2/2018 12:14

**Moved up [8]:** The results of our sensitivity experiments provided evidence that the magnitude of the simulated CH<sub>4</sub> emissions responds strongly to the value of  $f_{\text{CH}_4\text{anox}}$ .

Karel 26/2/2018 15:59

**Moved (insertion) [7]**

Karel 26/2/2018 16:01

**Deleted:** Our sensitivity experiments show that changes in the values of most of the

Karel 26/2/2018 16:01

**Deleted:** result in

1615 CH<sub>4</sub> emissions with the new formulation of the plant transport in the JSBACH-methane model. These results suggest that the revisited and simplified formulation for plant-mediated transport of gas allows a reduction in the uncertainties of methane transported through this pathway, which previously relied on predefined plant root characteristics that are often not available from observational studies. Instead, we define the volume in the soil that is occupied by roots.

1620 The lack of sensitivity in the CH<sub>4</sub> emissions to most of the selected parameters might ultimately be due to the explicit restriction of gas transport via diffusive processes modeled by Fick's first law (plant transport and molecular diffusion through snow) that was set in the model. The role of this restriction is to limit the diffusion of gas once the concentration gradient between two interfaces equals zero i.e. it reaches equilibrium. Thus, this restriction takes place when the concentration gradient between e.g. the gas in the soil pore spaces and within  
1625 the plant's roots (for plant-mediated transport) or between the gas in the soil pore spaces and the atmosphere above the snow layer (for diffusion of gas through the snow), equals zero. Because the transport pathways can occur in parallel (except for diffusion with and without a snow layer), or emissions can be shifted in time, the modeled total CH<sub>4</sub> emissions may not be influenced by the set of parameters tested here. Finally, changes in the threshold depth of  
1630 snow that limit the diffusion of gas through this layer revealed some differences in the partitioning of the methane flux into the four transport pathways. These differences indicate that a thinner threshold depth favors the other three transport pathways. However, the resulting total CH<sub>4</sub> emissions with the three tested snow threshold depths were not statistically different.

#### 4.2. Year-round model methane emissions

1635 We simulated for the first time year-round methane emissions in a Northeast Siberian region centered on the city of Chersky. Our results showcase the ability of the improved JSBACH-methane model to reproduce seasonality in the CH<sub>4</sub> emissions when compared to fluxes measured by EC and chambers in a study site near Chersky. The different transport pathways in this process-based model play an important role to define the timing of the year-round  
1640 emissions since they are closely linked to the soil physical state and speed of transport processes by their definition. During the growing season, plant-mediated transport dominated the emissions, contributing about 61.4 % in 2014 and 61.7 % in 2015 of the total annual CH<sub>4</sub> emissions, followed by ebullition (33.9 % and 35.7 %) and molecular diffusion during summer when snow is not hindering the emissions (0.02 % for both years). These patterns agree  
1645 well with the findings presented in Kwon et al. (2016) for the CH<sub>4</sub> emissions measured with chambers at the Chersky floodplain, and by Kutzbach et al. (2004) and Knoblauch et al.

Karel 3/3/2018 13:50

Deleted: . .

... [20]

Karel 3/3/2018 13:51

Deleted: of

Karel 3/3/2018 13:52

Deleted: C

Karel 27/2/2018 12:17

Deleted: , including emissions during the non-growing season

Karel 21/2/2018 15:02

Deleted: eddy covariance

1655 (2016) in the Lena River Delta. In these works is shown that the dominant CH<sub>4</sub> transport pathway in tundra wetland ecosystems (about 70-90 % of the total annual emissions) is diffusion through the aerenchyma structures of the plants when they are present. Methane emissions during the non-growing season contributed 4.7 % and 2.7 % of the annual methane emissions in 2014 and 2015, respectively.

1660 As for the methane oxidation, the bulk soil oxidation accounts for about 1 % of the total methane production during the growing season at grid cell scale, and only about 0.6 % for rhizospheric CH<sub>4</sub> oxidation (results not shown). This leads to most of the methane that is produced in the soil to be emitted to the atmosphere through the different transport pathways. Past observational and laboratory studies have estimated the methane oxidation in boreal and tundra soils. Whalen and Reeburgh (2000) showed that about 55 % of the CH<sub>4</sub> diffusing from saturated boreal soils, were oxidized while reaching the surface. Through bottle incubations, Knoblauch et al. (2016) measured the volumetric CH<sub>4</sub> oxidation potential of soil and moss samples collected from ponds of the Lena Delta. The authors found that the fraction of produced CH<sub>4</sub> that is oxidized before it is emitted was between 61 and 78 % using a stable isotope approach. In samples from pond areas without vascular plants, the fraction increased up to 90 % of the total produced CH<sub>4</sub> following a potential methanogenesis approach, and from diffusive CH<sub>4</sub> fluxes into the bottom water this was between 63 % and 94 %. Berestovskaya et al. (2005) measured CH<sub>4</sub> oxidation rates of different soil samples from the Russian Arctic tundra and found that generally the rates of methane oxidation exceeded those to the rates of methane production especially at temperatures of 5 °C. For this to happen, methane-oxidizing bacteria rapidly consumes the methane released from the freshly thawed tundra soils and the methane already deposited in the unfrozen soil, and this takes place even before methanogens produce new methane. Based on these scarce observations in boreal soils, the oxidation processes in our model are still far off and need to be revisited in order to improve the contribution of the methane oxidation processes into the total methane emissions.

1680 The JSBACH-methane model does not explicitly consider specific mechanisms related to the carbon decomposition and thaw in Arctic permafrost and wetland ecosystems, such as: CH<sub>4</sub> production in the soil from root exudates (Knoblauch et al., 2016; Ström et al., 2012), vertical transport of soil organic matter and its vertically resolved decomposition (Braakhekke et al., 2011, 2013; Koven et al., 2015), and microbial community dynamics (McCalley et al., 2014) involved in anoxic CH<sub>4</sub> oxidation or the production of CH<sub>4</sub> in anaerobic microsites confined in oxic soils. Although these processes might contribute substantially to the dynamics of CH<sub>4</sub>,

Karel 3/3/2018 13:54

Deleted: , who found evidence...s ... [21]

Karel 23/2/2018 18:00

Formatted ... [22]

Karel 27/2/2018 12:22

Deleted: (Berestovskaya et al., 2005; Whalen and Reeburgh, 2000)

Karel 27/2/2018 12:18

Formatted ... [23]

Karel 23/2/2018 18:09

Deleted: . ... [24]

1710 research on these processes in soil-permafrost and wetland environments is still lacking or poorly understood with controversial results so far (Bridgham et al., 2013).

At the grid cell scale, the characteristics defined in the model input parameters exert an important influence on the spatial heterogeneity and temporal variability of the modeled environmental controls and CH<sub>4</sub> emissions. For example, in the model domain the soil depths range between 0.1 to 10.6 m (Fig. S4c; grid cell A is 0.89 m and grid cell B is 10.6 m), whereas the depth of the root zone is from 0.1 to 0.89 m (Fig. S4d; grid cell A is 0.72 m and grid cell B is 0.67 m). Also, the cover fraction of vegetation differs among grid cells, and in this model, the coverage of C3 grasses is particularly relevant for CH<sub>4</sub> emissions through the plants roots, e.g. 33.3 % in the area of grid cell A and 91.6 % in grid cell B (Fig. S1). Finally, grid cell A has lower soil moisture and soil ice content relative to the pore volume in the top five soil layers, and larger inundated area, compared to grid cell B (Fig. S8a, b, and d). These differences predominantly explain the shift in the dominant growing season CH<sub>4</sub> transport pathways and seasonal changes between grid cells (Fig. S8e and f).

1720 To further demonstrate the heterogeneity in the modeled total CH<sub>4</sub> emissions, we show in Fig. S5 the time series of the daily CH<sub>4</sub> fluxes in 2014 and 2015, for nine model grid cells (grid cell A and the eight grid cells surrounding it which includes grid cell B). In this area of the domain, the range of the mean emissions is between 24 to 75 mg CH<sub>4</sub> m<sup>-2</sup> d<sup>-1</sup>, with similar values between years 2014 and 2015. To further analyze the spatial heterogeneity, more is discussed below in the context of spatial distribution of CH<sub>4</sub> fluxes in the entire model domain (Fig. S9).

1730 The modeled CH<sub>4</sub> emissions represent fluxes from exclusively inundated areas (water table at or above the surface), thus emissions from areas with a water table below the surface are neglected. In Figure A2b (Appendix A) are shown summertime CH<sub>4</sub> fluxes (June to August, 2014) measured with chambers in the Chersky floodplain (Kwon et al., 2016), plotted the water table in the chamber microsite at the time of the flux measurements. CH<sub>4</sub> oxidation predominantly exceeded production in dry microsities (water tables were below the surface up to about 10 cm), and this was evidenced by a small uptake of CH<sub>4</sub> (on average 3 mg CH<sub>4</sub> m<sup>-2</sup> d<sup>-1</sup>). The fluxes in these dry plots were almost negligible during the growing season. Thus, the modeled fluxes of CH<sub>4</sub> represent the majority of the emissions in this tundra ecosystem.

1740 Our results show a good agreement between the modeled CH<sub>4</sub> emissions (at the grid cell scale) and measured CH<sub>4</sub> emissions with EC and chambers. Overall, the modeled year-round and measured methane emissions at daily temporal resolution are in the same order of magnitude, and both fall within their monthly range of variability. In both the EC footprint area and

Karel 3/3/2018 14:01

Deleted:

Karel 26/2/2018 14:57

Formatted: Subscript

Karel 26/2/2018 15:02

Formatted: Subscript

Karel 26/2/2018 15:27

Deleted: we observed that the heterogeneity in the prescribed input parameters in the model domain, such as the initial soil depth, ultimately control the variability of the modeled environmental characteristics. The contrasting coverage of C3 grasses in two neighboring model grid cells

Karel 26/2/2018 15:39

Deleted: s

Karel 23/2/2018 11:24

Formatted: Subscript

Karel 23/2/2018 12:01

Formatted: Subscript

Karel 23/2/2018 13:29

Formatted: Subscript

Karel 23/2/2018 13:30

Formatted: Subscript

Karel 23/2/2018 13:44

Formatted: Superscript

Karel 23/2/2018 13:44

Formatted: Superscript

Karel 23/2/2018 13:30

Formatted: Subscript

Karel 22/2/2018 15:44

Deleted:

Karel 22/2/2018 13:59

Deleted: 0

Karel 21/2/2018 15:02

Deleted: eddy covariance

model grid cell area, the methane emissions are not spatially homogeneous but bound to the distribution of wetland (inundated) areas, which are also linked to the type of vegetation. This was demonstrated for summer of 2014, where EC CH<sub>4</sub> fluxes are in closer agreement to the model methane emissions after a linear scaling approach of the wet soil areas in the EC footprint.

Karel 23/2/2018 13:48  
Formatted: Subscript

In the model, CH<sub>4</sub> emissions integrated in our study region were on average 22.5 mg CH<sub>4</sub> m<sup>-2</sup> d<sup>-1</sup> during the growing season of 2014 and 2015. These modeled values are also in good agreement with measurements in other Arctic wetland areas influenced by permafrost using eddy towers, chambers, and more recently with airborne techniques. Kutzbach et al., (2004) reported CH<sub>4</sub> emissions of 28 mg CH<sub>4</sub> m<sup>-2</sup> d<sup>-1</sup> measured with chambers during the onset of the growing season from a polygon center of the wet tundra in the Lena Delta. For a variety of locations in polygons of the same region, Sachs et al. (2010) reported mean summer methane emissions of about 55 mg CH<sub>4</sub> m<sup>-2</sup> d<sup>-1</sup>. Knoblauch et al. (2016) presented mean summer fluxes of 46 mg CH<sub>4</sub> m<sup>-2</sup> d<sup>-1</sup> also measured with chambers at the margins of ponds also in Lena Delta. Larger summer methane emission values have been reported elsewhere, e.g. from automatic chambers at the Zackenberg research station, with maximum emissions of about 168 mg CH<sub>4</sub> m<sup>-2</sup> d<sup>-1</sup> at the onset of the growing season (Mastepanov et al., 2008). Merbold et al. (2009) reported CH<sub>4</sub> emissions of ~600 mg CH<sub>4</sub> m<sup>-2</sup> d<sup>-1</sup> measured by chambers at the peak of the growing season (August) in 2005 in the Chersky floodplain.

Karel 3/3/2018 14:19  
Deleted: Lena Delta

Karel 3/3/2018 14:20  
Deleted: ,

Karel 3/3/2018 14:20  
Deleted: and for the same study site,

At the lower end of the observational data, Wille et al. (2008) measured CH<sub>4</sub> emissions of about 30 mg CH<sub>4</sub> m<sup>-2</sup> d<sup>-1</sup> during mid-summer in the Lena Delta. The authors argued that the measured values were generally lower than other estimates and that the main controlling factors of their measurements were low soil temperatures and the influence of atmospheric turbulence during their period of study. Rinne et al. (2007) reported CH<sub>4</sub> fluxes of about 84 mg CH<sub>4</sub> m<sup>-2</sup> d<sup>-1</sup> measured using EC at a boreal fen in southern Finland. Eddy covariance CH<sub>4</sub> fluxes measured in the Alaskan tundra showed a larger range of values, with an average of 32 mg CH<sub>4</sub> m<sup>-2</sup> d<sup>-1</sup> during the onset of the growing season (Zona et al., 2016). Finally, airborne measurements of CH<sub>4</sub> emissions from wetlands in Alaska were estimated to be about 56 mg CH<sub>4</sub> m<sup>-2</sup> d<sup>-1</sup> (Chang et al., 2014).

Karel 3/3/2018 14:21  
Deleted: also

Karel 21/2/2018 15:02  
Deleted: eddy covariance

#### 4.3. Representation of inundated fractions of the grid cell

In this model version, we incorporated the TOPMODEL approach to explicitly model the distribution of inundated areas according to the topography profile. Although this is still only a robust approximation, the implementation of this approach enabled the representation of wetlands in the highly heterogeneous landscape of northeastern Siberia, which is not possible

Karel 3/3/2018 14:21  
Deleted:

Karel 2/3/2018 12:36  
Deleted: improved the ability of the model to represent wetlands

1800 with the traditional hydrology scheme of JSBACH because it does not allow standing water (Kaiser et al., 2017; Hagemann and Stacke, 2015). In contrast to standard remote sensing products, the highly resolved product of Reschke et al. (2012) is the best data available so far for our application. After TOPMODEL parameter adjustments, still large differences remain between  $w_{mod}$  and  $w_{rs}$ , however, most of these can be attributed to uncertainties due to the model technique to simulate wetlands and its horizontal resolution.

- Karel 2/3/2018 12:36  
**Deleted:** . Furthermore, this was a considerable improvement to alleviate restrictions associated
- Karel 2/3/2018 12:37  
**Deleted:** , which
- Karel 2/3/2018 12:37  
**Deleted:** modeling of grid cells with

1805 In the model, the fraction of the grid cell that becomes inundated refers to the area where the water table lies at or above the soil surface and varies with changes in available solid (snow) and liquid water (precipitation) leading to a 15-day time step. However, in nature, most wetlands have periods of the year when no visible standing water is above the surface, and the water table is located few cm below the surface (Bridgham et al., 2013; Kwon et al., 2016).

- Karel 2/3/2018 13:23  
**Deleted:** I

1810 Previous studies have demonstrated the dependence of CH<sub>4</sub> emissions on the location of the water table in tundra ecosystems (e.g. Helbig et al., 2017a; Kwon et al., 2016; Merbold et al., 2009; Sturtevant et al., 2012; Zona et al., 2009) and as shown before, the work by Kwon et al. (2016) revealed that CH<sub>4</sub> fluxes measured by chambers in the Chersky floodplain are significantly influenced by the location of the water table at the plot scale. Larger CH<sub>4</sub> emissions

- Karel 2/3/2018 13:27  
**Deleted:** can sometimes lie just

- Karel 2/3/2018 13:27  
**Deleted:** works

1815 were measured in sites where the water table was at or above the surface compared to drier sites. With the TOPMODEL approach it is not possible to characterize the location of inland water bodies (i.e. lakes), and the explicit location of peatlands is also not taken into account because the model only considers mineral soils. This separation would help to identify the inundated portions of land with more or less relative input of organic carbon to better localize the methane emissions. The lack of organic layers representation in the model is mainly due to the difficulties of coupling sub-grid scale hydrology and carbon cycle in a holistic manner. The model however, considers the amount of carbon that is available in the soil, based on a soil carbon and litterbag approach, and that one for decomposition and production of methane.

- Karel 2/3/2018 14:32  
**Deleted:** (e.g. Kwon et al., 2016; Merbold et al., 2009; Sturtevant et al., 2012(Zona et al., 2016))

- Karel 23/2/2018 14:02  
**Deleted:** .

- Karel 23/2/2018 13:54  
**Deleted:** T

- Karel 23/2/2018 14:02  
**Deleted:** , with I

1825 Future important advancements in our model are necessary in the context of a process-based representation of peatland extent as well as the CH<sub>4</sub> balance in non-inundated areas; currently, these are not taken into account in our study, contrary to Kaiser et al., (2017) for a site level study. This is especially relevant for the applicability of this model to other regions where uptake of methane in dry areas might play a substantial role (e.g. Flessa et al., 2008; Jørgensen et al., 2015).

- Karel 23/2/2018 14:05  
**Deleted:** However, although CH<sub>4</sub> oxidation predominantly exceeds production in dry sites, low CH<sub>4</sub> fluxes during the growing season were measured in areas where the water table was located below the soil surface.

- Karel 26/2/2018 11:25  
**Deleted:** Further

- Karel 2/3/2018 13:29  
**Deleted:** improvements in the model

- Karel 23/2/2018 14:16  
**Deleted:** are needed to better simulate

- Karel 2/3/2018 13:29  
**Deleted:** emissions

- Karel 23/2/2018 14:17  
**Deleted:** areas, as discussed below

1830

#### 4.4. Impact of the revised model structure

The model reproduces well the observed temporal trends in the CH<sub>4</sub> emissions, and patterns can be linked to changes in the environmental controls. However, integrating the TOPMODEL approach into JSBACH led to a decoupling of some physical soil state variables. Soil moisture content, soil ice content and soil temperature influence the heat capacity of the soil and the ice content (i.e. soil freeze and thaw processes), and control the accumulation of gas, microbial activity, diffusion rates of gases, and the amount of oxygen in the soil (Sturtevant et al., 2012; Wickland et al., 1999; Pirk et al., 2016). In the JSBACH-methane model, soil moisture of the ice-free soil pores in the inundated part of the grid cell was set to 95 % saturation, for purposes of justifying inundation in the TOPMODEL approach. Although, the temperature and ice conditions in the soil are not influenced by this change, this leads to a missing link in terms of the distribution of soil water to soil ice or soil moisture. However, a direct connection between each of these physical variables and the CH<sub>4</sub> processes is definitively present.

#### 4.5.

Between data years, the soil temperature in summer of 2014 was lower from mid-June than at the same period during 2015, leading to a phase lag in the maximum summer CH<sub>4</sub> emissions of nearly a month earlier in 2015. However, during the autumn of 2015, the soil was colder than in 2014, with more soil ice content and less methane production during this period of the year. This translates into lower CH<sub>4</sub> emissions to the atmosphere from November 2015 until the end of the year than during the same period in 2014. Because seasonal changes in soil wetness must be taken into account for modeling year-round gas emissions in permafrost Arctic tundra environments (Pirk et al., 2016), the JSBACH-methane version used for this work requires further improvements to better integrate the TOPMODEL approach, using a fully mechanistic thermal and hydrology scheme at landscape scale able to interact with inundated area fractions at grid cell scale (Stacke and Hagemann, 2012).

#### 4.6. Simulation of grid cell soil temperature

Large uncertainties in the simulation of CH<sub>4</sub> emissions from northern wetlands with models come from limitations in the representation of freezing and thawing soil processes, snow layer dynamics, and the robust mapping of the distribution of wetlands (Bridgham et al., 2013). Kaiser et al., (2017) reported that the process-based JSBACH-methane module considers the effects of permafrost thawing and freezing, thus also the seasonal changes of the physical state of the soil on CH<sub>4</sub> processes. However, our analysis of the soil temperature profiles showed that during the cold season the simulated soil temperatures are nearly 10 °C lower

Karel 3/3/2018 14:31

Moved (insertion) [10]

Karel 3/3/2018 14:31

Formatted: Font:(Default) Times New Roman

Karel 3/3/2018 14:31

Formatted: List Paragraph, Left, Indent: Left: 0", Hanging: 0.39". Outline numbered + Level: 2 + Numbering Style: 1, 2, 3, ... + Start at: 1 + Alignment: Left + Aligned at: 0.25" + Indent at: 0.55"

Karel 3/3/2018 14:31

Deleted: .

Karel 2/3/2018 14:39

Moved (insertion) [9]

Karel 3/3/2018 14:31

Moved up [10]: Impact of the revised model structure .

Karel 3/3/2018 14:37

Deleted: (Stacke and Hagemann, 2012). .

Karel 26/2/2018 11:19

Formatted: Font:Not Bold

Karel 3/3/2018 14:33

Deleted: The model reproduces well the observed temporal trends in the CH<sub>4</sub> emissions, and patterns can be linked to changes in the environmental controls. However, as a result of introducing the TOPMODEL approach to allow the representation of inundated areas, the connection among the soil characteristics of the inundated part of the grid cell has been compromised in this model version. Namely, the soil moisture content is no longer connected to the soil ice content and to the soil temperature. Still, in this model version the soil ice content controls the pore space available for CH<sub>4</sub> transport, and the soil temperature influences, among other ... [25]

Karel 2/3/2018 14:39

Moved up [9]: However, a direct connection between each of these physical v... [26]

Karel 3/3/2018 14:38

Deleted:

Karel 3/3/2018 14:37

Deleted: into the grid cell thermal and hydrology schemes

Karel 2/3/2018 14:47

Deleted: the poor

Karel 2/3/2018 14:47

Deleted: (Ekici et al., 2014)

Karel 2/3/2018 14:47

Deleted: for the emission of gas during the cold season

Karel 2/3/2018 14:47

Deleted: .

Karel 2/3/2018 14:47

Deleted: the

1950 than the values measured on site. Moreover, they gradually increase through spring and  
summer to reach values similar to the measurements. In contrast, the soil temperature season-  
al cycle observed in the Chersky floodplain shows strong links to thawing and freezing pro-  
cesses (Göckede et al., 2017). These differences could be related to a negative bias in soil  
moisture content at the grid cell scale – which is driven by non-inundated areas - used to cal-  
1955 culate the soil thermal regime. This limits the validity of the soil thermal properties as well as  
changes in latent heat. In addition, the carbon decomposition scheme used in this model ver-  
sion is driven by precipitation and atmospheric temperature. Therefore, actual changes in the  
soil temperature regime and wetness are not fully linked to the carbon dynamics. Finally, in  
addition to snow, near-surface vegetation in tundra environments (e.g., mosses and lichens)  
1960 are also effective thermal insulators of soil (Porada et al., 2016), regulating high surface tem-  
peratures in summer and cold temperatures during winter, and should be taken into account in  
a next version of the land surface model.

#### 4.7. Role of non-growing season CH<sub>4</sub> emissions

1965 In this work, we present, to our knowledge, the first simulated CH<sub>4</sub> emissions during the non-  
growing season with a land surface model at a regional scale. Our results show that changes  
in the snow layer depth control the temporal variation of the molecular diffusion of CH<sub>4</sub>  
through the snow. Our sensitivity studies corroborate that setting a thinner layer of snow as a  
threshold depth to switch to the CH<sub>4</sub> emission process during the cold season, only promotes  
1970 some changes in the partitioning of the methane flux among the four transport pathways. For  
example, a thinner snow layer promotes an earlier release of CH<sub>4</sub> than was otherwise emitted  
during late summer with a thicker layer of snow. However, the magnitude of the emissions  
through the snow is also determined by the amount of CH<sub>4</sub> that is produced, calculated from  
the decomposed carbon that is driven only by air temperature and precipitation in the carbon  
decomposition module. Changes in the physical properties of the snowpack (i.e. porosity and  
1975 density) defined in the model have no clear effect on the timing of the emissions through the  
snow; this may lead to the conclusion that our choice of values for the capacity of snow to  
transport CH<sub>4</sub> was large enough. The physical restriction of gas transport via diffusive pro-  
cesses modeled by Fick's first law ensures that only physically possible rates of gas transport  
are being modeled.

1980 In the recent work by Pirk et al. (2016), the authors demonstrated that the fluxes of CH<sub>4</sub>  
through the snowpack of permafrost Arctic wetlands during wintertime reflected a continuous  
emission of low amounts of gas still being produced in the soil, rather than solely the release  
of gas stored in the soil that was produced during the preceding growing season. These ob-

Karel 2/3/2018 14:51

Deleted: profiles

Karel 2/3/2018 14:52

Deleted: measured

Karel 2/3/2018 14:52

Deleted: display a pronounced seasonal cycle linked

Karel 2/3/2018 14:52

Deleted: the

Karel 2/3/2018 14:52

Deleted: in the soil

Karel 26/2/2018 21:48

Deleted: are

Karel 2/3/2018 14:52

Deleted: the lower

Karel 2/3/2018 14:53

Deleted: in the model

Karel 2/3/2018 14:53

Deleted: modeled heat capacity and thermal conductivity of the soil, ultimately failing to reproduce the zero curtain period. Thus, in order to improve the modeled winter emissions of methane, it is also mandatory to improve the representation of the soil moisture regime in the model.

Karel 3/3/2018 14:42

Deleted: Yasso07

2000 servations are in agreement with those from Mast et al. (1998), where the authors reported  
evidence of microbial activity throughout winter in subalpine soils permitted by the insulat-  
ing effect of the snow layer. The results of Pirk et al. (2016) showed that there was no appar-  
ent sink or source of CH<sub>4</sub> within the snowpack, and their measurements captured a linear  
2005 concentration gradient through the snow. (Pirk et al., 2016). This observation validates the  
application of Fick’s first law for diffusion of fluxes through the snow during winter, as ap-  
plied in our model configuration. However, our formulation does not take into account the  
“pressure pumping” process reported by Massman et al. (1997) and Bowling and Massman  
(2011) that is related to the persistent advection of gas enhanced by wind through the snow-  
2010 pack. Based on isotopic analysis of CO<sub>2</sub> through the snowpack of a mountain forest, Bowling  
and Massman (2011) found that in the presence of wind, the pressure pumping effect contrib-  
uted up to 11 % of the total emissions during winter.

Karel 3/3/2018 14:44

Deleted: pack

Our comparison at a grid cell scale to wintertime fluxes measured from EC at the Chersky  
floodplain (from January until March 2015 on average 3.8 mg CH<sub>4</sub> m<sup>-2</sup> d<sup>-1</sup>) shows that the  
modeled CH<sub>4</sub> emissions during this season (0.4 mg CH<sub>4</sub> m<sup>-2</sup> d<sup>-1</sup>) are consistently lower by  
2015 about one order of magnitude. The measured EC fluxes are similar to other measurements  
with other methods from earlier studies. The work by Panikov and Dedysh (2000) showed  
winter methane emissions measured by chambers of about 5.0 mg CH<sub>4</sub> m<sup>-2</sup> d<sup>-1</sup> from boreal  
peat bogs in western Siberia in mid-February. Pirk et al., (2016) measured CH<sub>4</sub> fluxes above  
the snowpack of about 2.4 mg CH<sub>4</sub> m<sup>-2</sup> d<sup>-1</sup>. In subalpine soils covered with snow, Mast et al.  
2020 (1998) reported average winter CH<sub>4</sub> emissions of 4.4 mg CH<sub>4</sub> m<sup>-2</sup> d<sup>-1</sup> in moist soils calculated  
from samples collected through the snowpack. However, our modeled winter CH<sub>4</sub> emissions  
are comparable to those reported by Smagin and Shnyrev (2015) of about 0.6 mg CH<sub>4</sub> m<sup>-2</sup> d<sup>-1</sup>  
measured by chambers during the coldest months of the year (February and March) in envi-  
ronments with different soil wetness in a West-Siberian bog landscape.

Karel 21/2/2018 15:02

Deleted: eddy covariance

Karel 3/3/2018 14:45

Deleted: (0.4 mg CH<sub>4</sub> m<sup>-2</sup> d<sup>-1</sup>)

Karel 21/2/2018 15:02

Deleted: eddy covariance

2025 Moreover, it is important to note that our results represent average values of a grid cell with a  
0.5° x 0.5° horizontal resolution, whereas measurements represent a much smaller spatial  
scale. Integrating the latter to the grid cell level must lead to an overestimation of the emis-  
sion values at the grid cell level.

Other works have reported large CH<sub>4</sub> emissions from dry areas during the non-growing sea-  
2030 son. Using EC measurements, Zona et al., (2016) showed large fluxes from dry areas of the  
Alaskan tundra during the zero curtain period. Also, the findings of Mastepanov et al. (2013),  
imply that a portion of the active layer still remains free of ice during late autumn, and mois-  
ture and temperature changes are limited by the low thermal conductivity and heat capacity

Karel 21/2/2018 15:02

Deleted: eddy covariance

Karel 3/3/2018 14:46

Deleted: T

Karel 26/2/2018 18:41

Deleted: Mastepanov et al. (2013)

of dry soils. In the model, the consistently lower CH<sub>4</sub> emissions during winter can be explained by a low bias in soil temperature, leading to a low bias also in methanogenesis and larger oxidation within the topsoil.

## 5. Conclusion and outlook

The refined configuration of the JSBACH-methane model presented in this study has the ability to represent grid cell scale year-round CH<sub>4</sub> emissions at a comparable magnitude to those measured by chambers and EC in the same study area. The model was successfully applied to a regional domain in a floodplain of Northeastern Siberia underlain by permafrost. The majority of the annual emissions take place through vascular plants. The seasonal transition of the four CH<sub>4</sub> transport pathways is mainly controlled by changes in the soil temperature, and only indirectly linked to soil moisture.

The findings of this study demonstrate that to improve the understanding of the interannual variability of CH<sub>4</sub> fluxes from wetlands in boreal permafrost areas, and to improve process model evaluation, more highly resolved temporal observational data is required, specially of year-round CH<sub>4</sub> EC fluxes and soil temperatures which are generally scarce and challenging for boreal and tundra areas. This is particularly important to improve modeling CH<sub>4</sub> emissions through snow, which in our model show a low bias when compared to EC measurements.

Finally, our model will greatly benefit from further improvements for regional simulations, which will also contribute to advancing the application to a global scale. In summary, the following model improvements are suggested: 1) a descriptive scheme for snow layer dynamics may benefit the simulation of wintertime CH<sub>4</sub> emissions, including pressure pumping effects due to advection of gas enhanced by wind, 2) improvements to prescribed model parameters such as soil depth until bedrock and initial soil moisture saturation, which are normally obtained from global scale configurations of JSBACH, 3) an improved connection between the TOPMODEL approach for simulating the inundated fractions in a model grid cell, and soil state variables such as soil moisture, soil temperature, and ice content. This in turn might lead to improvements in the soil thermal properties for dry versus wet areas, and to the representation of non-inundated areas to understand the dynamics of sources and sinks of CH<sub>4</sub>. This might be alleviated if sub-grid scale heterogeneity is included in future model developments.

4) finally, improving the temporal transitions and seasonality of the water table levels will help to better constrain the surface heterogeneity of hydrologic responses to permafrost thaw and the spatial distribution of carbon decomposition.

Deleted: ... [27]

Karel 2/3/2018 14:56

Deleted: work...has the ability to ... [28]

Karel 3/3/2018 14:49

Formatted ... [29]

Karel 2/3/2018 15:06

Deleted: Modeled ...H<sub>4</sub> emissions t ... [30]

Karel 3/3/2018 14:57

Formatted ... [31]

Karel 27/2/2018 12:45

Deleted: O...r model will greatly b ... [32]

Karel 2/3/2018 15:15

Deleted: the ...ynamics of the snow ... [34]

Karel 3/3/2018 14:50

Formatted ... [33]

Karel 3/3/2018 14:50

Formatted ... [35]

Karel 3/3/2018 14:51

Deleted: ... [36]

Karel 3/3/2018 14:51

Formatted ... [36]

Karel 3/3/2018 14:51

Deleted: I ... [37]

Karel 3/3/2018 14:51

Formatted ... [37]

Karel 3/3/2018 14:51

Deleted: ... [38]

Karel 3/3/2018 14:51

Deleted: Improvements to the ... [38]

Karel 3/3/2018 14:51

Formatted ... [39]

Karel 2/3/2018 15:16

Deleted: conditions ...uch as soil m ... [40]

Karel 3/3/2018 14:51

Formatted ... [41]

Karel 3/3/2018 14:59

Deleted: d ... [42]

Karel 3/3/2018 14:51

Formatted ... [42]

Karel 2/3/2018 15:16

Deleted: capacity and conductivity ... [43]

Karel 3/3/2018 14:51

Formatted ... [44]

Karel 3/3/2018 15:13

Formatted ... [45]

Karel 3/3/2018 14:57

Deleted: ... [46]

Karel 3/3/2018 14:57

Formatted ... [46]

Karel 3/3/2018 14:57

Deleted: T ... [47]

Karel 3/3/2018 14:57

Formatted ... [47]

Karel 3/3/2018 15:03

Deleted: integrated TOPMODEL sc ... [48]

Karel 26/2/2018 20:39

Deleted: Currently the model does ... [49]

Karel 3/3/2018 15:13

Formatted ... [50]

## 6. Code and data availability

The land surface model JSBACH used in this study is intellectual property of the Max Planck Society for the Advancement of Science, Germany. The JSBACH source code is distributed under the Software License Agreement of the Max Planck Institute for Meteorology and it can be accessed on personal request. The steps to gain access are explained under the following link: <http://www.mpimet.mpg.de/en/science/models/license/>. The EC dataset is available through the European Fluxes Database Cluster (site code: RU-Ch2). The chamber flux data is available upon request to M. Göckede (mgoeck@bgc-jena.mpg.de).

### Appendix A: Details on in-situ flux observation program.

#### *Uncertainty assessment in EC flux data.*

The uncertainty analysis for the EC flux data followed procedures well-established in literature (Aubinet et al., 2012), and was split into random and systematic errors. The largest sources of random errors are associated with the turbulent sampling and instrument issues. These errors were quantified for each 30 min flux value through the flux processing software TK3 (Mauder and Foken, 2015). Errors related to footprint uncertainties were not quantified, since there are no major transitions in biome types within the core areas of the flux footprints. Systematic errors can be introduced by unmet theoretical assumptions and methodological challenges, as well as by instrument calibration and data processing issues. To minimize this error, the instruments in the Chersky area were maintained and calibrated on regular basis. Data intercomparison with a second EC tower located 600 m away of the tower that is source of the data presented here yielded no systematic offset in the frequency distributions of wind speed, sonic temperature, and methane mixing ratios between the two towers. The TK3 software package contains all the required conversions and corrections for the flux data processing, and yielded good agreement in a comparison with EddyPro (Fratini and Mauder, 2014). To avoid methodological issues that may bias flux data results, we employed a rigid post-processing quality control and flagging system scheme based on well-established analyses for stationarity and well-developed turbulence (Foken and Wichura, 1996), followed by additional tests to flag implausible data points in the resulting flux time series. Further details on this analysis are presented in Kittler et al. (2017).

No  $u^*$ -threshold was applied to the flux dataset, since we determined stationarity of the signal and integral turbulence characteristics are also for nighttime conditions. This information facilitates identifying datasets with regular turbulent exchange also during stable stratification, therefore producing fewer gaps compared to a bulk exclusion of data during stable nighttime

Karel 2/3/2018 15:34

Formatted: Normal

Karel 2/3/2018 15:21

Deleted: The model code is available upon request to the corresponding author (kcastro@bgc-jena.mpg.de).

Karel 21/2/2018 15:02

Deleted: eddy covariance

Karel 2/3/2018 15:21

Deleted: s

Karel 2/3/2018 15:21

Deleted: will be made

Karel 27/2/2018 12:45

Formatted: Font:(Default) Times New Roman

Karel 27/2/2018 12:45

Formatted: Font:(Default) Times New Roman

Karel 27/2/2018 12:45

Formatted: Font:(Default) Times New Roman

Karel 27/2/2018 12:36

Deleted: ... [51]

Karel 27/2/2018 12:45

Formatted: Font:(Default) Times New Roman

Karel 26/2/2018 12:44

Formatted: Justified

2260 stratification through the  $u^*$ -filter method. After filtering out low-quality fluxes, the data  
coverage of methane fluxes was 86 % during the growing season and 67 % during the winter  
from the original full 30 min flux data set (Kittler et al., 2017). To produce a continuous flux  
record for quantification of long-term  $\text{CH}_4$  budgets, the remaining gaps in the data were filled  
by averaging the existing flux data within a moving window of 10-day length centered on the  
2265 gap. Uncertainties for gap-filled values were quantified as standard deviation within the cor-  
responding window, similar to the definition of gapfilling uncertainties for the  $\text{CO}_2$  flux via  
the marginal distribution sampling routine of Reichstein et al. (2005).

To produce aggregated uncertainty values for longer time periods, we applied the procedures  
suggested in Rannik et al. (2016). All random errors were combined by considering them as  
independent variables that normally decrease with the length of the averaging period. Aver-  
2270 aged over 2014 and 2015, the  $\text{CH}_4$  flux uncertainty based on the 30 min data is  $7.4 \pm 8.3 \text{ nmol}$   
 $\text{m}^{-2} \text{ s}^{-1}$ , a result comparable to  $4.7 \pm 3.8 \text{ nmol m}^{-2} \text{ s}^{-1}$  reported for a fen ecosystem by Jammet et  
al. (2017).

#### *Source-weight function of the EC flux data.*

2275 We conducted a source weight analysis (i.e., footprint analysis), to determine the fractional  
contribution of different land cover types within the field of view of the EC flux tower.  
Source weight functions for each 30-min flux measurement were computed based on the La-  
grangian stochastic footprint model of Rannik et al. (2003). Footprints were accumulated,  
analyzed and interpreted using an approach presented by Göckede et al. (2006, 2008). We  
2280 projected these footprints onto a land cover map from WorldView-2 with 2 m horizontal res-  
olution (Fig. A1). In the context of the presented study, we aggregated the originally identi-  
fied 22 land cover classes into 9 classes to concentrate on the dominant elements of the vege-  
tation community structure.

2285 Since the EC tower is situated on a slightly elevated patch of tundra, tussocks and shrubs fea-  
turing various levels of wetness (red and orange colors in Fig. A1) dominate the immediate  
surroundings. Even though inundated parts of the study area, in this case identified by the  
prevalence of the cotton grass *Eriophorum angustifolium* (blue-ish colors in Fig. A1), are  
dominating the area encircled by the 10 % isoline that is used here to mark the boundary of  
the cumulative footprint area, they are mostly present in the outer reaches, therefore combin-  
2290 ing just about 26 % of the total flux signal sampled by the eddy system. Another 31 % is con-  
tributed by wet to moist tussock tundra with some shrubs. Overall coverage fractions within  
the major wetness categories remain approximately constant between tower footprint and two  
larger regions covered within the same WorldView-2 dataset, indicating that this composition

Karel 26/2/2018 16:10

Deleted: (Reichstein et al., 2005)

Karel 26/2/2018 14:10

Formatted: Font color: Background 1

2295 of wetness levels is typical for the Kolyma floodplain ecosystems analyzed within the context  
of this study.

Flux chamber observations.

2300 As shown in the study of Kwon et al. (2016), in the Chersky site were located two transects  
of 10 permanently installed PVC collars for flux chamber measurements. With distances of  
approximately 25 m between individual microsites, both transects cover a distance of ~225 m  
within a drained and a control section in this area. Site locations were selected quasi-  
randomly to reflect the dominant microsite characteristics (e.g., vegetation composition, wet-  
ness level) that were observed at each of the target locations. With a chamber footprint of  
60 cm x 60 cm, this technique allowed studying microsites with rather homogeneous envi-  
ronmental conditions, as compared to the EC fluxes with often heterogeneous footprint areas.  
2305 Details on the chamber program, overall methane flux rates observed, and functional rela-  
tionships with e.g. soil temperature, vegetation and wetness levels are provided in Kwon et  
al. (2017).

2310 Figure A2a displays average flux rates for wet and dry microsites observed within a drained  
and control transects during sampling campaigns in summer 2014 (Kwon et al., 2016). These  
results demonstrate that methane release rates were virtually zero in the absence of standing  
water. At some of the dry microsites, defined by having the water table below the surface (on  
average up to 10 cm), slightly negative CH<sub>4</sub> flux rates were predominantly observed (mean of  
3 mg CH<sub>4</sub> m<sup>-2</sup> d<sup>-1</sup>) and almost negligible emissions, indicating the oxidation of methane (up-  
take) under highly aerobic conditions. Thus, the methane emissions in this tussock tundra  
2315 ecosystem of Northeastern Siberia take place predominantly in wet areas.

7. **Special issue statement**

This manuscript is a contribution to the special issue dedicated to the project: “Changing  
Permafrost in the Arctic and its Global Effects in the 21st Century (PAGE21)”.

2320 8. **Acknowledgements**

This work was supported through funding by the European Commission (PAGE21 project,  
FP7-ENV-2011, Grant Agreement No. 282700, and PerCCOM project, FP7-PEOPLE-2012-  
CIG, Grant Agreement No. PCIG12-GA-201-333796), the German Ministry of Education  
and Research (CarboPerm-Project, BMBF Grant No. 03G0836G), and the AXA Research  
2325 Fund (PDOC\_2012\_W2 campaign, ARF fellowship M. Göckede). We thank Andrew Durso  
for the English proofread of this manuscript.

Karel 27/2/2018 12:34  
Formatted: Font:Not Bold

Karel 26/2/2018 12:41  
Deleted: ... [52]

Karel 26/2/2018 18:47  
Deleted: KCM

Karel 26/2/2018 18:47  
Deleted:

Karel 27/2/2018 12:34  
Deleted:

## 9. References

- 2335 Aubinet, M., Vesala, T., and Papale, D.: Eddy Covariance - A practical guide to measurement and data analysis, Springer, Dordrecht, Heidelberg, London, New York, 2012.
- Beer, C.: Soil science: the Arctic carbon count, *Nature geoscience*, 1, 569-570, 2008, 10.1038/ngeo292.
- 2340 Berestovskaya, I. I., Rusanov, I. I., Vasil'eva, L. V., and Pimenov, N. V.: The processes of methane production and oxidation in the soils of the Russian Arctic tundra, *Microbiology*, 74, 221-229, 2005, 10.1007/s11021-005-0055-2.
- Beven, K. J. and Kirkby, M. J.: A physically based, variable contributing area model of basin hydrology, *Hydrological Sciences Bulletin*, 24, 43-69, 1979, 10.1080/02626667909491834.
- 2345 Blanc-Betes, E., Welker, J. M., Sturchio, N. C., Chanton, J. P., and Gonzalez-Meler, M. A.: Winter precipitation and snow accumulation drive the methane sink or source strength of Arctic tussock tundra, *Global Change Biology*, 22, 2818-2833, 2016, 10.1111/gcb.13242.
- 2350 Bohn, T. J., Melton, J. R., Ito, A., Kleinen, T., Spahni, R., Stocker, B. D., Zhang, B., Zhu, X., Shroeder, R., Glagolev, M. V., Maksyutov, S., Brovkin, V., Chen, G., Denisov, S. N., Eliseev, A. V., Gallego-Sala, A., McDonald, K. C., Rawlins, M. A., Riley, W. J., Subin, Z. M., Tian, H., Zhuang, Q., and Kaplan, J. O.: WETCHIMP-WSL: intercomparison of wetland methane emissions models over West Siberia, *Biogeosciences*, 12, 3321-3349, 2015, 10.5194/bg-12-3321-2015.
- Bowling, D. R. and Massman, W. J.: Persistent wind-induced enhancement of diffusive CO<sub>2</sub> transport in a mountain forest snowpack, *Journal of Geophysical Research*, 116, G04006, 2011, 10.1029/2011JG001722.
- 2355 Braakhekke, M. C., Beer, C., Hoosbeek, M. R., Reichstein, M., Kruijt, B., Schrumpf, M., and Kabat, P.: SOMPROF: A vertically explicit soil organic matter model, *Ecological Modelling*, 222, 1712-1730, 2011, 10.1016/j.ecolmodel.2011.02.015.
- 2360 Braakhekke, M. C., Wutzler, T., Beer, C., Kattge, J., Schrumpf, M., Ahrens, B., Schöning, I., Hoosbeek, M. R., Kruijt, B., Kabat, P., and Reichstein, M.: Modeling the vertical soil organic matter profile using Bayesian parameter estimation, *Biogeosciences*, 10, 399-420, 2013, 10.5194/bg-10-399-2013.
- Brovkin, V., Boysen, L., Raddatz, T., Gayler, V., Loew, A., and Claussen, M.: Evaluation of vegetation cover and land-surface albedo in MPI-ESM CMIP5 simulations, *Journal of Advances in Modeling Earth Systems*, 5, 48-57, 2013, 10.1029/2012MS000169.
- 2365 Chadburn, S. E., Krinner, G., Porada, P., Bartsch, A., Beer, C., Marchesini, L. B., Boike, J., Ekici, A., Elberling, B., Friborg, T., Hugelius, G., Johanson, M., Kuhry, P., Kutzbach, L., Langer, M., Lund, M., Parmentier, F.-J. W., Peng, S., van Huissteden, J., Wang, T., Westermann, S., Zhu, D., and Burke, E. J.: Carbon stocks and fluxes in the high latitudes: using site-level data to evaluate Earth system models, *Biogeosciences*, 14, 5143-5169, 2017, 10.5194/bg-14-5143-2017.
- 2370 Chang, R. Y. W., Miller, C. E., Dinardo, S. J., Karion, A., Sweeney, C., Daube, B. C., Henderson, J. M., Mountain, M. E., Eluszkiewicz, J., Miller, J. B., Bruhwiler, L. M. P., and

- 2375 Wofsy, S. C.: Methane emissions from Alaska in 2012 from CARVE airborne observations, *Proceedings of the National Academy of Sciences*, 111, 16694-16699, 2014, 10.1073/pnas.1412953111.
- Chen, X., Bohn, T. J., and Lettenmaier, D. P.: Model estimates of climate controls on pan-Arctic wetland methane emissions, *Biogeosciences*, 12, 6259-6277, 2015, 10.5194/bg-12-6259-2015.
- 2380 Christensen, T. R., Johansson, T., Åkerman, H. J., Mastepanov, M., Malmer, N., Friborg, T., Crill, P., and Svensson, B. H.: Thawing sub-arctic permafrost: effects on vegetation and methane emissions, *Geophysical Research Letters*, 31, L04501, 2004, 10.1029/2003GL018680.
- 2385 Conrad, R.: Contribution of hydrogen to methane production and control of hydrogen concentrations in methanogenic soils and sediments, *FEMS Microbiology Ecology*, 28, 193-202, 1999, 10.1111/j.1574-6941.1999.tb00575.x.
- Cresto Aleina, F., Brovkin, V., Muster, S., Boike, J., Kutzbach, J., Sachs, T., and Zuyev, S.: A stochastic model for the polygonal tundra based on Poisson-Voronoi diagrams, *Earth System Dynamics*, 4, 187-198, 2013, 10.5194/esd-4-187-2013.
- 2390 Cresto Aleina, F., Runkle, B. R. K., Brücher, T., Kleinen, T., and Brovkin, V.: Upscaling methane emission hotspots in boreal peatlands, *Geoscientific Model Development*, 9, 915-926, 2016, 10.5194/gmd-9-915-2016.
- Davidson, S. J., Santos, M. J., Sloan, V. L., Reuss-Schmidt, K., Phoenix, G. K., Oechel, W. C., and Zona, D.: Upscaling CH<sub>4</sub> fluxes using high-resolution imagery in Arctic tundra ecosystems, *Remote Sensing*, 9, 1227, 2017, 10.3390/rs9121227.
- 2395 Domine, F., Barrere, M., Sarrazin, D., Morin, S., and Arnaud, L.: Automatic monitoring of the effective thermal conductivity of snow in a low-Arctic shrub tundra, *The Cryosphere*, 9, 1265-1276, 2015, 10.5194/tc-9-1265-2015.
- 2400 Dutta, K., Schuur, E. A., Neff, J. C., and Zimov, N.: Potential carbon release from permafrost soils of Northeastern Siberia, *Global Change Biology*, 12, 2336-2351, 2006, 10.1111/j.1365-2486.2006.01259.x.
- Ekici, A., Beer, C., Hagemann, S., Boike, J., Langer, M., and Hauck, C.: Simulating high-latitude permafrost regions by the JSBACH terrestrial ecosystem model, *Geoscientific Model Development*, 7, 631-647, 2014, 10.5194/gmd-7-631-2014.
- 2405 Flessa, H., Rodionov, A., Guggenberger, G., Fuchs, H., Magdon, P., Shibistova, O., Zrazhevskaya, G., Mikheyeva, N., Kasansky, O. A., and Blodau, C.: Landscape controls of CH<sub>4</sub> fluxes in a catchment of the forest tundra ecotone in northern Siberia, *Global Change Biology*, 14, 2040-2056, 2008, 10.1111/j.1365-2486.2008.01633.x.
- Foken, T. and Wichura, B.: Tools for quality assessment of surface-based flux measurements, *Agricultural and Forest Meteorology*, 78, 83-105, 1996, 10.1016/0168-1923(95)02248-1.
- 2410 Fratini, G. and Mauder, M.: Towards a consistent eddy-covariance processing: an intercomparison of EddyPro and TK3, *Atmospheric Measurement Techniques*, 7, 2273-2281, 2014, 10.5194/amt-7-2273-2014.

- Friborg, T., Christensen, T. R., and Sogaard, H.: Rapid response of greenhouse gas emission to early spring thaw in a subarctic mire as shown by micrometeorological techniques, *Geophysical Research Letters*, 24, 3061-3064, 1997, 10.1029/97GL03024.
- 2415
- Göckede, M., Foken, T., Aubinet, M., Aurela, M., Banza, J., Bernhofer, C., Bonnefond, J. M., Brunet, Y., Carrara, A., Clement, R., Dellwik, E., Elbers, J., Eugster, W., Fuhrer, J., Granier, A., Grünwald, T., Heinesch, B., Janssens, I. A., Knohl, A., Koeble, R., Laurila, T., Longdoz, B., Manca, G., Marek, M., Markkanen, T., Mateus, J., Matteucci, G., Mauder, M., 2420  
Migliavacca, M., Minerbi, S., Moncrieff, J., Montagnani, L., Moors, E., Ourcival, J.-M., Papale, D., Pereira, J., Pilegaard, K., Pita, G., Rambal, S., Rebmann, C., Rodrigues, A., Rotenberg, E., Sanz, M. J., Sedlak, P., Seufert, G., Siebicke, L., Soussana, J. F., Valentini, R., Vesala, T., Verbeeck, H., and Yakir, D.: Quality control of CarboEurope flux data - Part 1: Coupling footprint analyses with flux data quality assessment to evaluate sites in forest 2425  
ecosystems, *Biogeosciences*, 5, 433-450, 2008, 10.5194/bg-5-433-2008.
- Göckede, M., Kittler, F., Kwon, M. J., Burjack, I., Heimann, M., Kolle, O., Zimov, N., and Zimov, S.: Shifts in permafrost ecosystem structure following a decade-long drainage increase energy transfer to the atmosphere, but reduce thaw depth, *The Cryosphere*, 11, 2975-2996, 2017, 10.5194/tc-11-2975-2017.
- 2430
- Göckede, M., Markkanen, T., Hasager, C. B., and Foken, T.: Update of a footprint-based approach for the characterisation of complex measurement sites, *Boundary Layer Meteorology*, 118, 635-655, 2006, 10.1007/s10546-005-6435-3.
- Goll, D. S., Brovkin, V., Liski, J., Raddatz, T., Thum, T., and Todd-Brown, K. E. O.: Strong dependence of CO<sub>2</sub> emissions from anthropogenic land cover change on initial land cover and soil carbon parameterization, *Global Biogeochemical Cycles*, 29, 1511-1523, 2015, 10.1002/2014GB004988.
- 2435
- Grant, R. F.: Simulation of methanogenesis in the mathematical model Ecosys, *Soil Biology and Biochemistry*, 30, 883-896, 1998, 10.1016/S0038-0717(97)00218-6.
- Hagemann, S. and Stacke, T.: Impact of the soil hydrology scheme on simulated soil 2440  
moisture memory, *Climate Dynamics*, 44, 1731-1750, 2015, 10.1007/s00382-014-2221-6.
- Helbig, M., Chasmer, L. E., Kljun, N., Quinton, W. L., Treat, C. C., and Sonnentag, O.: The positive net radiative greenhouse gas forcing of increasing methane emissions from a thawing boreal forest-wetland landscape, *Global Change Biology*, 23, 2413-2427, 2017b, 10.1111/gcb.13520.
- 2445
- Helbig, M., Quinton, W. L., and Sonnentag, O.: Warmer spring conditions increase annual methane emissions from a boreal peat landscape with sporadic permafrost, *Environmental Research Letters*, 12, 2017a, 10.1088/1748-932/aa8c85.
- Hugelius, G., Strauss, J., Zubrzycki, S., Harden, J. W., Schuur, E. A., Ping, C.-L., Schirmer, L., Grosse, G., Michaelson, G. J., Koven, C. D., O'Donnell, J. A., Elberling, B., 2450  
Mishra, U., Camill, P., Yu, Z., Palmtag, J., and Kuhry, P.: Estimated stocks of circumpolar permafrost carbon with quantified uncertainty ranges and identified data gaps, *Biogeosciences*, 11, 6573-6593, 2014, 10.5194/bg-11-6573-2014.

- 2455 Jammet, M., Crill, P., Dengel, S., and Friborg, T.: Large methane emissions from a subarctic lake during spring thaw: mechanisms and landscape significance, *Journal of Geophysical Research: Biogeosciences*, 120, 2289-2305, 2015, 10.1002/2015JG003137.
- Jammet, M., Dengel, S., Kettner, E., Parmentier, F.-J. W., Wik, M., Crill, P., and Friborg, T.: Year-round CH<sub>4</sub> and CO<sub>2</sub> flux dynamics in two contrasting freshwater ecosystems of the subarctic, *Biogeosciences*, 14, 5189-5216, 2017, 10.5194/bg-14-5189-2017.
- 2460 Jørgensen, C. J., Lund Johansen, K. M., Westergaard-Nielsen, A., and Elberling, B.: Net regional methane sink in High Arctic soils of northeast Greenland, *Nature Geoscience*, 8, 20-23, 2015, 10.1038/NGEO2305.
- 2465 Kaiser, S., Göckede, M., Castro-Morales, K., Knoblauch, C., Ekici, A., Kleinen, T., Zubrzycki, S., Sachs, T., Wille, C., and Beer, C.: Process-based modelling of the methane balance in periglacial landscapes (JSBACH-methane), *Geoscientific Model Development*, 10, 333-358, 2017, 10.5194/gmd-10-333-2017.
- Kattsov, V. M. and Walsh, J. E.: Twentieth-century trends of Arctic precipitation from observational data and climate model simulation, *Journal of Climate*, 13, 1362-1370, 2000, 10.1175/1520-0442(2000)013<1362:TCTOAP>2.0.CO;2.
- 2470 Kim, Y., Ueyama, M., Nakagawa, F., Tsunogai, U., Harazono, Y., and Tanaka, N.: Assessment of winter fluxes of CO<sub>2</sub> and CH<sub>4</sub> in boreal forest soils of central Alaska estimated by the profile method and the chamber method: a diagnosis of methane emission and implications for the regional carbon budget, *Tellus*, 59B, 223-233, 2007, 10.1111/j.1600-0889.2006.00233.x.
- 2475 Kittler, F., Burjack, I., Corradi, C. A. R., Heimann, M., Kolle, O., Merbold, L., Zimov, N., Zimov, S., and Göckede, M.: Impacts of a decadal drainage disturbance on surface-atmosphere fluxes of carbon dioxide in a permafrost ecosystem, *Biogeosciences*, 13, 5315-5332, 2016, 10.5194/bg-13-5315-2016.
- 2480 Kittler, F., Heimann, M., Kolle, O., Zimov, N., Zimov, S., and Göckede, M.: Long-term drainage reduces CO<sub>2</sub> uptake and CH<sub>4</sub> emissions in a Siberian permafrost ecosystem, *Global Biogeochemical Cycles*, 31, 1704-1717, 2017, 10.1002/2017GB005774.
- Kleinen, T., Brovkin, V., and Schuldt, R. J.: A dynamic model of wetland extent and peat accumulation: results for the Holocene, *Biogeosciences*, 9, 235-248, 2012, 10.5194/bg-9-235-2012.
- 2485 Knoblauch, C., Spott, O., Evgrafova, S., Kutzbach, L., and Pfeiffer, E.-M.: Regulation of methane production, oxidation, and emission by vascular plants and bryophytes in ponds of the northeast Siberian polygonal tundra, *Journal of Geophysical Research: Biogeosciences*, 120, 2525-2541, 2016, 10.1002/2015JG003053.
- 2490 Knorr, W.: Annual and interannual CO<sub>2</sub> exchanges of the terrestrial biosphere: process-based simulations and uncertainties, *Global Ecology and Biogeography*, 9, 225-252, 2000, 10.1046/j.1365-2699.2000.00159.x.
- Koven, C. D., Lawrence, D. M., and Riley, W. J.: Permafrost carbon-climate feedback is sensitive to deep soil carbon decomposability but not deep soil nitrogen dynamics,

- Proceedings of the National Academy of Sciences, 112, 3752-3757, 2015,  
10.1073/pnas.1415123112.
- 2495 Kutzbach, L., Wagner, D., and Pfeiffer, E.-M.: Effect of microrelief and vegetation on methane emission from wet polygonal tundra, Lena Delta, Northern Siberia, *Biogeochemistry*, 69, 341-362, 2004, 10.1023/B:BIOG.0000031053.81520.db.
- 2500 Kwon, M. J., Beulig, F., Ilie, I., Wildner, M., Küsel, K., Merbold, L., Mahecha, M. D., Zimov, N., Zimov, S., Heimann, M., Schuur, E. A., Kostka, J. E., Kolle, O., Hilke, I., and Göckede, M.: Plants, microorganisms, and soil temperatures contribute to a decrease in methane fluxes on a drained Arctic floodplain, *Global Change Biology*, 23, 2396-2412, 2017, 10.1111/gcb.13558.
- 2505 Kwon, M. J., Beulig, F., Ilie, I., Wildner, M., Küsel, K., Merbold, L., Mahecha, M. D., Zimov, N., Zimov, S. A., Heimann, M., Schuur, E. A., Kostka, J. E., Kolle, O., Hilke, I., and Göckede, M.: Plants, microorganisms, and soil temperatures contribute to a decrease in methane fluxes on a drained Arctic floodplain, *Global Change Biology*, 23, 2396-2412, 2016, 10.1111/gcb.13558.
- 2510 Lawrence, D. M., Koven, C. D., Swenson, S. C., Riley, W. J., and Slater, G.: Permafrost thaw and resulting soil moisture changes regulate projected high-latitude CO<sub>2</sub> and CH<sub>4</sub> emissions, *Environmental Research Letters*, 10, 094011, 2015, 10.1088/1748-9326/10/9/094011.
- 2515 Liljedahl, A. K., Boike, J., Daanen, R. P., Fedorov, A. N., Frost, G. V., Grosse, G., Hinzman, L. D., Lijma, Y., Jorgenson, J. C., Matveyeva, N., Necsoiu, M., Reynolds, M. K., Romanovsky, V. E., Schulla, J., Tape, K. D., Walker, D. A., Wilson, C. J., Yabuki, H., and Zona, D.: Pan-Arctic ice-wedge degradation in warming permafrost and its influence on tundra hydrology, *Nature geoscience*, 9, 2016, 10.1038/NGEO2674.
- Massman, W. J., Sommerfeld, R. A., Mosier, A. R., Zeller, K. F., Hehn, T. J., and Rochelle, S. G.: A model investigation of turbulence-driven pressure-pumping effects on the rate of diffusion of CO<sub>2</sub>, N<sub>2</sub>O, and CH<sub>4</sub> through layered snowpacks, *Journal of Geophysical Research*, 102, 18851-18863, 1997, 10.1029/97JD00844.
- 2520 Mast, M. A., Wickland, K. P., Striegl, R. T., and Clow, D. W.: Winter fluxes of CO<sub>2</sub> and CH<sub>4</sub> from subalpine soils in Rocky Mountain National Park, Colorado, *Global Biogeochemical Cycles*, 12, 607-620, 1998, 10.1029/98GB02313.
- 2525 Mastepanov, M., Sigsgaar, C., Tagesson, T., Ström, L., Tamstorf, M. P., and Christensen, T. R.: Revisiting factors controlling methane emissions from high-Arctic tundra, *Biogeosciences*, 10, 5139-5158, 2013, 10.5194/bg-10-5139-2013.
- Mastepanov, M., Sigsgaard, C., Dlugokencky, E. J., Houweling, S., Ström, L., Tamstorf, M. P., and Christensen, T. R.: Large tundra methane burst during onset of freezing, *Nature*, 456, 628-631, 2008, 10.1038/nature07464.
- Mauder, M. and Foken, T.: *Eddy-Covariance Software TK3*. 2015.
- 2530 McCalley, C. K., Woodcroft, B. J., Hodgkins, S. B., Wehr, R. A., Kim, E.-H., Mondav, R., Crill, P. M., Chanton, J. P., Rich, V. I., Tyson, G. W., and Saleska, S. R.: Methane dynamics regulated by microbial community response to permafrost thaw, *Nature*, 514, 478-481, 2014, 10.1038/nature13798.

- 2535 McGuire, A. D., Koven, C., Lawrence, D. M., Clein, J. S., Xia, J., Beer, C., Burke, E., Chen, G., Chen, X., Delire, C., Jafarov, E., MacDougall, A. H., Marchenko, S., Nicolsky, D., Peng, S., Rinke, A., Saito, K., Zhang, W., Alkama, R., Bohn, T. J., Ciais, P., Decharme, B., Ekici, A., Gouttevin, I., Hajima, T., Hayes, D. J., Ji, D., Krinner, G., Lettermaier, D. P., Luo, Y., Miller, P. A., Moore, J. C., Romanovsky, V., Schädel, C., Shaefer, K., Schuur, E. A., Smith, B., Sueyoshi, T., and Zhuang, Q.: Variability in the sensitivity among model simulations of permafrost and carbon dynamics in the permafrost region between 1960 and 2009, *Global Biogeochemical Cycles*, 30, 2016, 10.1002/2016GB005405.
- 2540 Melton, J. R., Wania, R., Hodson, E., Poulter, B., Ringeval, B., Spahni, r., Bohn, T., Avis, C. A., Beerling, D. J., Chen, G., Eliseev, A. V., Denisov, S. N., Hopcroft, P. O., Lettenmaier, D. P., Riley, W. J., Singarayer, J. S., Subin, Z. M., Tian, H., Zurcher, S., Brovkin, V., van Bodegom, P. M., Kleinen, T., Yu, Z., and Kaplan, J. O.: Present state of global wetland extent and wetland methane modelling: conclusion from a model intercomparison project (WETCHIMP), *Biogeosciences*, 10, 753-788, 2013, 10.5194/bg-10-753-2013.
- 2550 Merbold, L., Kutsch, W. L., Corradi, C., Kolle, O., Rebmann, C., Stoy, P. C., Zimov, S. A., and Schulze, E.-D.: Artificial drainage and associated carbon fluxes (CO<sub>2</sub>/CH<sub>4</sub>) in a tundra ecosystem, *Global Change Biology*, 15, 2599-2614, 2009, 10.1111/j.1365-2486.2009.01962.x.
- 2555 Mi, Y., van Huissteden, J., Parmentier, F.-J. W., Gallagher, A., Budishchev, A., Berridge, C. T., and Dolman, A. J.: Improving a plot-scale methane emission model and its performance at a northeastern Siberian tundra site, *Biogeosciences*, 11, 3985-3999, 2014, 10.5194/bg-11-3985.
- Panikov, N. S. and Dedysh, S. N.: Cold season CH<sub>4</sub> and CO<sub>2</sub> emission from boreal peat bogs (West Siberia): winter fluxes and thaw activation dynamics, *Global Biogeochemical Cycles*, 14, 1071-1080, 2000, 10.1029/1999BG900097.
- 2560 Pirk, N., Tamstorf, M. P., Lund, M., Mastepanov, M., Pedersen, S. H., Mylius, M. R., Parmentier, F.-J. W., Christiansen, H. H., and Christensen, T. R.: Snowpack fluxes of methane and carbon dioxide from high Arctic tundra, *Journal of Geophysical Research: Biogeosciences*, 121, 2016, 10.1002/2016JG003486.
- Porada, P., Ekici, A., and Beer, C.: Effects of bryophyte and lichen cover on permafrost soil temperature at large scale, *The Cryosphere*, 10, 2291-2315, 2016, tc-10-2291-2016.
- 2565 Preuss, I., Knoblauch, C., Gebert, J., and Pfeiffer, E.-M.: Improved quantification of microbial CH<sub>4</sub> oxidation efficiency in Arctic wetland soils using carbon isotope fractionation, *Biogeosciences*, 10, 2539-2552, 2013, 10.5194/bg-10-2539-2013.
- 2570 Prigent, C., Papa, F., Aires, F., Rossow, W., and Matthews, E.: Global inundation dynamics inferred from multiple satellite observations, 1993-2000, *Journal of Geophysical Research*, 112, 2007, 10.1029/2006JD007847.
- Raddatz, T., Reick, C., Knorr, W., Kattge, J., Roeckner, E., Schnur, R., Schnitzler, K.-G., Wetzel, P., and Jungclaus, J.: Will the tropical land biosphere dominate the climate-carbon cycle feedback during the twenty-first century?, *Climate Dynamics*, 29, 565-574, 2007, 10.1007/s00382-007-0247-8.

- 2575 Rannik, U., Markkanen, T., Raittila, J., Hari, P., and Vesala, T.: Turbulence statistics inside and over forest: influence on footprint prediction, *Boundary Layer Meteorology*, 109, 163-189, 2003, 10.1023/a:1025404923169.
- Rannik, U., Peltola, O., and Mammarella, I.: Random uncertainties of flux measurements by the eddy covariance technique, *Atmospheric Measurement Techniques*, 9, 5163-5181, 2016, 10.5194/amt-9-5163-2016.
- 2580 Reichstein, M., Falge, E., Baldocchi, D., Papale, D., Aubinet, M., Berbigier, P., Bernhofer, C., Buchmann, N., Gilmanov, T., Granier, A., Grünwald, T., Havránková, K., Ilvesniemi, H., Janous, D., Knohl, A., Laurila, T., Lohila, A., Loustau, D., Matteucci, G., Meyers, T., Miglietta, F., Ourcival, J.-M., Pumpanen, J., Rambal, S., Rotenberg, E., Sanz, M., Tenhunen, J., Seufert, G., Vaccari, F., Vesala, T., Yakir, D., and Valentini, R.: On the separation of net ecosystem exchange into assimilation and ecosystem respiration: review and improved algorithm, *Global Change Biology*, 11, 1424-1439, 2005, 10.1111/j.1365-2486.2005.001002.x.
- 2585 Reick, C., Raddatz, T., Brovkin, V., and Gayler, V.: Representation of natural and anthropogenic land cover change in MPI-ESM, *Journal of Advances in Modeling Earth Systems*, 5, 459-482, 2013, 10.1002/jame.20022.
- 2590 Reschke, J., Bartsch, A., Schlaffer, S., and Schepaschenko, D.: Capability of C-Band SAR for Operational Wetland Monitoring at High Latitudes, *Remote Sensing*, 4, 2923-2943, 2012, 10.3390/rs4102923.
- 2595 Riley, W. J., Subin, Z. M., Lawrence, D. M., Swenson, S. C., Torn, M. S., Meng, L., Mahowald, N. M., and Hess, P.: Barriers to predicting changes in global terrestrial methane fluxes: analyses using CLM4Me, a methane biogeochemistry model integrated in CESM, *Biogeosciences*, 8, 1925-1953, 2011, 10.5194/bg-8-1925-2011.
- 2600 Ringeval, B., Friedlingstein, P., Koven, C., Ciais, P., de Noblet-Ducoudré, N., Decharme, B., and Cadule, P.: Climate-CH<sub>4</sub> feedback from wetlands and its interaction with the climate-CO<sub>2</sub> feedback, *Biogeosciences*, 8, 2137-2157, 2011, 10.5194/bg-8-2137-2011.
- Rinne, J., Riutta, T., Pihlatie, M., Aurela, M., Haapanala, S., Tuovinen, J.-P., Tuittila, E.-S., and Vesala, T.: Annual cycle of methane emission from a boreal fen measured by eddy covariance technique, *Tellus*, 59B, 449-457, 2007, 10.1111/j.1600-0889.2007.00261.x.
- 2605 Sachs, T., Giebels, M., Boike, J., and Kutzbach, L.: Environmental controls on CH<sub>4</sub> emission from polygonal tundra on the microsite scale in the Lena river delta, Siberia, *Global Change Biology*, 16, 3096-3110, 2010, 10.1111/j.1365-2486.2010.02232.x.
- Saltelli, A., Chan, K., and Scott, E. M.: *Sensitivity Analysis*, John Wiley & Sons, Ltd., 2000.
- 2610 Saunio, M. and al., e.: The global methane budget 2000-2012, *Earth System Science Data*, 8, 697-751, 2016, 10.5194/essd-8-697-2016.
- Schuldt, R. J., Brovkin, V., Kleinen, T., and Winderlich, J.: Modelling Holocene carbon accumulation and methane emissions of boreal wetlands - an Earth system model approach, *Biogeosciences*, 10, 1659-1674, 2013, 10.5194/bg-10-1659-2013.

- 2615 Schuur, E. A., Bockheim, J., Canadell, J. G., Euskirchen, E., Field, C. B., Goryachkin, V., Hagemann, S., Kuhry, P., Lafleur, P. M., Lee, H., Mazhitova, G., Nelson, F. E., Rinke, A., Romanovsky, V. E., Shiklomanov, N., Tarnocai, C., Venevsky, S., Vogel, J. G., and Zimov, S.: Vulnerability of permafrost carbon to climate change: implications for the global carbon cycle, *BioScience*, 58, 701-714, 2008, 10.1641/B580807.
- 2620 Schuur, E. A., McGuire, D., Schädel, C., Grosse, G., Harden, J. W., Hayes, D. J., Hugelius, G., Koven, C. D., Kuhry, P., Lawrence, D. M., Natali, S. M., Olefeldt, D., Romanovsky, V. E., Schaefer, K., Turetsky, M. R., Treat, C. C., and Vonk, J. E.: Climate change and the permafrost carbon feedback, *Nature*, 520, 171-179, 2015, 10.1038/nature14338.
- 2625 Serreze, M. C., Walsh, J. E., Chapin III, F. S., Osterkamp, T. E., Dyurgerov, M., Romanovsky, V., Oechel, W. C., Morison, J., Zhang, T., and Barry, R. G.: Observational evidence of recent change in the Northern high-latitude environment, *Climatic Change*, 46, 159-207, 2000, 10.1023/A:1005504031923.
- Smagin, A. V. and Shnyrev, N. A.: Methane fluxes during the cold season: distribution and mass transfer in the snow cover of bogs, *Eurasian Soil Science*, 48, 823-830, 2015, 10.1134/S1064229315080086.
- 2630 Song, C., Xu, X., Sun, X., Tian, H., Sun, L., Miao, Y., Wang, X., and Guo, Y.: Large methane emission upon spring thaw from natural wetlands in the northern permafrost region, *Environmental Research Letters*, 7, 2012, 10.1088/1748-9326/7/3/034009.
- 2635 Stacke, T. and Hagemann, S.: Development and evaluation of a global dynamical wetlands extent scheme, *Hydrology and Earth System Sciences*, 16, 2915-2933, 2012, 10.5194/hess-16-2915-2012.
- Stocker, B. D., Spahni, R., and Joos, F.: DYPTOP: a cost-efficient TOPMODEL implementation to simulate sub-grid spatio-temporal dynamics of global wetlands and peatlands, *Geoscientific Model Development*, 7, 3089-3110, 2014, 10.5194/gmd-7-3089-2014.
- 2640 Ström, L., Tagesson, T., Mastepanov, m., and Christensen, T. R.: Presence of *Eriophorum scheuchyeri* enhances substrate availability and methane emission in an Arctic wetland, *Soil Biology and Biogeochemistry*, 45, 61-70, 2012, 10.10/j.soilbio.2011.09.005.
- 2645 Sturtevant, C. S., Oechel, W. C., Kim, Y., and Emerson, C. E.: Soil moisture control over autumn season methane flux, Arctic Coastal Plain of Alaska, *Biogeosciences*, 9, 1423-1440, 2012, 10.5194/bg-9-1423-2012.
- 2650 Tagesson, T., Mastepanov, M., Mölder, M., Tamstorf, M. P., Eklundh, L., Smith, B., Sigsgaard, C., Lund, M., Ekber, A., Falk, J. M., Friberg, T., Christensen, T. R., and Ström, L.: Modelling of growing season methane fluxes in a high-Arctic wet tundra ecosystem 1997-2010 using in situ and high-resolution satellite data, *Tellus B*, 65, 19722, 2013, 10.3402/tellusb.v65i0.19722.
- Tarnocai, C., Canadell, J. G., Schuur, E. A., Kuhry, P., Mazhitova, G., and Zimov, S.: Soil organic carbon pools in the northern circumpolar permafrost region, *Global Biogeochemical Cycles*, 23, GB2023, 2009, 10.1029/2008GB003327.

- 2655 Thum, T., Räisänen, P., Sevanto, S., Tuomi, M., Reick, C., Vesala, T., Raddatz, T., Aalto, T., Järvinen, H., Altimir, N., Pilegaard, K., Nagy, Z., Rambal, S., and Liski, J.: Soil carbon model alternatives for ECHAM5/JSBACH climate model: evaluation and impacts on global carbon cycle estimates, *Journal of Geophysical Research*, 116, G02028, 2011, 10.1029/2010JG001612.
- 2660 Tokida, T., Mizoguchi, M., Miyazaki, T., Kagemoto, A., Nagata, O., and Hatano, R.: Episodic release of methane bubbles from peatland during spring thaw, *Chemosphere*, 70, 165-171, 2007, 10.1016/j.chemosphere.2007.06.042.
- Tuomi, M., Laiho, R., Repo, A., and Liski, J.: Wood decomposition model for boreal forests, *Ecological Modelling*, 222, 709-718, 2011, 10.1016/j.ecolmodel.2010.10.025.
- 2665 Tuomi, M., Thum, T., Järvinen, H., Fronzek, S., Berg, B., Harmon, M., Trofymow, J. A., Sevanto, S., and Liski, J.: Leaf litter decomposition - estimates of global variability based on Yasso07 model, *Ecological Modelling*, 220, 3362-3371, 2009, 10.1016/j.ecolmodel.2009.05.016.
- 2670 Viovy, N. and Ciais, P.: CRUNCEP data set for 1901-2015, Version 7.0, [https://esgf.extra.cea.fr/thredds/catalog/store/p529viovy/cruncep/V7\\_1901\\_2015/catalog.html](https://esgf.extra.cea.fr/thredds/catalog/store/p529viovy/cruncep/V7_1901_2015/catalog.html), 2016.
- Walter, B. P. and Heimann, M.: A process-based, climate-sensitive model to derive methane emissions from natural wetlands: application to five wetland sites, sensitivity to model parameters, and climate, *Global Biogeochemical Cycles*, 14, 745-765, 2000, 10.1029/1999GB001204.
- 2675 Wania, R., Ross, I., and Prentice, I. C.: Implementation and evaluation of a new methane model within a dynamic global vegetation model: LPJ-WHyMe v1.3.1, *Geoscientific Model Development*, 3, 565-584, 2010, 10.5194/gmd-3-565-2010.
- 2680 Whalen, S. C. and Reeburgh, W. S.: Interannual variations in tundra methane emission: a 4-year time series at fixed sites, *Global Biogeochemical Cycles*, 6, 139-159, 1992, 10.1029/92GB00430.
- Whalen, S. C. and Reeburgh, W. S.: Methane oxidation, production, and emission at contrasting sites in a boreal bog, *Geomicrobiology Journal*, 17, 237-251, 2000, 10.1080/01490450050121198.
- 2685 Wickland, K. P., Striegl, R. G., Schmidt, S. K., and Mast, M. A.: Methane flux in subalpine wetland and unsaturated soils in the southern Rocky Mountains, *Global Biogeochemical Cycles*, 13, 101-113, 1999, 10.1029/1998GB900003.
- Wille, C., Kutzbach, L., Sachs, T., Wagner, D., and Pfeiffer, E.-M.: Methane emission from Siberian arctic polygonal tundra: eddy covariance measurements and modeling, *Global Change Biology*, 14, 1395-1408, 2008, j.1365-2486.2008.01586.x.
- 2690 Xu, X., Elias, D. A., Graham, D. E., Phelps, T. J., Carroll, S. L., Wulfschleger, S. D., and Thornton, P. E.: A microbial functional group-based module for simulating methane production and consumption: application to an incubated permafrost soil, *Journal of Geophysical Research: Biogeosciences*, 120, 1315-1333, 2015, 10.1002/2015JG002935.

Karel 3/3/2018 15:14

Formatted: Default Paragraph Font, Font:(Default) Times New Roman, Check spelling and grammar

- 2695 Xu, X., Riley, W. J., Koven, C. D., Billesbach, D. P., Chang, R. Y.-W., Commane, R., Euskirchen, E. S., Hartery, S., Harazono, Y., Iwata, H., McDonald, K. C., Miller, C. E., Oechel, W. C., Poulter, B., Raz-Yaseef, N., Sweeney, C., Torn, M., Wofsy, S. C., Zhang, Z., and Zona, D.: A multi-scale comparison of modeled and observed seasonal methane emissions in northern wetlands, *Biogeosciences*, 13, 5043-5056, 2016, 10.5194/bg-13-5043-2016.
- 2700 Zhu, Q., Liu, J., Peng, C., Chen, H., Fang, X., Jiang, H., Yang, G., Zhu, D., Wang, W., and Zhou, X.: Modelling methane emissions from natural wetlands by development and application of the TRIPLEX-GHG model, *Geoscientific Model Development*, 7, 981-999, 2014, 10.5194/gmd-7-981-2014.
- 2705 Zona, D., Gioli, B., Commane, R., Lindaas, J., Wofsy, S. C., Miller, C. E., Dinardo, S. J., Dengel, S., Sweeney, C., Karion, A., Chang, R. Y.-W., Henderson, J. M., Murphy, P. C., Goodrich, J. P., Moreaux, V., Liljedahl, A., Watts, J. D., Kimball, J. S., Lipson, D. A., and Oechel, W. C.: Cold season emissions dominate the Arctic tundra methane budget, *Proceedings of the National Academy of Sciences*, 113, 40-45, 2016, 10.1073/pnas.1516017113.
- 2710 Zona, D., Oechel, W. C., Kochendorfer, J., Paw U, K. T., Salyuk, A. N., Olivas, P. C., Oberbauer, S. F., and Lipson, D. A.: Methane fluxes during the initiation of a large-scale water table manipulation experiment in the Alaskan Arctic tundra, *Global Biogeochemical Cycles*, 23, GB2013, 2009, 10.1029/2009GB003487.

2715

**Table 1.** Summary of the most relevant prescribed parameters in the JSBACH-methane control and reference simulations.

Parameter	Description	Value	Unit
$\chi_{\min\_cti}$	Threshold to define maximum areas that can be flooded in a grid cell (TOPMODEL)	12	[-]
$f$	Exponential decay of transmissivity with depth (TOPMODEL)	2.0	[-]
$d_r$	Root diameter	2	mm
$r$	Resistance factor of root exodermis	0.8	[-]
$h_{exo}$	Thickness of exodermis	0.06	mm
$R_{fr}$	Principal fraction of the pore-free soil volume occupied by roots	40	%
$\phi$	Porosity of snow	0.64	[-]
$h_{snow}$	Snow depth threshold	5	cm
$f_{CH_4^{anox}}$	Fraction of anoxic decomposed carbon that becomes $CH_4$	0.5	[-]
$D_{air}^{CH_4}$	Diffusion coefficient of $CH_4$ in free air at 0 °C and 1 atm	$1.95 \times 10^{-5}$	$m^2 s^{-1}$
$D_{air}^{O_2}$	Diffusion coefficient of $O_2$ in free air at 0 °C and 1 atm	$1.82 \times 10^{-5}$	$m^2 s^{-1}$
$\rho_{ice}$	Ice density	910	$kg m^{-3}$
$\rho_{snow}$	Snow density	330	$kg m^{-3}$
(Together with $\rho_{ice}$ leads to: $\phi=0.64$ and $\tau=0.77$ )			

2720

Karel 27/2/2018 12:46

Formatted: List Paragraph

Karel 27/2/2018 12:46

Deleted: -

-

Karel 26/2/2018 14:34

Deleted: -

**Table 2.** Results from sensitivity experiments (the specific descriptions of the parameters listed below are given in Table 1). Statistical  $p$ -values are given for the experiments whose results significantly differ from the results in the reference simulation.

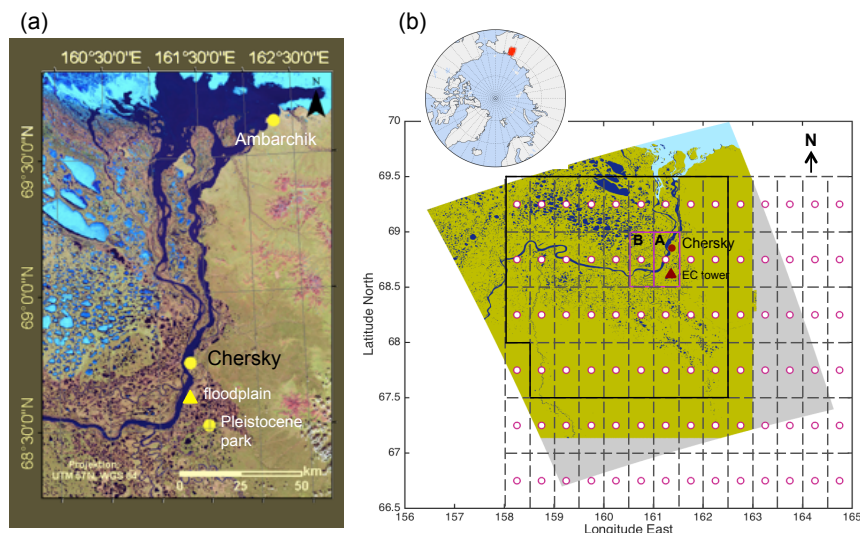
Variable	Value	Unit	Annual mean of total CH <sub>4</sub> / (mg CH <sub>4</sub> m <sup>-2</sup> d <sup>-1</sup> )
$\chi_{\text{min\_cti}}$	11		4.2 ± 5.0*
	12 <sup>§</sup>	[-]	6.2 ± 7.3
	13		9.2 ± 10.7*
$d_t$	2 <sup>§</sup>		6.2 ± 7.3
	5	mm	6.2 ± 7.3
	8		6.2 ± 7.3
$R_{f_t}$	0.2		6.2 ± 7.3
	0.4 <sup>§</sup>	[-]	6.2 ± 7.3
	0.6		6.2 ± 7.3
$\phi$	0.64 <sup>§</sup>		6.2 ± 7.3
	0.71	[-]	6.2 ± 7.3
	0.86		6.2 ± 7.3
$h_{\text{snow}}$	1		6.2 ± 7.3
	3	cm	6.2 ± 7.3
	5 <sup>§</sup>		6.2 ± 7.3
$f_{\text{CH4anox}}$	0.1		1.2 ± 1.4*
	0.3	[-]	3.7 ± 4.3*
	0.5 <sup>§</sup>		6.2 ± 7.3

<sup>§</sup>parameter value in reference simulation; \*significant at  $p < 0.001$

Karel 5/3/2018 10:22

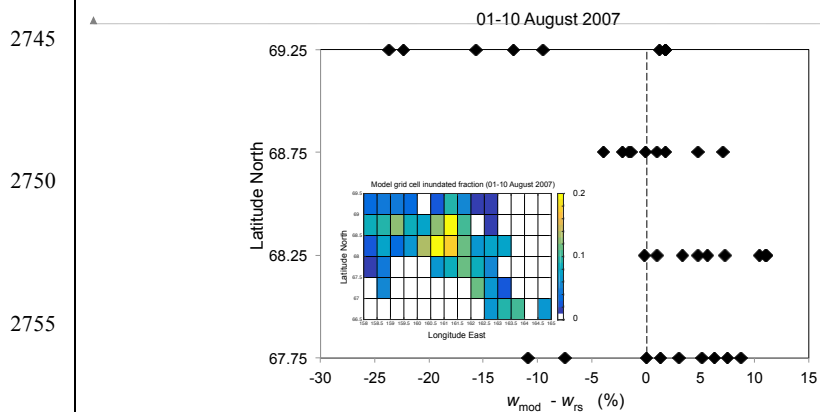
Formatted: Left

**Figures**



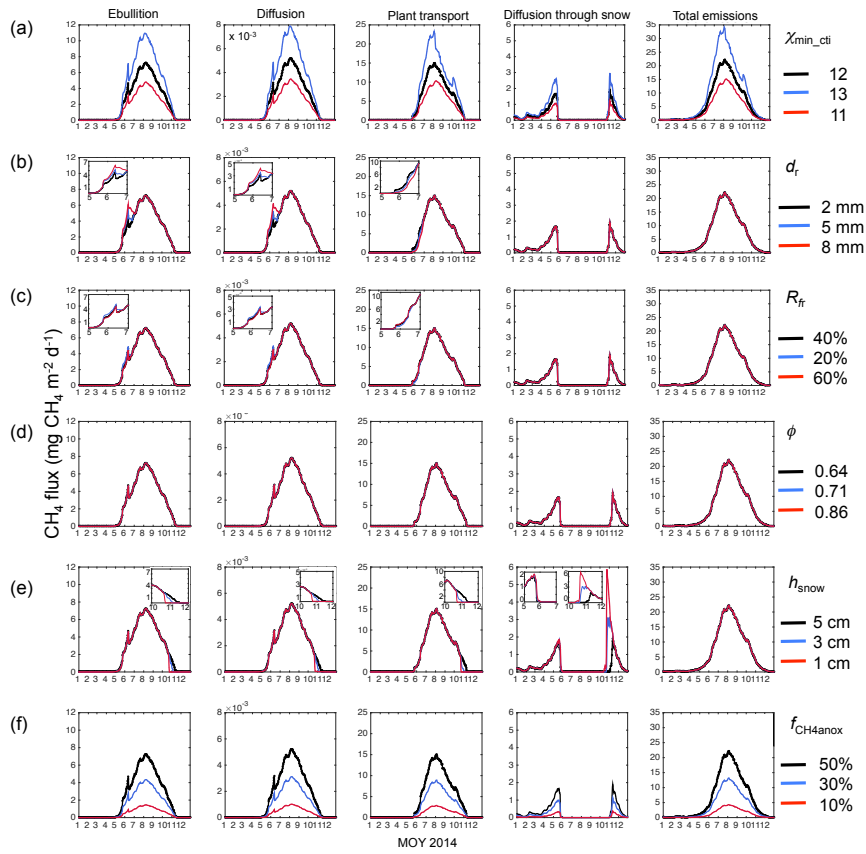
Unknown  
Formatted: Font:(Default) Times New Roman, Bold

2735 **Figure 1** – a) MODIS image showing the heterogeneous landscape in most of the model domain in Northeast Siberia, also showing the location of nearby cities and the floodplain, b) geographical location of the model domain used in this study also depicted with the mid-points of the model grid cells (pink circles) and boundaries (dashed lines) underlain by a geotiff image (data from 01-10 July 2007) from the EAWS product. The boundaries of the grid cells A and B are delimited with pink lines. The continuous dark line delimits the 35 model grid cells used for the evaluation of modeled inundated areas against the EAWS product.



Unknown  
Formatted: Font:(Default) Times New Roman

2750 **Figure 2** – Latitudinal distribution of the difference between the fractions of the grid cell inundated areas simulated with TOPMODEL in JSBACH-methane ( $w_{mod}$ ) and the inundated areas estimated from the EAWS product ( $w_{rs}$ ) for the same grid cells (01-10 August 2007). Inset figure is the mean spatial distribution of the fraction of inundated areas in the model domain for 01-10 August 2007. Grid cells with inundated areas < 1 % are not shown.



2765

2770

**Figure 3** – Results from the sensitivity experiments for the six selected parameters described in Table 2. Daily methane emissions for the individual transport pathways and total methane emissions are shown. The inset figures in some of the panels are zooms to periods of time where larger differences between signals are depicted.

Unknown  
Formatted: Font:(Default) Times New Roman

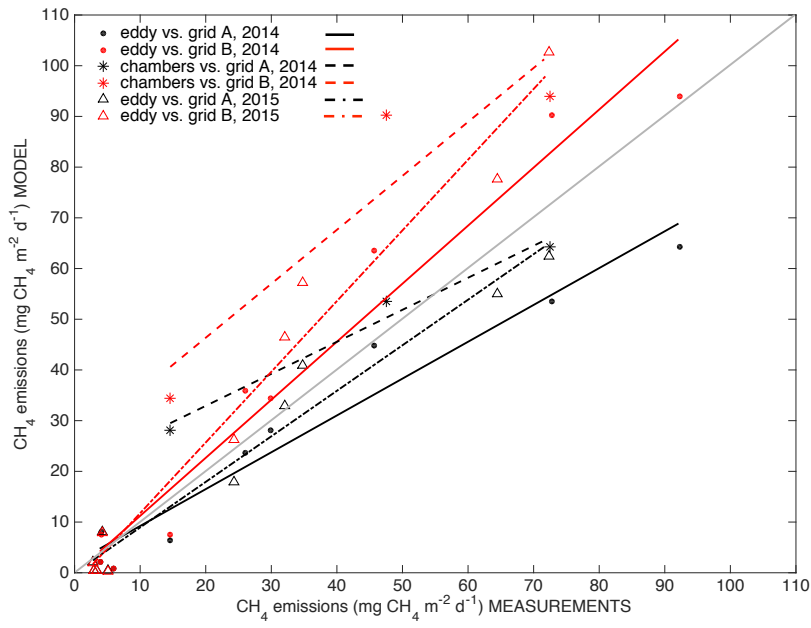
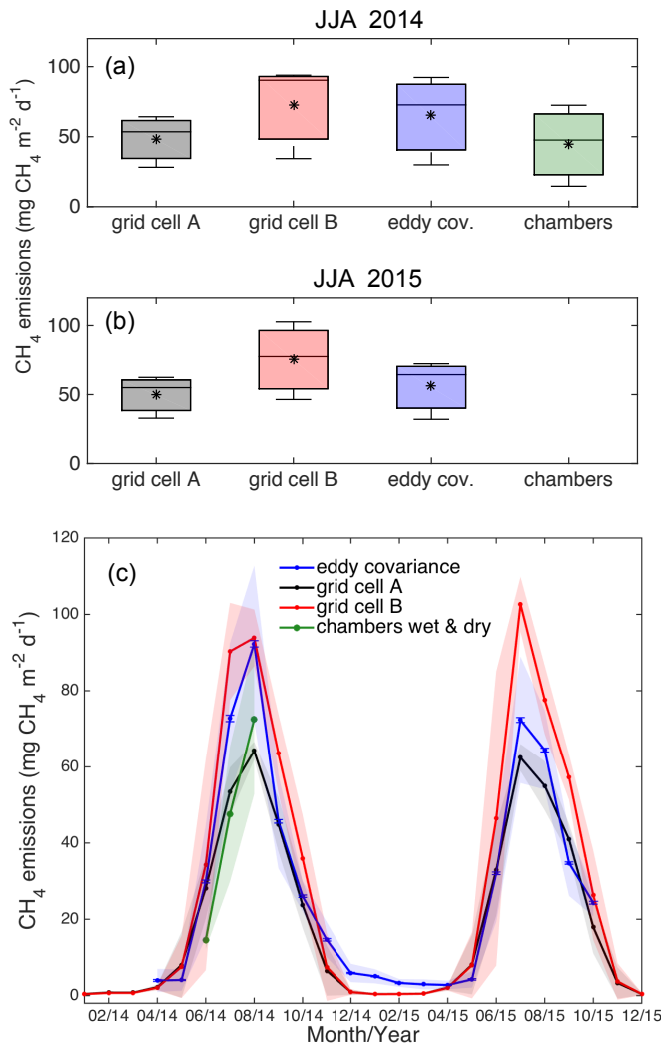


**Figure 4** – Comparison between modeled CH<sub>4</sub> emissions and flux measurements by chambers and EC in the Chersky floodplain: correlation between results for model grid cells A and B and measurements during 2014 and 2015 (the light grey line is the 1:1 line).

2775

Unknown

Formatted: Font:(Default) Times New Roman



Unknown  
**Formatted:** Font:(Default) Times New Roman, Bold

**Figure 5** – Box plot for summer (JJA) methane emissions from model grid cells A and B, eddy covariance and chamber flux measurements for a) 2014 and b) 2015 (without chamber flux measurements). The central horizontal line on each box is the median for each data set and whiskers are the minimum and maximum values; c) time series of monthly CH<sub>4</sub> emissions for 2014 and 2015 for grid cells A and B in the model, from eddy covariance as well as chamber flux measurements. Shaded areas depict one standard deviation of the monthly mean of each data set calculated from the daily resolution model output. Error bars in the EC fluxes are the uncertainty of the monthly averages of the gapfilled and quality checked signal.

2820

2825

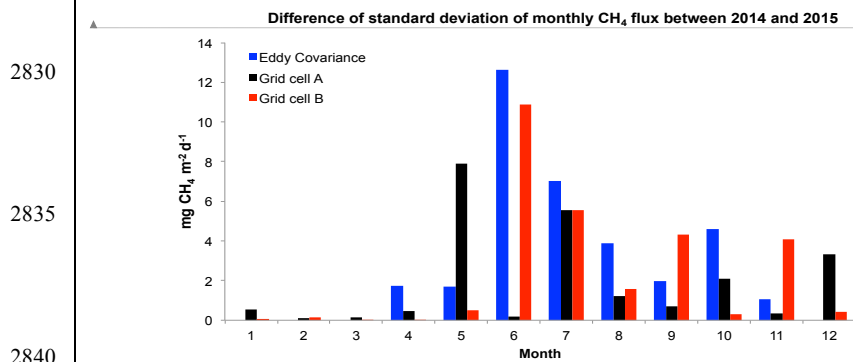


Figure 6 – Comparison of the standard deviation of the monthly fluxes between 2014 and 2015.

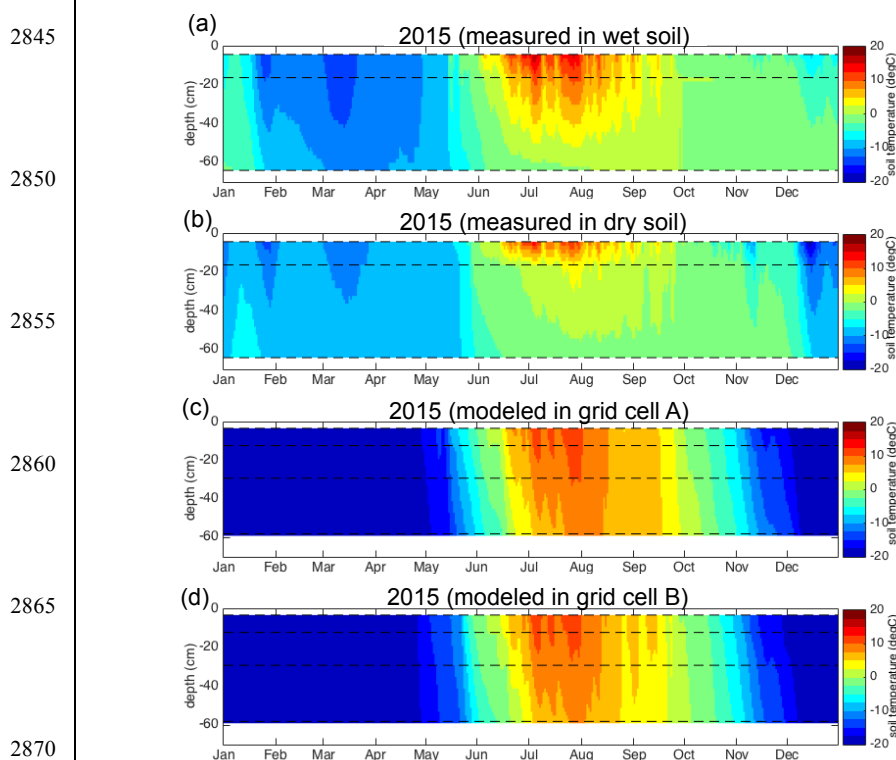
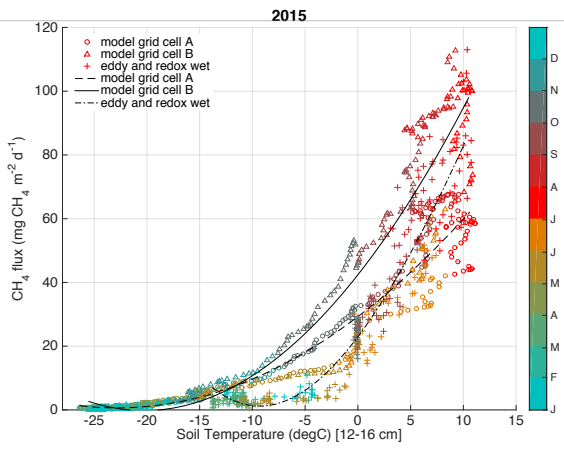


Figure 7 – Hovmöller diagrams showing the time evolution of the vertical profiles of daily soil temperature during 2015 from eddy covariance fluxes measured a) at the wet plot and b) at the dry plot and from the model data c) grid cell A and d) grid cell B. The data were interpolated linearly from the depths where data is available (4, 16 and 64 cm in the sensors of redox systems and 3, 12, 29, and 58 cm in the model).

Unknown  
Formatted: Font:(Default) Times New Roman

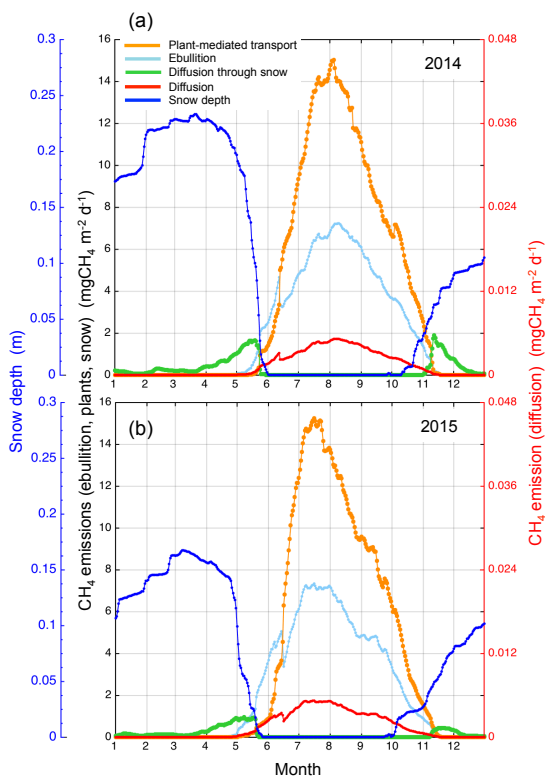
Unknown  
Formatted: Font:(Default) Times New Roman

2880  
2885  
2890  
2895  
2900  
2905  
2910  
2915  
2920  
2925



Unknown  
Formatted: Font:(Default) Times New Roman

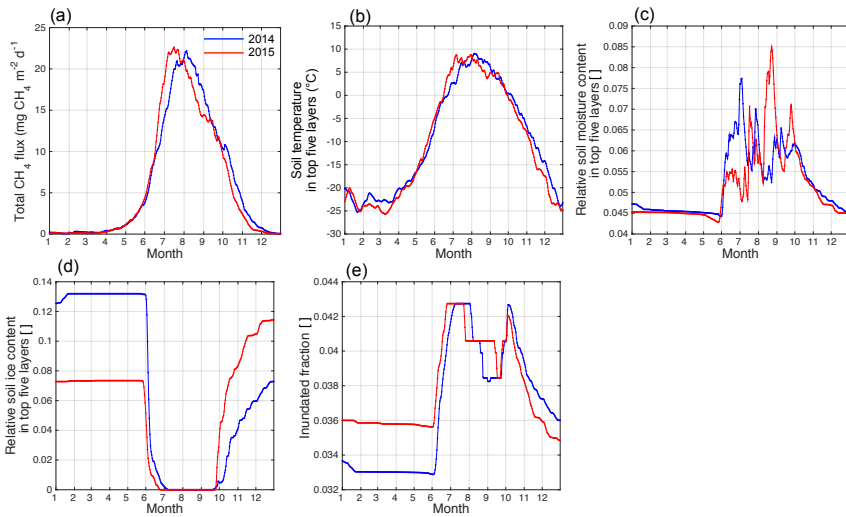
Figure 8 – Model soil temperatures at 12 cm depth and measured values at 16 cm depth measured at a wet site, against the total methane emissions for grid cell A and B in 2015.



Unknown  
Formatted: Font:(Default) Times New Roman

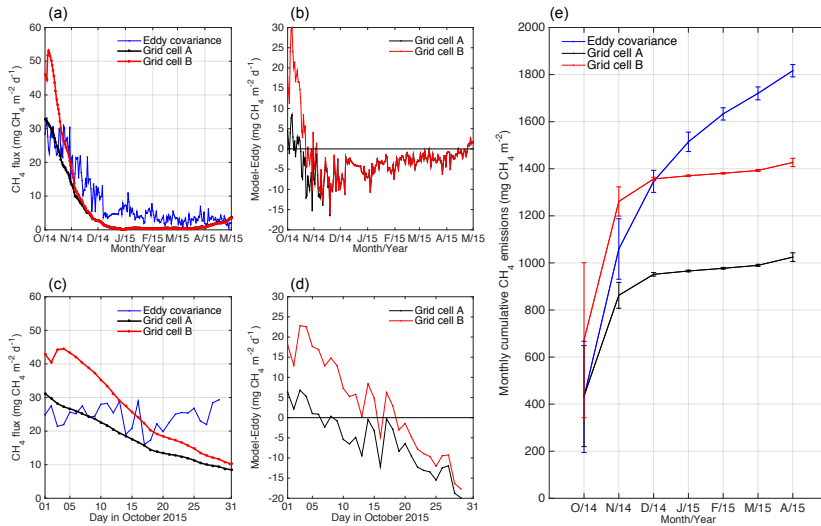
Figure 9 – Year-round mean simulated CH<sub>4</sub> emissions of the model domain through different pathways and domain mean snow depth for a) 2014 and b) 2015.

Karel 5/3/2018 10:38  
Formatted: Justified



2930

**Figure 10** – Mean daily ancillary variables and CH<sub>4</sub> emissions in the model domain in 2014 and 2015: a) total CH<sub>4</sub> emissions, b) mean soil temperature in the root zone (top five soil layers), c) domain mean relative soil moisture content in the top five soil layers, d) domain mean relative soil ice content in the top five soil layers, e) inundated fraction of the grid cell



2935

**Figure 11** – Time series of the daily mean of methane emissions through snow from eddy covariance measurements and model data for grid cell A and B during: a) October 2014 to March 2015 and c) October 2015; the difference between grid cell A and B, and the eddy covariance data are shown in panels b) and d) for the same period of time; e) cumulative CH<sub>4</sub> emissions for the period from the end of autumn in 2014 until the end of spring in 2015 for the same data sets. Error bars in each data set are the standard deviation of the monthly-accumulated fluxes.

2940

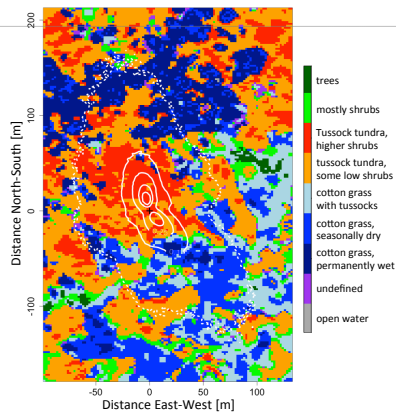
Unknown  
Formatted: Font:(Default) Times New Roman

Unknown  
Formatted: Font:(Default) Times New Roman

2945

2950

2955



Unknown  
 Formatted: Font:(Default) Times New Roman, Bold

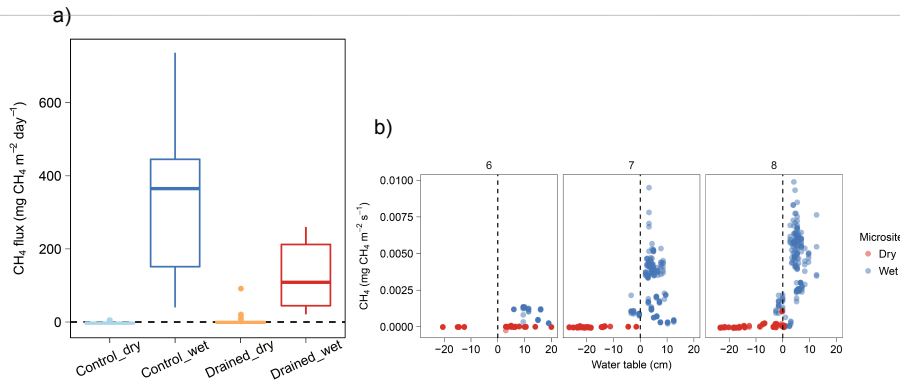
2960

Figure A1: Accumulated source weight function for the EC tower in a control area within the Chersky study site, based on data from the growing season (mid June – mid September) in 2014. Solid white isolines indicate the 80, 60, 40, and 20 % levels, the dashed line is the 10 % level. Background colors indicate aggregated land cover classes based on WorldView-2 data.

2965

2970

2975



Unknown  
 Formatted: Font:(Default) Times New Roman, Bold

2980

Figure A2 - Daily methane flux rates a) aggregated from flux chamber measurements within the growing season of 2014. Measurements are separated into drained (1 wet microsite, 9 dry microsites) and control (8 wet microsites, 2 dry microsites) transects; b) flux rates against the water table at each microsite. Dry plots had a water table at or below the surface (up to 10 cm), whereas wet plots had a water table at or above the surface.

Karel 5/3/2018 10:22  
 Formatted: Left